TRANSPORT OF BEDLOAD BY TRANSLATION WAVES IN AN ALLUVIAL CHANNEL

A thesis presented for the degree of
Doctor of Philosophy in Civil Engineering
at the University of Canterbury
Christchurch, New Zealand

by

GEORGE A. GRIFFITHS

January 1976

ABSTRACT

The response of an alluvial reach to imposed steady water flows and to gradually varying triangular translation waves is examined. Two cases are considered with each flow type; firstly, an equilibrium inflow of bed sediment and secondly, no bedload inflow. Accepted principles of bedload transportation are critically reviewed and are used to qualitatively predict the reach response to the passage of triangular flood waves.

The assumptions made in the general mathematical model for the situation are criticised and questions are posed relating to this little explored phenomemon. These theoretical predictions, assumptions and questions are tested, verified or answered experimentally.

This is achieved by examining the reach behaviour for both flow types, one case at a time, under comparable conditions. That is, the experimentally determined wave state parameters are compared, at selected intervals, with steady flow data. In this process the non-steady flow is treated as a finite series of steady states. The steady water flow parameters were obtained from experiments designed to reproduce, as far as possible, the conditions pertaining to the wave's passage through the same alluvial reach.

In the equilibrium bedload inflow case the inflow and outflow water and sediment hydrographs were similar and non-steady equilibrium transport could be defined. For the range of conditions treated no significant difference was found between the measured and comparable steady transport rates. This result, combined with an observed small variation in resistance, implies that the use of steady state resistance and equilibrium transport formulae in the mathematical model is justified. Therefore the performance of the mathematical model will be limited only by the agreement between the selected bedload transport formula and the steady flow data. A rational adjustment procedure is given to improve this agreement.

In the no bedload inflow or non-equilibrium case magnitude differences occurred between the measured non-steady and the comparable steady transport rates. It is thought that a bed response effect was involved; this effect diminishes as the downstream end of the scour

region associated with the passage of a wave is approached. The error introduced by this response effect and the use of equilibrium formulae in a non-equilibrium situation will render the model performance poor when the reach length is less than the scour hole length. Improvement can be expected as the reach length is proportionally increased.

However, in both cases, the sediment yield can be estimated at a point, as a wave passes, if the corresponding steady flow transport conditions are known.
Other aspects of the reach response which receive attention include initial motion, bedforms, flow resistance and stage-discharge relations.

ACKNOWLEDGEMENTS

The research for this thesis was carried out in the Department of Civil Engineering, University of Canterbury. Facilities and equipment were provided by its Head, Professor H.J. Hopkins.

I acknowledge the assistance received during the course of this project and extend my thanks to:

Dr. A.J. Sutherland, my supervisor, for his encouragement, guidance and helpful criticism throughout the study;

Professor I.R. Wood, Dr. B.W. Hunt and Dr. R.N. Weisman of the academic staff for rewarding discussions;

the Technical Staff of the Civil Engineering Department for their aid with the experimental program. I wish to thank particularly Mr. J. Sheard for numerous practical suggestions, and also Messrs. A. Stokes, H. Pearce and F. Archer for assistance with the construction of equipment and the performance of experiments;

Mrs. A. Watt for typing the manuscript;

Mr. H. Patterson for photographic work;

Mr. L. Brown of the Geological Survey and

Mr. J. Haywood of the Tussock Grasslands and Mountain Lands Institute for comment on natural channel aspects;

the Staff of the North Canterbury Catchment Board for equipment and data.

I appreciate the interest and criticisms made by visitors to the Civil Engineering Department, principally, Professor H.W. Shen of Colorado State University, Professor F.M. Henderson of the University of Newcastle, Professor A.J. Raudkivi of the University of Auckland and Dr. S.M. Thompson of the Ministry of Works and Development.

This study was financially supported by the Ministry of Works and Development, New Zealand.

TABLE OF CONTENTS

Page

Page

APPENDIX E - EXPERIMENTAL RESULTS

Page

LIST OF FIGURES

LIST OF PLATES

Page

LIST OF TABLES

LIST OF SYMBOLS

(Note: Symbols or uses of a symbol occurring in one section only are generally not listed)

a,b	Constants in equilibrium bedload transport formula
B	Bulk specific dry weight of sediment in the bed
C	Chezy resistance coefficient
c	Wave velocity relative to the bank
D	Diameter of particles
D_{90}	Diameter of particles in a sample 90% of which is finer
e	2.71828
exp(x)	Exponential function (of x)
f(x)	Function (of x), a general notation
Fr	Froude number
G_T	Sediment yield per unit width
ΔG_T	Proportional difference in sediment yield
g	The acceleration of gravity
g_s	Sediment discharge per unit width (dry weight)
$g_{s_{av}}$	Average sediment discharge of a wave per unit width, G_T/T
g_{se}	Equilibrium sediment discharge per unit width
k_s	Height of surface roughness projections
L	Reach length
L_s	Length of scour hole
max	Subscript, maximum
min	Subscript, minimum
N	Dimensionless erosion rate
n	Manning's resistance coefficient
o	Subscript relating to steady flow conditions or indicating a reference parameter
p	Porosity
Q	Water discharge

q	Water discharge per unit width
q_{av}	Average water discharge of a wave per unit width
q_s	Equivalent steady water discharge per unit width
R	Hydraulic mean radius
r	Ratio of bedslope to waveslope
S_a	Acceleration slope
S_e	Energy slope
S_f	Friction slope
S_o	Bed slope
S_s	Solid : fluid density ratio, $\rho s/\rho$
T	Wave period
t	time
u	Velocity of water
u_*	shear velocity
u_{*max}	Shear velocity at wave peak
w	Subscript relating to a wave
X_l	Particle shear Reynolds number u_*D/ν
x	Spatial coordinate along the direction of flow
Y	Shields Entrainment Function $\rho u_*^2/\gamma_s D$
y	Vertical depth of flow
y_{crit}	Flow depth when critical transport conditions obtain
y_s	Flow stage or height of water surface above datum
z	Bedload or height of bedsurface above datum
$\bar{z}$	Mean bedlevel
z_f	Limiting depth of scour
γ	Specific weight of water
γ_s	Submerged specific weight of sediment, $\gamma(S_s - 1)$
δ	Boundary layer thickness
Θ	Water temperature
λ	Wavelength or scale

μ	Dynamic viscosity of water
ν	Kinematic viscosity of water
ρ	Density of water
ρ_s	Density of sediment
τ	Variable of integration
τ_c	Shear stress at the threshold of bed motion
τ_o	Shear stress at the bed
ϕ	Einstein bed-load function
ψ	Einstein flow intensity function $1/Y$

CHAPTER 1

INTRODUCTION

1.1 PROBLEM STATEMENT

The major portion of the central mountainous regions of both islands of New Zealand is composed of relatively undifferentiated, extensively fractured sedimentary rocks. Material eroded from this source consists, for the most part, of hard, coarse, rounded, durable alluvium. During the Pleistocene period vast quantities of this debris were transported by water and ice and deposited in the intermontane basins and valleys. Contemporaneously extensive deltas and alluvial plains were formed in some cases, and built up further in others on the seaward margins of the higher relief. Large rivers, with a pronounced shingle* phase, still traverse these surfaces. Their stabilisation in regard to mitigation of flooding and sediment inflow into hydroelectric and irrigation schemes is of economic importance and has been a matter of concern since European settlement.

Nowadays it is generally recognised that the bulk of the annual sediment discharge of many rivers and streams may be transported in a relatively short period of time by a few storm runoffs. During these the discharge of the river or stream is continuously varying. (Bennett [1]). Computational treatment of the flow component of this two phase system has met with a large measure of success. How the sediment phase is to be dealt with is not clearly defined. What is clear, in this regard, in the New Zealand situation is that the bedload fraction of the sediment load is bringing about the important channel changes and is causing the more severe problems. (Henderson [2]).

* Shingle denotes the material in transit on the riverbeds as opposed to the underlying more heterogeneous gravel deposits.

Consequently there is a need for theoretical and laboratory research coupled with field investigations directed firstly;at understanding the physics of the phenomenon of bedload transportation by flood or translation** waves, and secondly; at making quantitative predictions of transport rates and associated system behaviour, in particular the effect of bedforms, the estimation of roughness and the derivation of water and sediment rating curves.

This project is an exploratory one and attempts to meet, in a preliminary sense, the initial requirements of the above prescription.

1.2 SCOPE OF THE INVESTIGATION

This thesis details a theoretical and experimental study of the response of an alluvial reach to both steady and non-steady water inflows, both transporting and not transporting bedload initially. The fluid phase is restricted to flows which can be approximated as one-dimensional and to long wave type transients (i.e. where the ratio of depth, y , to wave length λ , $y/\lambda << 1$). The sediment phase consists of uniform, non-cohesive, gravel particles.

Chapter 2 includes a brief discussion of background papers, current research directions and analytic models. A number of specific problems to be examined in this thesis are posed.

In Chapter 3 the physical system of the study is defined and its response predicted qualitatively. Mathematical models are critically reviewed and developed. A set of experiments designed to give physical insight and to test the models is presented. Other effects are discussed.

** The definition and principal properties of translation waves are given in Appendix A.1.

Chapter 4 is devoted to a description of the experimental work. Sections are included on the objects and general form of the experiments and the experimental procedures and measurements.

Results of the experimental investigation are presented in graphical form and are discussed in Chapter 5.

A set of conclusions, practical implications, and recommendations for future work is given in the final chapter.

All theoretical and experimental details, calculations and results not directly relevant to the main line of the discussion are relegated to the Appendices.

CHAPTER 2

BACKGROUND DISCUSSION

2.1 SYNOPSIS

In this chapter reasons are given for approaching non-steady sediment transport phenomena in alluvial channels from steady state considerations. Then follows a brief review of contributions made to the derivation of a mathematical model. The paucity of experimental data is noted and possible research directions are indicated. A series of questions is posed relating to the problem.

2.2 HISTORICAL NOTE

Until recently research in the field of sediment transport has been almost exclusively concerned with steady uniform flow conditions with regard to water discharge as well as sediment load. (See, for example, the work edited by Shen [3] and the reviews written by Graf [4] and Yalin [5].)

It is recognised that many of the dynamic processes shaping a river bed are related to non-uniform and non-steady conditions. Examples include the processes of aggradation and degradation. Nevertheless Gessler [6] argues, it seems acceptable to use steady state sediment transport equations in mathematical models of these situations. Gessler's argument for this approach is that the sediment transport equations used are unreliable under many conditions and will therefore contain errors which are likely to be substantially larger than those due to a slight degree of non-steadiness. This approach is reasonable when disturbances in transport characteristics propagate slowly.

In regard to the circumstances outlined in 1.1 the question arises as to whether it is valid to use steady state formulae in what is clearly a markedly transient situation. The answer to this

question is not known. However, this is no reason why a start, based on steady state considerations, should not be made even if the research only succeeds in indicating more precisely the areas of uncertainty. Alternatively, it may be possible to derive an empirical model commensurate with the accuracy of those existing for the steady state. Irrespective of these arguments, attempts at modelling the transient situation have been made by de Vries [7,8,9], Wu [10], Chang [11], Miloradov and Muskatirovic [12] and Sakhan et al [13], amongst others. Essentially, the work of these authors has been concerned with formulating an analytical model where the water behaviour is described by the St. Venant Equations and the sediment behaviour by the Exner erosion equation and an equilibrium transport formula. For the simplest one-dimensional case the model* takes the form

Water:

$$\frac{\partial u}{\partial t} + u\frac{\partial u}{\partial x} + g\frac{\partial y}{\partial x} = g\left(\frac{\partial z}{\partial x} - \frac{u^2}{C^2 y}\right) \qquad \ldots (2.1)$$

$$\frac{\partial y}{\partial t} + u\frac{\partial y}{\partial x} + y\frac{\partial u}{\partial x} = 0 \qquad \ldots (2.2)$$

Sediment:

$$\frac{\partial g_s}{\partial x} + B\frac{\partial z}{\partial t} = 0 \qquad \ldots (2.3)$$

$$g_s = f(u, \text{parameters}). \qquad \ldots (2.4)$$

de Vries [9] developed a number of closed form solution models for river bed variations based on this equation set but involving, with other simplifications, the assumption of a constant water discharge.

* A description of these equations is given in Appendix A.2. Properties of the model are discussed in 3.3.2.1(b).

He treated numerically the case of steady withdrawal of cooling water from a natural river with some degree of success (de Vries [8]). It was assumed here that both the Froude number and the celerity of the resulting bottom disturbance were small. In discussing aggradation and degradation (de Vries [9]) he points out that the hydraulic roughness is time dependent and may exhibit hysteresis effects.

Finite difference schemes for the numerical solution of the equation set have been proposed by Wu [10], who replaced equation (2.4) by various specific formulae and by Miloradov and Muskatirovic [12] who took into account a complex cross section with developed meanders.

Perhaps the most comprehensive theoretical treatment is that of Sakhan et al [13] who employed a systems engineering approach. A simulation model was developed in terms of a generalised version of equations 2.1 → 2.3 combined with a stochastic sediment transfer equation which included the effect of bedload. Graphical results were presented demonstrating the operation of the model when applied to the problem of routing a hypothetical input hydrograph and suspended sediment discharge through a long alluvial reach; the bedload discharge at the upstream end being computed directly by the model. Sensitivity analysis on different parameters showed that the response of the hydrographs of water, suspended sediment and bedload discharge agree with what might be expected from field observations. Specific results relevant to this study were:

1) The shapes of the upstream and downstream bedload hydrographs were similar.
2) At the downstream end the peaks of the bedload hydrographs and the water hydrograph occurred at the same time regardless of bed slope and median grain size (3 slopes and 2 median sizes). The magnitudes of the bedload hydrograph peaks decreased with decreasing bed slope and increasing sediment size.

This work is of value conceptually and also because it gives insight into the movements of sediments relative to the flow.

Experimental data on sediment transportation by non-steady flows is extremely limited both in scope and quantity. de Vries [8] created a transition phase between two steady flow equilibrium transport states by suddenly altering the water level in a flume. He found that the reaction of the bed was slow and questioned the use of an equilibrium transport formula to describe local temporary transport for a non-steady state. Sutherland and Griffiths [14] compared, experimentally, non-steady bedload transport by translation waves with steady bedload transport under comparable conditions. For the degradational case, in which no sediment was introduced at the upstream end of the test reach, it was found that translation waves exhibited transport rates which were less than comparable steady rates. The qualitative reason given for this difference was that changes in entrainment and transport rates occur more slowly than changes in discharge. An equivalent steady discharge which produced the same sediment yield as a translation wave could be defined.

Bedform response to non-steady flows and its relationship with stage discharge curves has also been studied experimentally. Such work is reviewed in Chapter 3 where these effects are examined.

It seems to the author that the properties and response of the mathematical model for non-steady sediment transportation have been reasonably well explored theoretically. What is required now is both field and laboratory data to test the range of applicability of the model and to ascertain which, if any, of the assumptions made in its derivation are unreasonable. Concurrently it would be worthwhile to examine the physics of the phenomenon with a view to discovering simplifications in the model or possibly, a more rational theory.

2.3 PROBLEMS CONSIDERED

It is proposed to study theoretically and experimentally the response of an alluvial reach to steady and to gradually varying non-steady flows* both transporting and not transporting sediment at the upstream end. The case of a non-steady flow initially transporting sediment corresponds physically to the situation of a flood wave, whose transport capacity** is satisfied, moving through a river reach. The case of an initially clear water non-steady flow corresponds to the non-steady release of water from a dam or similar structure.

There are a number of specific questions that can be asked concerning the response of an alluvial reach under the conditions stated above. Those considered to be of major importance are listed below. This study is directed at answering those questions in an attempt to clarify a scantily researched and little understood section of sediment transportation mechanics. Answers obtained theoretically and/or experimentally are presented in 6.3. More than one answer may be given to a question as different boundary conditions are discussed. These results form the principal original contribution of this work.

The questions are:

1) Can a quantitative estimate be made of the point of initial motion on a bed of uniform stones?

2) If an equilibrium bedload formula can be found to match experimental data (slopewise) can its magnitude be adjusted correspondingly in a non-arbitrary quantitative manner?

(3) Is there a difference between the nature of the sediment motion under a translation wave and that of a steady flow in the same reach whose discharge is, say, the same as the maximum wave discharge?

* Specifically triangular translation or flood waves. A definition and the basic properties of translation waves are given in Appendix A.1.

** This concept is defined in 3.2.2 1(b)

(4) Can a wave be associated with an equilibrium transport rate?

(5) How is a wave affected by the sediment motion beneath it?

(6) In an alluvial reach are the inflow and outflow water and sediment hydrographs of similar shape?

(7) Do temporal and/or spatial lags, that is, time delays and/or spatial separations occur between constant or changing water and sediment discharges when observed from a fixed point?

(8) Do magnitude lags, that is, differences between the amount of sediment actually being transported and the amount of sediment capable of being transported by a water flow exist?

(9) Can an equilibrium transport formula be used to estimate the sediment discharge of a wave as it passes a fixed point?

(10) Can a wave be replaced by a steady discharge which produces the same yield and how may such a discharge be defined?

(11) If a steady flow equilibrium condition is attained in an alluvial reach and the sediment inflow is then halted, it is known that degradation ensues. What is the extent of this degradation?

(12) Do bedforms appear during the passage of a wave and if so how do they develop and what are their characteristics?

(13) Does the flow resistance change during the passage of a wave?

(14) What do the stage-discharge relations look like and what are the reasons for their assuming a particular shape?

(15) Can a mathematical model, which takes the effects of (12), (13) into account, be used to predict the reach response to given water and sediment inflows?

(16) Can a scale model be used to predict the reach response as in (15) in a natural channel?

CHAPTER 3

THEORETICAL CONSIDERATIONS

3.1 SYNOPSIS

In this section the physical system to be examined in this thesis is defined. From considerations of accepted principles of bedload transportation the qualitative response of the system is predicted for differing initial and boundary conditions. Analytic models are critically reviewed and in one case further developed. A set of experiments, relevant to local field conditions, is designed. The object of these experiments is firstly; to gain further understanding of the mechanics of the transportation process and secondly; to test two major assumptions in the models. A brief treatment of what are regarded as secondary aspects of the system's behaviour occupies the remainder of the chapter.

3.2 PRINCIPLES OF BEDLOAD TRANSPORTATION

3.2.1 Physical System

The physical system can be viewed as a more idealised version of that examined by Einstein [15], that is, a constant width finite length channel of constant initial slope whose bed is composed of uniform non-cohesive gravel-size particles. Water flows, at constant temperature, which may or may not contain bed sediment are introduced at the upstream end. The turbulent boundary layer is fully developed throughout the reach. Specifically, two types of flow will be discussed; steady uniform flows and gradually varied non-steady flows in the form of triangular translation waves.

Such a reach can be considered as a non-linear system*. Of interest is the response of the system to both types of flow in regard to equilibrium

* In the precise sense of system's engineering. Systems theory proves useful in deducing certain aspects of the reach response. See A.4.2.

and non-equilibrium bedload transport conditions. The system itself, together with its component variables, both independent and dependent, is shown diagrammatically in Fig. 1.

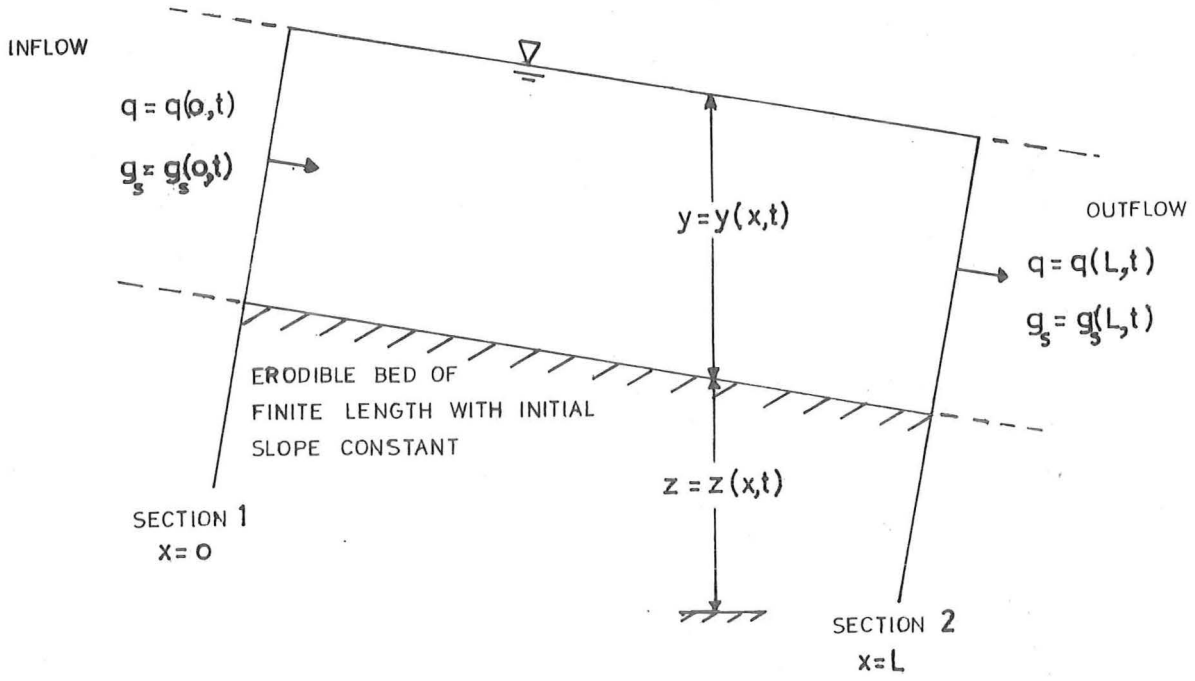

Fig.1 - REACH SYSTEM

Initial and boundary conditions treated are:

Case 1 (Equilibrium Transport)

a) Sediment - constant inflow $g_s(o,t) = \text{constant}$

$g_s(L,t) = \text{constant}$

Water - constant inflow $q(o,t) = \text{constant}$

$q(L,t) = \text{constant}$

b) Sediment - triangular inflow $g_s(o,o) = 0$

$g_s(L,o) = 0$

$g_s(o,o < t < T) = f(t)$

Water - triangular inflow imposed on initial base flow q_o at critical transport conditions*

$q(o,o) = q_o$

$q(L,o) = q_o$

$q(o,o < t < T) = f(t)$

Case 2 (Non-Equilibrium Transport)

a) Sediment - no inflow $g_s(o,t) = 0$

Water - constant inflow $q(o,t) =$ constant

$q(L,t) =$ constant

b) Sediment - no inflow $g_s(o,o) = 0$

$g_s(L,o) = 0$

$g_s(o,t) = 0$

Water - triangular inflow imposed on baseflow q_o at critical transport conditions

$q(o,o) = q_o$

$q(L,o) = q_o$

$q(o,o < t < T) = f(t)$

3.2.2 Equilibrium Transport

Case 1(a) Steady uniform flow.

This case has received extensive treatment, the best known being that of Einstein [15]. He stated that the equilibrium bedload transport rate obtains if, at each section, sediment is transported at a rate equal to the capacity of the flow. For our system this implies

$$g_s = g_s(x,t) = g_{se} = \text{constant} \qquad \ldots (3.1)$$

$$\frac{dg_s}{dt} = 0 \qquad \ldots (3.2)$$

* Steady uniform flow where initial motion conditions pertain on the bed. (See 3.4).

and the yield per unit width in time t is given by

$$\int_t g_s(x,\tau)\Big|_{x = L} d\tau = g_{se} t = G_T \qquad \ldots (3.3)$$

From experimental work Einstein [15]* deduced that the laws of equilibrium transport may be used to describe the bedload transport on a changing bed, provided it is possible to describe the bed and the flow locally during the transition.

The above can be expressed in a single principle, namely, that a relationship exists between the discharge of the bedload and the characteristics of the flow. There is, in addition, another important principle to be stated here. This is the principle of continuity. Relative to our system it implies that the difference between the inflow and outflow of sediment is balanced by a nett gain or loss of sediment within the reach, thus

$$\int_L \left(\frac{\partial g_s}{\partial x} + B \frac{\partial z}{\partial t}\right) dx = 0 \qquad \ldots (3.4)$$

These principles, which Colby [17] calls "the principles of scour and fill" are now applied to the non-steady case.

Case 1(b) Translation Waves.

Consider the introduction of a long translation wave at the upstream end of the test reach. Suppose, since the transport potential of the wave is finite, that each segment of it is transporting bedload to full capacity as it enters the reach. Then, neglecting energy losses, if the wave is routed through the reach the nett result, by the principle of continuity, will be that the inflow and outflow sediment hydrographs

* A comprehensive discussion of this work is given by Shen [16].

will be equal and there will be no change in mean bed level. Alternatively, since it is known that the water hydrographs change little with respect to distance in such conditions (Henderson [18]) it follows that the mean velocity and depth of each segment change little and consequently neither does its transporting capability. This implies the above nett result. But, throughout the wave, that is from segment to segment, the transport capacity and thus the intensity of the bedload transport do vary, being a minimum at the front and tail and a maximum at the wave peak. There is no conflict between the physics of the particle motion in this case and the steady case. An interchange process of varying intensity will exist between the particles of the bed and those in transit. These statements will hold true whether the initial transport conditions are above or below critical and whether the wave length is greater or less than the length of the reach. To an observer travelling with the wave the entire motion will appear to be an equilibrium situation. To a stationary observer it will appear to be a non-steady equilibrium condition. Thus Case 1(b) can be regarded as non-steady equilibrium transport.

There must be limits on the intensity and response of the entrainment - deposition process, for example under shock conditions or very high Froude Numbers where deep bed movement occurs, Hill [19]. However there is no reason to suppose, since material is supplied to the bed in each wave segment and conditions are mildly transient, that there will be lags between the sediment and water discharges temporally, spatially or in relative magnitude. A temporal lag is a time delay between a change in water discharge and a change in sediment discharge.

A spatial lag would exist if the position at which a change in water discharge occurred did not correspond with the position at which the related change in sediment discharge occurred. Temporal and spatial

lags are related herein for a stationary observer at a point. For example a time delay between the arrival of the water peak of a hydrograph and the sediment peak at a point would be associated with a spatial delay. The distinction is made to allow for the case of the moving observer and to enable separate description, should it be required.

A lag in relative magnitude is a difference between the actual bedload discharge at a point and the capacity bedload discharge of the water flow at that point. Such a lag occurs whenever the transport potential of the water flow is not satisfied.

The non-steady equilibrium transport situation may be illustrated mathematically. To a moving observer

$$\int_{\lambda} g_s(x,\tau)\Big|_{t=\tau} dx = G_T \qquad \ldots (3.5)$$

λ = wave length

and to the stationary observer

$$\int_{T} g_s(x,\tau)\Big|_{x=L} d\tau = G_T \qquad \ldots (3.6)$$

Further, to an observer moving with the wave

$$\frac{dg_s}{dt} = \frac{\partial g_s}{\partial x}\left(\frac{dx}{dt}\right)_w + \frac{\partial g_s}{\partial t} = 0 \qquad \ldots (3.7)$$

as in (3.2) where $(dx/dt)_w$ is the moving observer's velocity.

3.2.3 Non-Equilibrium Transport

Case 2(a) Steady uniform flow.

Presume that upstream of section 1 ($x = 0$) the bed is fixed. Then, provided critical transport conditions are exceeded, entrainment will occur where the clear water flow encounters the loose bed. A physical example of this situation is the case where steady flow equilibrium transport conditions obtain (3.2.2 1(a)). At $t = 0$, $x = 0$ the sediment inflow is stopped, say, by removing a sediment inflow hopper positioned here in a flume.

Each segment of the flow will seek to satisfy its transport capacity and a scour hole will develop, its depth being such that critical conditions obtain on the base of the hole. With the stipulation that the reach is infinitely long the length of the scour hole will increase indefinitely. Downstream of the point of transition between the extending excavation and the original bed, equilibrium transport conditions must be present. The reason is that here the transport capacity of the flow is realized.

By continuity the nett amount of material in transport, adjusted for porosity, must equal the volume of the scour hole.

Thus

$$B \int_{L_s} (z_o - z)(x,\tau) \Big|_{t=\tau} dx = g_s t = G_T \qquad \ldots (3.8)$$

z_o = original bed level.

Case 2(b) Translation Waves.

The system response here will be similar to that outlined in Case 2(a). Each segment of the wave, upon reaching the movable bed, will begin to entrain sediment. Entrainment will continue until the segment reaches full capacity, the scour hole being deepened and extended.

As the wave is of finite length so will be the degraded region. Continuity of volume must be satisfied, the material in transit downstream of the scour hole being in a state of non-steady equilibrium transport. Consequently after the wave has left the scour hole

$$B \int_{L_s} (z_o - z)(x,\tau)\Big|_{t=\tau} dx = \int_{\lambda} g_s(x,\tau)\Big|_{t=\tau} dx = G_T \qquad \ldots (3.9)$$

Eqn. (3.9) allows an estimate of the scour hole length L_s to be made; the L.H.S. may be approximated by

$$n_s (Z_f L_s) B \qquad \ldots (3.10)$$

Z_f = limiting depth of scour.

where n_s is a shape factor. The R.H.S. is simply

G_T

thus from (3.10) $$L_s \simeq \frac{G_T}{n_s Z_f B} \qquad \ldots (3.11)$$

and in a flume experiment $\lambda \simeq 0[10^3]$, $G_T \simeq 0[10^3]$, $Z_f \simeq 0[10^{-1}]$

$B \simeq 0[10^4]$, $n_s \simeq [10°]$

which implies that $\frac{L_s}{\lambda} \simeq 0[10^{-3}]$

(The ratio L_s/λ is used in 6.4).

The question of lags presents a more difficult problem in this case of non-equilibrium transport. Two degrees of unsteadiness are involved: non-steady water flow and non-equilibrium transport. These should not cause temporal or spatial lags (3.2.2 1(b)) in the distribution of sediment throughout the waves because at all points as

the transport capacity increases there is sediment available to be entrained. There may however be magnitude differences between the measured transport rates and the transporting capacities. What is unknown here is the bed response to variform water transients.

3.2.4 Composite System Response

The response of the reach, as predicted from the principles of bedload transportation and outlined above, is summarized diagramatically in Fig. 2.

3.3 MODELS

3.3.1 Introduction

The emphasis, in the context of mathematical modelling of two phase flows in an alluvial reach, has been placed on uniform or quasi-uniform steady situations. Albiet, ie as was indicated in 2.2, a start has been made with the non-steady regime.

It is not proposed to present a new mathematical model but to test experimentally the more significant assumptions in the existing one. As some elements of the non-steady model are based on steady state formulae it is pertinent to review these briefly in the light of performance.

3.3.2 Equilibrium Transport

Case 1(a) Steady uniform flow.

A bedload equation is by definition an equation which relates the bedload transport per unit width of bedlayer to the local flow. At best it can predict the capacity of a given flow to transport sediment of a given size. For a reach one hopes to obtain a relationship of the form

$$g_s = f(q) \qquad \text{(sediment rating curve)}$$

STEADY FLOWS

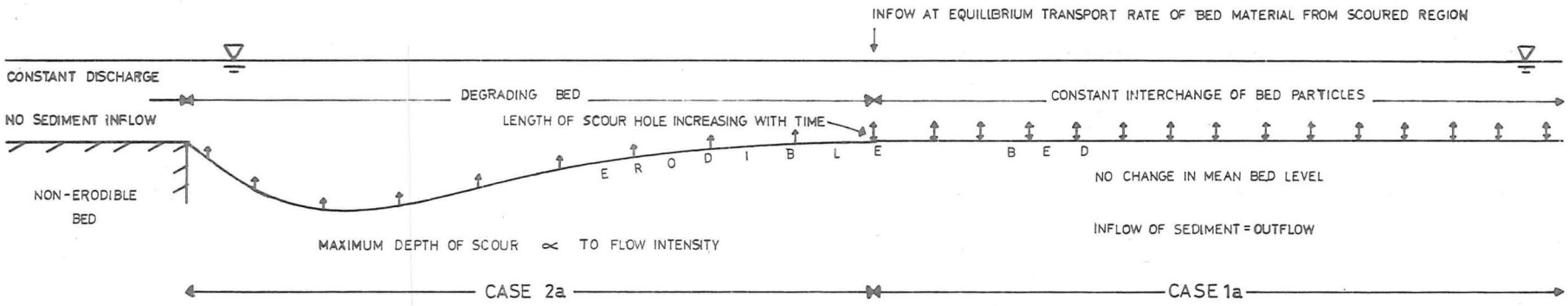

NON-STEADY FLOWS

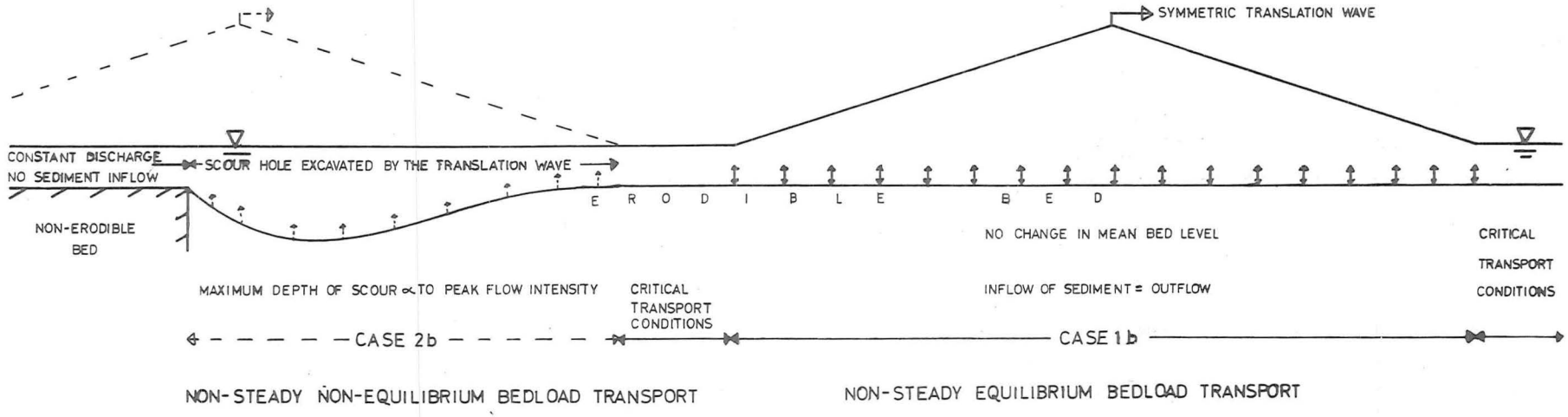

Fig.2 - THEORETICAL COMPOSITE SYSTEM RESPONSE

Explicitly $g_s = a\,q^b$

where often $a = 0[10^1]$, $b = 0[10^0]$ (with SI units)

The performance of equations of this type is generally poor because they are not wholly rational and the majority were developed in laboratory flumes for a narrow range of conditions. White et al [20]* have extensively tested equilibrium bedload formulae with both field and flume data.

Case 1(b) Translation Waves.

(i) Mathematical model.

A problem can be specified from the dynamic viewpoint by the fulfilment of certain universal balance relations, the delineation of constitutive relations that express specific properties of the materials themselves and the satisfaction of appropriate boundary conditions. For our system four balance relations are required, namely, momentum and mass balance for both fluid and sediment. All of these expressions are available except for sediment momentum. In the absence of such, a formula of the type described in 3.3.2 1(a) is used. This, in addition to the abovementioned first order, quasi-linear, hyperbolic partial differential equations can be written, for the idealised reach as

Fluid: $$\frac{\partial u}{\partial t} + u\frac{\partial u}{\partial x} + g\frac{\partial y}{\partial x} = g(S_o - S_f) \qquad \ldots (3.12)$$

$$\frac{\partial y}{\partial t} + u\frac{\partial y}{\partial x} + y\frac{\partial u}{\partial x} = 0 \qquad \ldots (3.13)$$

Sediment: $$\frac{\partial g_s}{\partial x} + B\frac{\partial z}{\partial t} = 0 \qquad \ldots (3.14)$$

$$g_s = a\,q^b \qquad \ldots (3.15)$$

where S_o = bedslope $= -\frac{\partial z}{\partial x}$, B = bulk specific dry weight of sediment in the bed.

* This work is used in D.2.

$S_f = \frac{u^2}{C^2 y}$, where the Chezy expression is used.

Appropriate initial and boundary conditions have been detailed in 3.2.1 1(b).

If sediment motion is not considered the St. Venant Equations (3.12), (3.13), apply. Numerical solutions of these have proved highly successful in the prediction of flume and natural channel transient flows. (Gunaratnam and Perkins [21]). The basic questions remain. How well do equations 3.14 and 3.15 represent the sediment motion and what effect does this motion have on the fluid behaviour? An answer to the former part will depend on the validity of two assumptions. Firstly the description of the friction slope by a steady state equation and secondly, the estimation of the bedload transport by an equilibrium transport formula. The assumptions can only be tested by experimental investigation. Such an investigation is described later herein. This may also indicate whether simplifications in general and those made in certain cases (Henderson [22]) in the St. Venant Equations are applicable. As to the effect of sediment motion on fluid behaviour how much clarification will be gained is not clear as the translation wave length must be substantially longer than the test reach if fluid conditions are to be simulated*. Nonetheless the general effect can be determined by the application of linear systems theory. Full details have been worked out in A.4 but the essence is that after linearization the equations 3.12 to 3.15 can be combined into the single linear partial differential equation

$$\left[gy_o\left(1 + \frac{baq_o^{b-1}}{B}\right) - u_o^2\right]\frac{\partial^2 q}{\partial x^2} - 2u_o\frac{\partial^2 q}{\partial x \partial t} - \frac{\partial^2 q}{\partial t^2} - 3gS_o\frac{\partial q}{\partial x} - \frac{2gS_o}{u_o}\frac{\partial q}{\partial t} = 0 \qquad \ldots(3.16)$$

where subscripted variables are reference variables.

* Details in 3.3.4.

The impulse response of Eq. 3.16 (A.4.2) reveals that the general effect of the bedload motion on the dynamic wave behaviour is negligible. It tends to increase the diffusion or spread of the transient and decrease the speed of the front part of the wave.

When bedforms develop the resistance coefficient is substantially increased. Consequently the wave velocity is reduced and subsidence, which cannot be predicted by linear theory, is enhanced in the crest region of non-kinematic waves. (A.4.2.)

(ii) Experimental Model.

The object of the experimental model is principally,to compare both steady flow experimental values and those predicted by steady flow equilibrium transport formulae, with instantaneous bedload transport rate measurements obtained when a translation wave traverses the same test reach. That is to say, the translation wave is to be treated as a finite series of steady discharges which, as far as possible, reproduce the conditions of the wave itself.

In regard to the fluid flow the degree of approximation involved in this comparison process can be estimated.

Consider the momentum equation for the non-steady water phase

$$\frac{\partial u}{\partial t} + u\frac{\partial u}{\partial x} + g\frac{\partial y}{\partial x} = g\left(-\frac{\partial z}{\partial x} - \frac{u^2}{C^2 y}\right)$$

This equation may be rewritten as

$$S_a + S_e + S_f = 0$$

where S_a = acceleration slope $= \frac{1}{g}\frac{\partial u}{\partial t}$

S_e = energy slope $= +\frac{\partial z}{\partial x} + \frac{\partial y}{\partial x} + \frac{u}{g}\frac{\partial u}{\partial x}$

S_f = friction slope $= \frac{u^2}{C^2 y}$

and for steady uniform flows

$$S_o = S_f \Rightarrow -\frac{\partial z}{\partial x} = \frac{u^2}{C^2 y}$$

If the bed slope S_o is held constant for both steady and non-steady experiments then differences arising from the varying water motion will be due to the influence of the convective and spatial acceleration terms and the wave slope. In fact the contribution of these elements in this and other steep slope applications is an order of magnitude less than that of S_o. (Gunaratnam and Perkins [21]). Thus the degree of approximation in the fluid flow comparison is small. The remaining term is the friction slope which is intimately connected with the alluvial bed behaviour. Therefore deviations between the compared steady and the non-steady transport rates will largely be due to bed response effects. This is the reason why the model has been designed as below.

Details of the practical aspects are as follows:

A set of equilibrium transport experiments will be performed with identical bed slopes for, on the one hand, a triangular translation wave and, on the other, a series of constant water discharges ranging in magnitude up to the peak flow of the wave. In both cases the criteria of equilibrium will be when inflow sediment rates match outflow rates and no change occurs in the mean bed level. A trial and error process is involved owing to the bedslope restriction.

The mechanics of the comparison procedure to be carried out using the experimental data is given below and illustrated in Fig. 3(a).

At any time t_H during the passage of a wave the relevant system variables, that is, the water discharge q, the sediment discharge g_s, the mean stage y_s, the bedslope S_o, and the mean bed level z will have specific known values.

In the non-steady case, (right hand column of Fig. 3(a))

$$t_H \rightarrow \{q(t) \ , \ g_s(t) \ , \ y_s(t)\} \qquad S_o, z \ \text{constant}$$

Now in the steady case the relationships (Fig. 3(a))

$$y_s \quad v \quad q$$

$$g_s \quad v \quad q$$

are known. We can therefore equate the steady and non-steady water surface levels, thus

$$y_s = y_s(t)\Big|_{t = t_H}$$

Then $y_s \ v \ q$ implies q (uniform steady)

and $y_s(t)\Big|_{t = t_H}$ implies $q(t)\Big|_{t = t_H}$ (non-steady)

Two values of q are obtained; one, a uniform flow value and the other; a non-steady flow value. They differ because of the loop rating between $y_s(t)$ and $q_s(t)$. (Dashed line in plot y_s v q (steady), Fig. 3(a)). When these two values of water discharge are applied to the plot

$$g_s \quad v \quad q \quad \text{(steady)}$$

two values of steady sediment discharge are obtained. A mean value should be taken. This is the comparable sediment discharge and we have obtained under comparable conditions the relation

$$g_s \sim g_s(t)\Big|_{t = t_H}$$

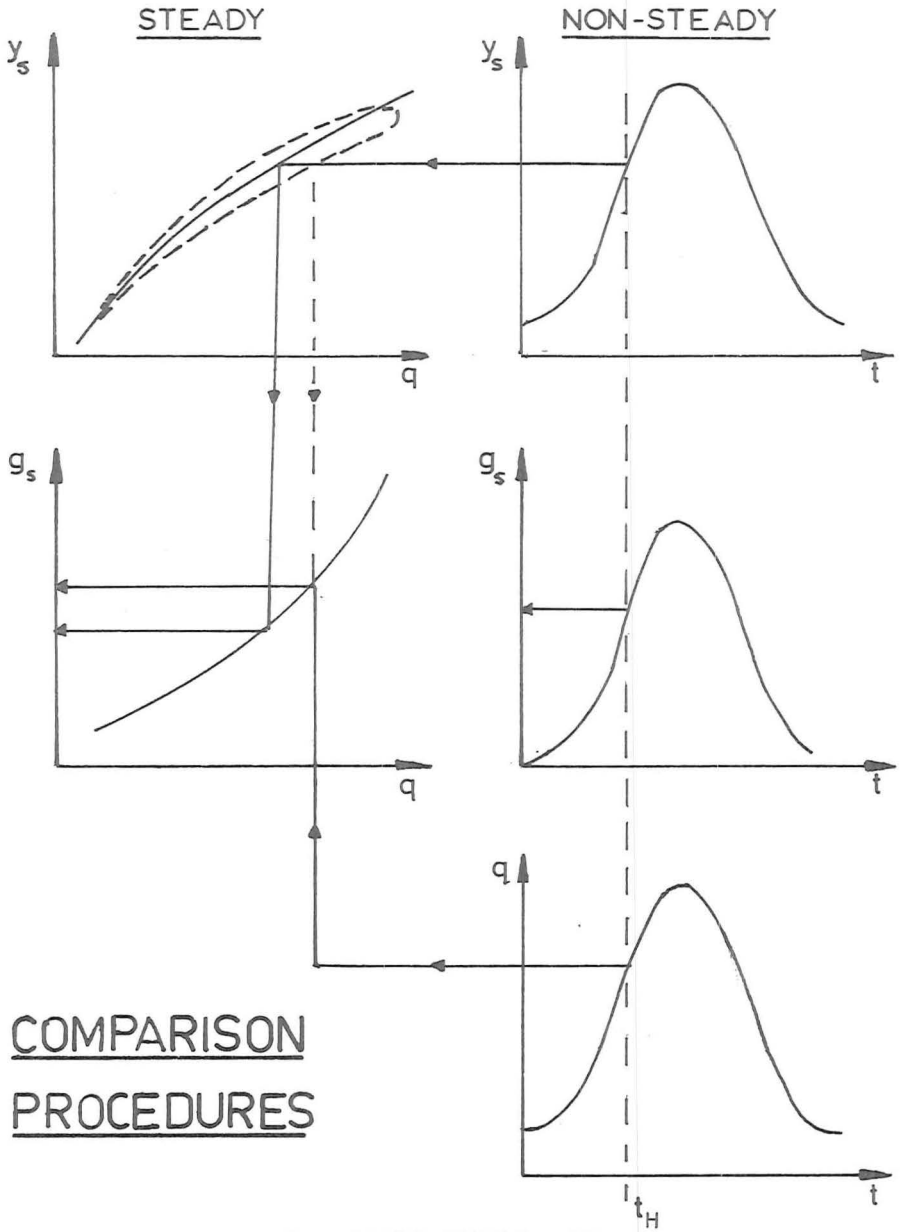

Fig. 3a - EQUILIBRIUM TRANSPORT

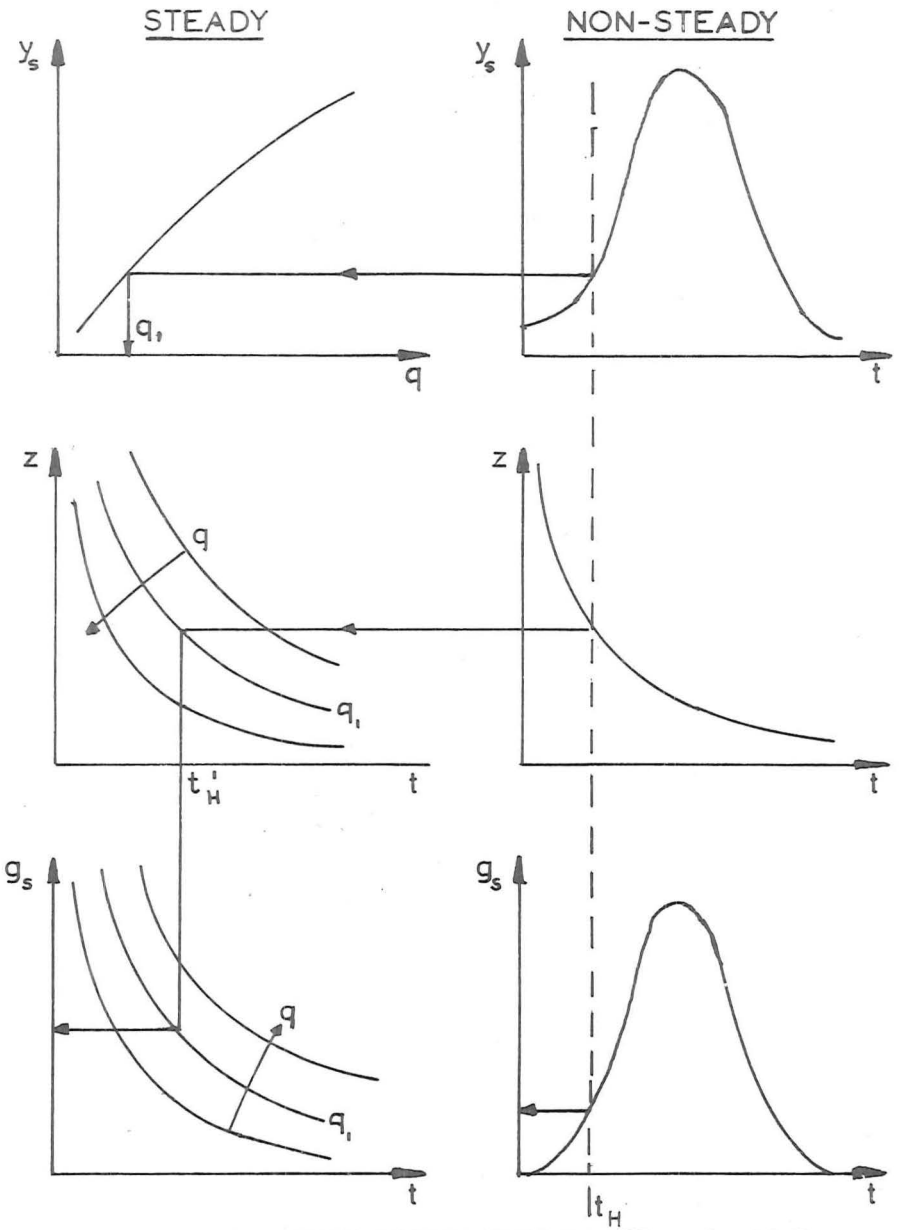

Fig. 3b - NON-EQUILIBRIUM TRANSPORT

A comparable steady state sediment outflow hydrograph can be derived by repeating this procedure for differing values of t_H . This may then be compared with the measured hydrograph to see if differences occur. Comparable conditions can now be defined as occurring when the system parameters, with the exception of the bedload transport rate, approximately correspond.

The operation of the experimental model will also permit observation of the physical processes and will yield data concerning initial motion, bedforms, flow resistance and stage discharge relationships.

3.3.3 Non-Equilibrium Transport

Case 2(a) Steady uniform flow

This case is the channel degradation problem. In previous work interest has centred around estimating the bedlevel behaviour as a function of time. The computational process involves the following steps, (Gessler [6]) in an alluvial reach or flume.

(i) Evaluation of the water surface profile and energy grade line along a given profile.

(ii) Evaluation of the sediment transport along the channel by means of an equilibrium transport formula.

(iii) Application of the sediment continuity equation over segments of the channel in order to find the amount of degradation.

(iv) Determination of the new profile.

From step (iv) one returns to step (i).

Objections to this procedure include the use of an equilibrium transport formula in a degradational situation and the neglect of the material already in transport. This neglect occurs because the time interval between the time steps at which the process (i) to (iv) is carried out is short (e.g. 1 minute). Sediment transported in one

step may not have left the reach before a new value is computed. Consequently the transporting capacity for the new step will be reduced. The general effect of the two objections is an overestimation of the depth of degradation. Field applications reported by Komura and Simmons [23] show such a consequence. The contribution of the above objections to their observations is uncertain because of the presence of such factors as bank erosion, meandering and vegetation. Tinney [24] used a similar technique, to that outlined, to predict the experimental results of Newton [25]. However the mentioned problems were circumvented by adjusting coefficients in order to fit the measured bedloads. A non-steady transport equation is required to clear the matter up.

Case 2(b) Translation Waves

(i) Mathematical Model

Analytically the only difference between this case and that of equilibrium transport by translation waves is in the upstream boundary condition for the sediment. Here the inflow is zero. The same criticisms apply (3.3.2.1(b)(i)) but in a more severe sense because the situation is a non-equilibrium one.

(ii) Experimental Model

This is as before (3.3.2.1(b)(ii)) except that no sediment will be added to the flows at the upstream section and degradation will ensue.

The mechanics of the comparison process to be carried out using the experimental data is given below and illustrated in Fig. 3(b).

At any time t_H during the passage of a wave the relevant system variables, as defined in the equilibrium transport comparison procedure 3.3.2.1(b)(ii), q , z , y_s , g_s will have specific known mean values.

In the non-steady case;

$$t_H \rightarrow \{ q(t) , z(t) , y_s(t) , g_s(t) \}$$

Now in the steady case the relationships (Fig. 3(b))

$$y_s \quad v \quad q$$

$$z \quad v \quad q , t$$

$$g_s \quad v \quad q , t$$

are known. We can therefore equate the non-steady and steady water surface levels, thus

$$y_s = y_s(t)\Big|_{t = t_H}$$

For this value of y_s the relation y_s v q yields a value, say, q_1. The mean bed levels may also be equated, thus

$$z = z(t)\Big|_{t = t_H}$$

which from $z \quad v \quad q , t$ where $q = q_1$

gives a time value $t = t'_H$.

The comparable steady water discharge q_1 and t'_H can be used in the plot

$$g_s \quad v \quad q , t$$

to obtain the comparable steady bedload discharge g_s (steady). We have therefore obtained under comparable conditions the relation

$$g_s \sim g_s(t)\Big|_{t = t_H}$$

A comparable steady bedload discharge could also be found using $q(t)\Big|_{t = t_H}$ instead of q_1. A slightly different value would result and a mean could be taken.

Repetition of this procedure for different values of t_H allows a comparable steady state sediment outflow hydrograph to be derived. This can then be compared with the measured hydrograph to see if differences occur.

3.3.4 Scaling

In many New Zealand rivers the slope is steep, the bed, comprised of coarse alluvium, is wide and the flow in the central section is approximately two dimensional. It is not intended in this project to model a particular river although the same type of fluid and sediment is to be used in the experiments. Rather, the aim is merely to have the wave characteristics and basic system parameters covering and extending the upper range* of those observed in the field.

To achieve this it is necessary to determine the relevant scaling relationships.

Following Yalin [26] we assume that two phase motion due to a translation wave moving over a mobile bed is completely determined by the following characteristic parameters

$$u_* \ , \ T \ , \ y \ , \ \rho \ , \ \mu \ , \ \rho_s \ , \ \gamma_s \ , \ D$$

Application of the Buckingham π Theorem yields the dimensionless variables

* Particularly in regard to wave steepness.

$$X_1 = \frac{u_* D}{\nu} \qquad \nu = \mu/\rho$$

$$Y = \frac{\rho u_*^2}{\gamma_s D}$$

$$X_2 = \frac{\rho_s}{\rho} \qquad \ldots \quad (3.17)$$

$$X_3 = \frac{y}{D}$$

$$X_4 = \frac{u_* T}{y}$$

Since the model is geometrically similar, the grain Reynolds No. (X_1) is large (as the flow is rough turbulent) and the same materials are used, X_1 and X_2 may be ignored. Dynamic similarity is then given by

$$\lambda_Y = 1 , \quad \lambda_{X_3} = 1 , \quad \lambda_{X_4} = 1 \qquad \ldots \quad (3.18)$$

provided (Yalin [26]p.113)

$$\lambda_\ell > \simeq \left[\frac{70}{\frac{u_* k_s}{\nu}} \right]^{2/3} \qquad \ldots \quad (3.19)$$

where λ = scale , $k_s \simeq D$ and λ_ℓ = length scale.

The scale relationships between model and prototype obtained from λ_Y , λ_{X_3} , λ_{X_4} are

$$\lambda_{u_*} = \sqrt{\lambda_\ell}$$

$$\lambda_T = \sqrt{\lambda_\ell} \qquad \ldots \quad (3.20)$$

$$\lambda_D = \lambda_y = \lambda_\ell$$

where $\lambda_\rho = \lambda_{\gamma_s} = 1$

Identical equations have been obtained by a different method in Appendix A.3 because the dimensionless variables X , Y , X_2 , X_3 , X_4 are not unique.

For a typical New Zealand river $X_1 = \frac{u_* D}{\nu} \simeq 2 \times 10^4$ and thus condition (3.19) gives a minimum scale of $\frac{1}{40}$. A convenient model sediment has a grain size D_m of 4 mm and the prototype size $D_p \simeq 100$ mm (D_{90}).

Hence $$\lambda_\ell = \lambda_D = \frac{D_m}{D_p} = {}^1/_{25}$$

immediately from (3.20) $\lambda_T = {}^1/_5$

$$\lambda_{u_*} = \lambda_u = {}^1/_5$$

The most important aspect of the modelling problem is the rate of rise of the waves. In a very fast rising natural flood this may be 0.5 m/hr which corresponds to a model value of 0.1 m/hr. As non-steady transport effects will be more apparent under severe conditions a range from say 0.8 → 0.1 m/hr should be considered.

For steady subcritical flows the model roughness (a function of the sediment size), the flume dimensions and the available water discharge indicate a convenient bedslope. This bedslope and the sediment size dictate critical transport conditions - the initial condition for the non-steady flows (3.2.1). Consequently the stage-discharge relation is defined above the initial condition and this, together with the chosen rates of rise, prescribe the wave parameters.

Table 1 lists the order of relevant parameters of model and prototype. The range indicated is to be used in the experiments.

Parameter	Natural River (Very fast rising flood)	Experimental Model
Rate of Rise	0.5 m/hr	0.8 - 0.1 m/hr.
Ratio of Bedslope to waveslope	15	13 - 90
Ratio of wavelength to reach length	180	130 - 480
Ratio of wave velocity to uniform flow velocity	1.5	1.5

TABLE 1. Order of Model and Prototype Parameters.

3.4 INITIAL MOTION

3.4.1 Introduction

The classic work on the initial movement of grains from a cohesionless sediment bed was carried out by Shields [27]. He showed that the process was governed by the dimensionless relationship

$$\frac{\tau_o}{\gamma_s D} = f\left(\frac{u_* D}{\nu}\right)$$

or $$Y = f(X_1)$$

where Y = entrainment function

X_1 = particle Reynolds No.

Later writers, including Paintal [28], Vanoni et al [29], have noted that Shields' limiting value of the entrainment function for the fully rough turbulent zone pertains to a low but measurable rate of transport.

Critical conditions have been defined in various ways both qualitatively and quantitatively. (D.1.) In fact, experimentally, it is not possible to observe the real beginning of movement but only a certain degree of established movement. For this reason there is considerable scatter in the estimates of critical conditions. In these circumstances what appears to be needed is an arbitrary definition relating to whatever degree of movement is acceptable. This degree may vary from situation to situation.

3.4.2 Definition of the Beginning of Movement

Neill and Yalin [30] have met this requirement with the introduction of a new parameter n, which is the number of grains displaced per unit area per unit time. It is easily shown that the following dimensionless relationship obtains

$$\frac{nD^3}{u_*} = f\left(\frac{u_* D}{\nu} , \frac{\varrho u_*^2}{\gamma_s D}\right) \qquad \ldots \quad (3.21)$$

or $N = f(X_1 , Y)$

where N = dimensionless erosion rate.

The suggested criterion is $N = 1 \times 10^{-6}$.

Unfortunately only the probable form of this expression has been given, (Neill [31], in the case where X_1 is not significantly affected by Y, that is, for $X_1 > 70$ (rough turbulent conditions pertain at the bed). In this thesis the initial condition for non-steady flows, that is, the base flow on which the waves are superimposed, corresponds to critical conditions. An experimental plot* of the relationship $N = f(X_1 Y)$ can therefore be obtained. Furthermore the N value corresponding to criteria proposed by early writers for critical conditions can be found thus establishing relativity between the criteria for one value of D.

* Necessarily in the form $N = f(Y)$ since $D_{50} = 4$ mm in the experiments and thus $X_1 > 70$.

Clearly, further work is needed to test the usefulness of Neill's quantitative definition but the results to be presented herein are a useful start.

3.5 BEDFORMS AND FLOW RESISTANCE

3.5.1 Introduction

Researchers have had some success in describing empirically the relationships between bedform types and the gross parameters concerning the flow in rivers, canals and flumes. However the subject is not fully understood in regard to the mechanism of bedform development or the derivation of a resistance formula. The flow conditions to be studied herein belong to the lower flow regime of Simons and Richardson [32]. According to the predictor diagram of Znamenskaya [33] the bedform type to be expected is dunes - ripples do not form if the bed material size exceeds 0.6 mm (Simons and Richardson [34]).

3.5.2 Implications for this Study

Gee [35] examined bedform response in non-steady flows by forcing a transition of bedforms between two discrete equilibrium states. His principal conclusions, which strictly apply to sand size sediment, were that the sequence of bedforms associated with increasing or decreasing discharge was the same as observers have found using fixed depth techniques; that dune generation proceeded at greater efficiency than dune destruction, and that the bedload transport changes the bedform dimensions. Jensen [36] deserves mention as the only other known writer on this subject but the relevance of his results is questionable as he used polystyrene balls as his sediment.

The pertinence of Gee's [35] results in this context is that if dunes do appear and attain different development from that in corresponding steady flows then loops will be produced in the depth-discharge curves.

Furthermore, irrespective of how the flow resistance is assessed, whether by using the shear stress or the friction factor*, the resistance must be overestimated on the rising and underestimated on the falling stage.

3.6 STAGE-DISCHARGE RELATIONS

3.6.1 Introduction

The stage-discharge relation in natural channels is not necessarily single valued. Simons and Richardson [37] state that shifts in rating and hysteresis effects may occur due to scour and fill of the bed and banks, changes in energy gradeline slope and changes in resistance to flow resulting from changes in bed configuration.

Many predictors have been developed for these relations in alluvial channels (ASCE [38]) but of the techniques proposed most have inadequate reliability and scope.

Where large floods are concerned it appears necessary (Simons et al [39]) to rout both water and sediment discharge through the reach under study in the manner, for example, of Santos-Cayade and Simons [40]. Here, the water routing model estimates the flow depths for each discharge and the sediment rating model determines the bed elevation; the stage being the sum of the two.

3.6.2 Implications for this Study

Simons et al [41] explored the variation in the depth-discharge relation resulting from changes in bed configuration for a hydrograph routed through a flume. The hydrograph was achieved by step changes in discharge. In the lower flow regime the bed roughness began as dunes (baseflow condition) then shifted to plane bed. On the falling stage the plane bed persisted at lower depths and discharges illustrating the hysteresis effect. These experiments were performed with a sand bed;

* It is presumed that grain and form resistance are accounted for in both cases.

what the situation might be with steep waves and coarse alluvium is a partial object of this project.

Generally speaking the effect of scour and fill on the stage discharge relation may be eliminated by using a depth-discharge relation. Loops in the rating will therefore be due to changing resistance and dynamic effects of the wave motion. The latter have been estimated theoretically by Henderson [22]. He points out that there cannot be a unique stage-discharge relationship unless the flow is uniform; the reason being that during the progress of a translation wave the influence of slope terms other than the bedslope S_o prescribe that the discharge is not a function of depth alone.

If Q_o is the discharge as given by the uniform flow rating curve, that is,

$$Q_o = B_c C y \sqrt{y S_o}$$

B_c = channel width

then over the crest of the wave the equation

$$\frac{Q}{Q_o} = \left[1 + \frac{2}{3r^2} + \frac{5Fr^2}{6r^2} + \frac{1}{S_o c} \frac{\partial y}{\partial t} \left(1 - \frac{Fr^2}{4} \right) \right]^{1/2} \quad \ldots \quad (3.22)$$

is applicable; on the flanks

$$\frac{Q}{Q_o} = \left[1 + \frac{Fr^2}{2r^2} + \frac{1}{S_o c} \frac{\partial y}{\partial t} \left(1 - \frac{Fr^2}{4} \right) \right]^{1/2} \quad \ldots \quad (3.23)$$

where $r = S_o/S_w$ (bedslope/wave slope)

c = wave velocity

holds approximately. Values of the parameters in these equations for the most severe rate of rise to be treated herein are:

$r \simeq 14$, $c \simeq 1.5$ m/sec , $Fr^2 \simeq 0.33$, $\frac{\partial y}{\partial t} \simeq 2.3 \times 10^{-4}$ m/sec.

$S_o \simeq 0.002$, crest/flank division at $\pm 2y/S_o$ measured from the crest.

Substitution of these into the above equation yields

$$Q/Q_o \simeq 1.04 \quad \text{over the crest}$$

and

$$Q/Q_o \simeq 1.03 \quad \text{on the flanks.}$$

Thus the effect of the additional terms in

$$Q = B_c C y \left[y \left(S_o - \frac{\partial y}{\partial x} - \frac{u}{g} \frac{\partial u}{\partial x} - \frac{1}{g} \frac{\partial u}{\partial t} \right) \right]^{1/2} \qquad \ldots \quad (3.24)$$

is small as might be expected when the wave is kinematic in nature and is generated at the upstream end of the flume.
Therefore loops in the rating curves will be due mainly to changing resistance.

3.7 SUMMARY

It has been shown that the composite system response, for equilibrium and non-equilibrium transport conditions under both steady and non-steady flows, can be predicted in a general sense from the principles of bedload transportation. The use of steady state transport and resistance formulae is noted in the mathematical model for the non-steady two phase phenomenon. However, these formulae are not expected to cause large errors in the equilibrium transport situation. This comment does not apply to the non-equilibrium case where the system response is by no means clear. The experimental model compares instantaneous translation wave parameters periodically with those of comparable steady flows.
Its design is flexible enough to provide physical insight and data, on initial motion, bedforms and flow resistance, and stage-discharge

relationships. These latter two are intimately connected with each other and with the bedload transport rate.

Theoretical background for these various topics remains limited in scope and precision.

CHAPTER 4

EXPERIMENTAL PROGRAM AND PROCEDURES

4.1 SYNOPSIS

This chapter begins with a note on the objects of the experiments and then describes the program, the layout of the equipment, the procedures and the measurements taken to attain the stated objects. Appendix B contains details of the apparatus. The design of the experiments and the data collection methods are given in Appendix C. Conclusions relating to the general performance of the program and the equipment are presented in Chapter 6.

4.2 INTRODUCTION

4.2.1 Objects of the Experiments

These are; first, to observe and estimate the bedload transport rate at or near critical transport conditions; second, to measure experimental variables for steady and non-steady flows and for both equilibrium and non-equilibrium states so that the comparison procedures of 3.3.2 and 3.3.3 can be carried out; third, to study bedform development and its effect on resistance and on stage discharge relationships.

4.2.2 Experimental Program

Three series of experiments involving 120 runs in two flumes were completed. The nature of the runs and the constant parameters in each series are given below:

SERIES I (6 m flume, $S_o = 0.0044$, $D_{50} = 2.18$ mm)

Part 1 - Initial Motion

Part 2 -

(A) Steady state non-equilibrium transport

(B) Non-steady state non-equilibrium transport.

SERIES II (30 m flume, S_o = 0.0075, D_{50} = 4.02 mm)

Part 1 - Initial Motion

Part 2 -

(A) Steady state non-equilibrium transport

(B) Non-steady state non-equilibrium transport

Part 3 -

(A) Steady state equilibrium transport

(B) Non-steady state equilibrium transport

SERIES III (30 m flume, S_o = 0.002, D_{50} = 4.02 mm)

Part 1 - Initial Motion

Part 2 -

(A) Steady state non-equilibrium transport

(B) Non-steady state non-equilibrium transport

Part 3 -

(A) Steady state equilibrium transport

(B) Non-steady state equilibrium transport

Results and details of Series I have been presented by Sutherland and Griffiths [14]. Sediment sampling and tailgate problems (C.3.2, C.1.1(b)) which arose in Series II necessitated modifications to the apparatus and led to the execution of Series III. Herein conditions pertaining to Series II and III are described.

4.3 GENERAL FORM OF EXPERIMENTS

4.3.1 Design and Layout of Equipment

Experiments in Series II and III were performed in the 30 m tilting flume (B.1) set at a width of 0.305 m. The basic considerations were those of routing steady and non-steady water and sediment discharges through a test reach and of recording inflows and outflows and the system response.

Three different regions existed, namely, the inflow, the test section and the outflow. Of paramount importance in the design of the equipment was the prevention of non-uniformities in both types of discharge entering the test section. The following design elements were chosen;

INFLOW -

(1) a reception area for the piped water supply

(2) a contraction followed by screens and longitudinally placed plates to smooth and align the flow (B.6)

(3) a ramp leading onto a length of fixed rough bed where the turbulent boundary layer could develop (C.1.1(a))

(4) a sediment infeed device (B.2)

TEST SECTION -

(1) a length of loose bed composed of uniform gravel particles to a depth of 15 cm

(2) two partition boards to separate the test reach from the other regions (C.1.2)

OUTFLOW -

(1) a length of fixed bed where backwater effects occur (C.1.1(b))

(2) a sediment measuring device (B.3)

(3) a tailgate or other control at or near the outflow point (B.5)

(4) a settling tank to separate the sediment from the water returning to the laboratory system

4.3.2 Generation of Flow Conditions

A. Water Flow: The general circulation of the water was from a constant head tower via pipes to the flume. After passing through the flume and a series of channels and pits leading to a storage sump, it was then pumped back to the tower. Thus the flume itself was operated in open circuit fashion. Two valve-controlled pipes of different diameters were used for the water delivery. Of these, the smaller (76 mm) provided a baseflow and the larger (152 mm) provided higher steady discharges or, alternatively, by opening and closing the valve at a prescribed rate, non-steady flows. (C.2.1.) At the downstream end of the flume the exit backwater curve was controlled by a tailgate in Series II and a submerged weir in Series III. During non-steady runs the control was raised and lowered proportionally and in synchronisation with the opening and closing of the inlet valve. (C.1.1(b)).

B. Sediment Flow: When required, sediment was added to the water flow from a variable flow hopper, suspended just upstream of the test section by the laboratory crane, at a constant or prescribed rate. (C.3.1.).

In Series II the outflow sediment was sampled by periodic collection in a mesh basket placed adjacent to the downstream side of the tailgate. That sediment which was not trapped passed with the water flow into a settling tank, the water being returned to the system. In Series II all the sediment was collected in a basket suspended in a trap below the bed level at the end of the test section. (C.3.2.)

4.4 MEASUREMENTS AND PROCEDURES

4.4.1 Measurements

The following data were recorded. IIC or IIIC denotes nearly continuous recording (sampling at 30 sec to 60 sec intervals) for

Series II and Series III and IIS, IIIS denote sampling at 5 to 15 min intervals.

A. Steady Flows:

(1) Initial Motion

(i)	Water discharge	IIS, IIIS
(ii)	Sediment discharge	IIS, IIIS
(iii)	Water surface level	IIS, IIIS
(iv)	Bed level	IIS, IIIS
(v)	Water temperature	IIS, IIIS

(2) Equilibrium Transport

(i)	Outflow water discharge	IIS, IIIS
(ii)	Inflow sediment discharge	IIC, IIIC
(iii)	Outflow sediment discharge	IIS, IIIC
(iv)	Water surface level	IIS, IIIS
(v)	Bed level	IIS, IIIS
(vi)	Bed configuration	IIS, IIIS
(vii)	Water temperature	IIS, IIIS

(3) Non-equilibrium Transport

(i)	Outflow water discharge	IIS, IIIS
(ii)	Outflow sediment discharge	IIS, IIIC
(iii)	Water surface level	IIS, IIIS
(iv)	Bed level	IIS, IIIS
(v)	Bed configuration	IIS, IIIS
(vi)	Water temperature	IIS, IIIS

B. Non-steady Flows:

(1) Equilibrium Transport

(i)	Inflow water discharge	IIC, IIIC
(ii)	Inflow sediment discharge	IIC, IIIC
(iii)	Outflow sediment discharge	IIS, IIIC

(iv)	Water surface level	IIC, IIIC
(v)	Bed level	IIS, IIIS
(vi)	Bed configuration	IIS, IIIS
(vii)	Water temperature	IIS, IIIS

(2) Non-equilibrium Transport

(i)	Inflow water discharge	IIC, IIIC
(ii)	Outflow sediment discharge	IIS, IIIC
(iii)	Water surface level	IIC, IIIC
(iv)	Bed level	IIS, IIIS
(v)	Bed configuration	IIS, IIIS
(vi)	Water temperature	IIS, IIIS

Several of these measured variables can be used to compute other variables and parameters useful in evaluating flow and transport characteristics. The computed variables include:

(i) Mean velocity

(ii) Mean depth

(iii) Mean bedlevel

(iv) Water surface slope

(v) Shear velocity or stress

(vi) Kinematic viscosity

(vii) Reynolds number

(viii) Froude number

(ix) Resistance factors

(x) Wave parameters.

During the course of the steady experiments calibration values were derived from the measured variables. These included the inflow water discharge meter reading, the inflow pipe valve setting, the gate setting and the water surface level resistance probes' output. (B.4.) Details of the methods of measurement and computation of the above variables are given

in C1 to C7.

A schematic layout diagram of the apparatus and instrument stations comprises Fig. 4.

4.4.2 Procedures

A. Initial Motion Runs.

Considerable care was taken with the preparation of the bed. Minor irregularities were removed using a blade attached to the movable trolley. (C.4.) The entire test section was levelled in this manner after which the surface was lightly brushed, particular attention being paid to the observation area. (Fig. 4.) Water was then sprayed onto the bed to reduce the chance of grains lifting off due to surface tension. A hose was used to fill the flume, the tailgate being lowered (Series II) or raised (Series III). When the test section was submerged the hose was removed, the gate set, the 76 mm diameter pipe valve opened and the flow rate was gradually built up. Recordings were taken (4.4.1 A(1)) for a period of time which varied according to the rate of movement. Twelve runs were made in each series for water discharges near critical bed conditions.

B. Steady State Runs.

(1) Equilibrium Transport.

As above the bed was relaid and graded between runs. The run began with the setting of critical bed conditions. Then the gate was set approximately and the valve on the 152 mm pipe opened slowly to the required position. Sediment infeed was initiated at a preset rate, final gate adjustments made and recordings begun (4.1.1 A(2)). Two or three attempts were made for each discharge before a satisfactory equilibrium transport value was obtained. The prime requirement of 3.3.2 1(b)(ii) is that the bedslope has to be held constant. This meant that the sediment infeed rate had to be close to the output rate initially,

SERIES II EXPERIMENTS

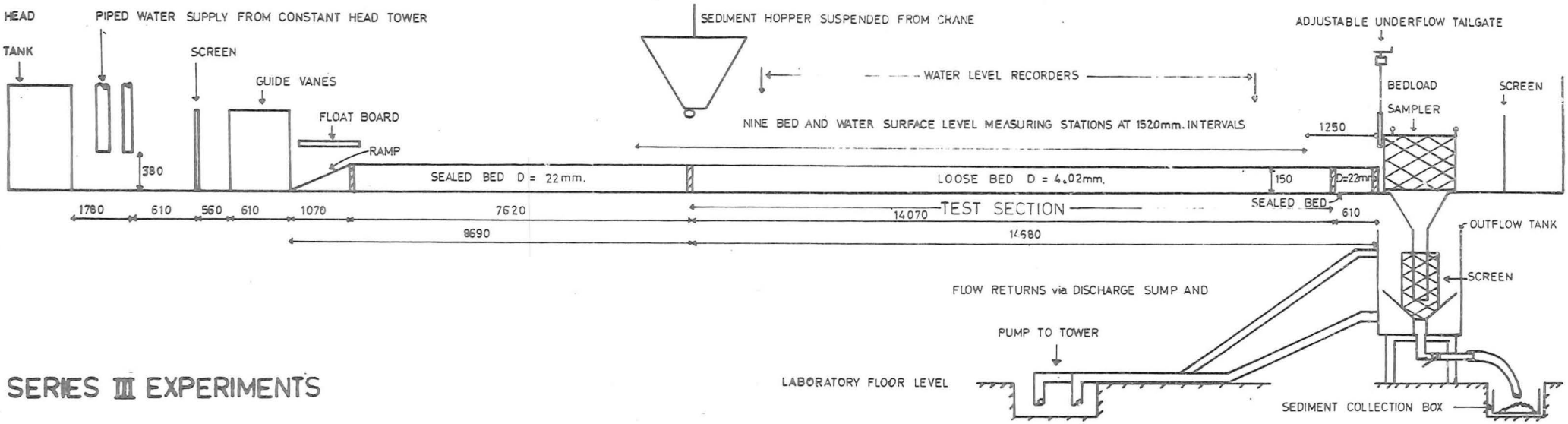

SERIES III EXPERIMENTS

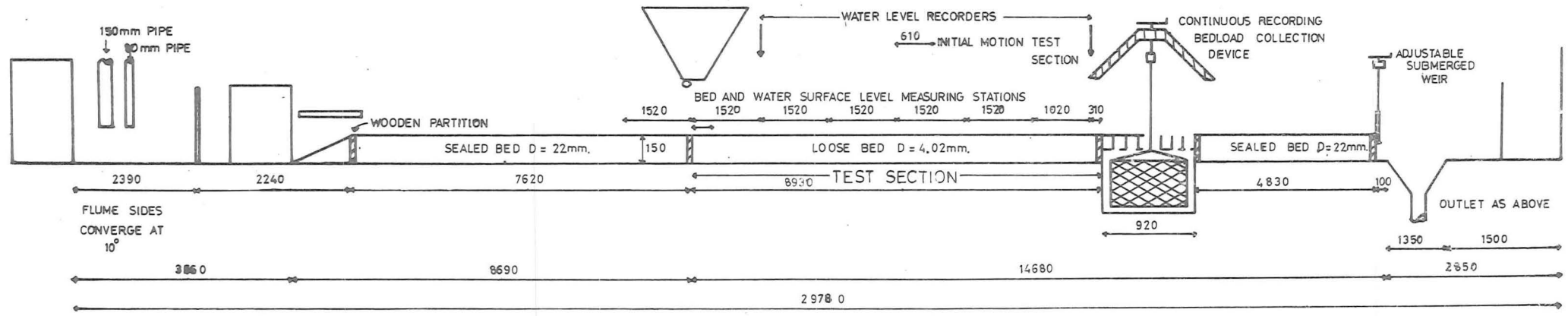

DIMENSIONS IN MILLIMETRES

Fig.4-SCHEMATIC FLUME ARRANGEMENT

otherwise almost irretrievable conditions would develop. That is, the bedslope would alter, local deposition or erosion would occur and a long period of time would be necessary to restore the conditions to those desired. Equilibrium flow was considered as established when the inflow and outflow sediment discharges were nearly equal and no change in the mean bed level occurred, the water surface being parallel to the bed and the bed configuration consistent throughout the reach. Time to stabilisation varied with discharge, the higher discharges taking less. Normally a period of two to three hours was involved as runs were continued longer than required to ensure the achievement of equilibrium conditions. In total some 45 runs were attempted of which about 18 were successful.

(2) Non-equilibrium Transport.

The procedure here was similar to that of section (1) except that no sediment was added to the flow. Recording (4.4.1 A(3)) began as soon as the water discharge was increased from the critical value. As non-equilibrium bed conditions pertained fewer runs were required, 25 being completed each lasting two hours.

C. Non-steady Runs.

(1) Equilibrium Transport.

Six symmetric translation waves of differing period and maximum discharge were selected for routing through the flume in which, initially, a critical transport condition baseflow was established. A translation wave was generated by opening and closing the valve on the larger inlet pipe, the settings, as a function of time, having been prescribed. Nearly simultaneously the downstream gate or weir was raised or lowered a proportional amount, again from predetermined settings. The variable flow rate hopper was operated to produce a sediment hydrograph of similar shape to the water hydrograph. As in section 4.2.2 A(1) several attempts

were made for each wave before success was attained. An equilibrium wave was considered to have been achieved when the inflow and outflow sediment hydrographs were nearly the same and the mean bed level remained unchanged, that is the bed slope remained constant. It is worth noting that the form of the inflow sediment hydrograph was determined, for the first attempt at a particular wave, from the steady state equilibrium transport values (obtained in Section B(1)) corresponding to selected discharges of the inflow water hydrograph. Apparatus was operated and recordings (4.4.1 B(1)) began as soon as the regulating valve started to open. Twenty runs of maximum duration 2 hrs were completed.

(2) Non-equilibrium Transport.

Similar procedures were used to that of Section 4.4.2 C(1) except for the sediment inflow which was zero in this case. As before waves were superimposed on an initial critical transport baseflow condition, the same inflow hydrographs being routed. Recordings taken were as in (4.4.1 B(2)) and fifteen runs were completed.

Plates (1, 2) show the deployment of the apparatus and operators during the course of a Series III non-steady equilibrium transport experiment.

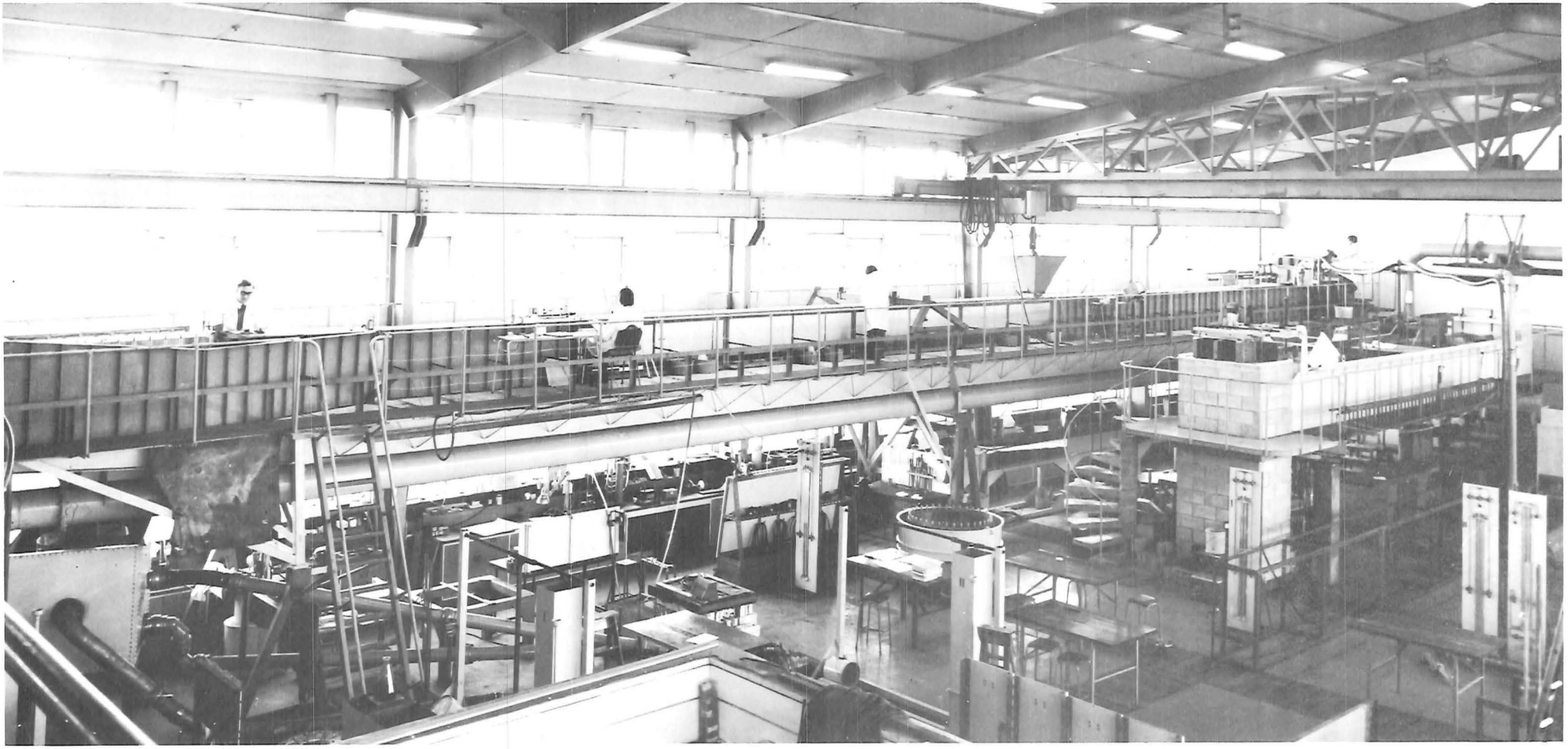

Plate 1 – GENERAL VIEW OF FLUME DURING A SERIES III NON-STEADY EQUILIBRIUM TRANSPORT EXPERIMENT

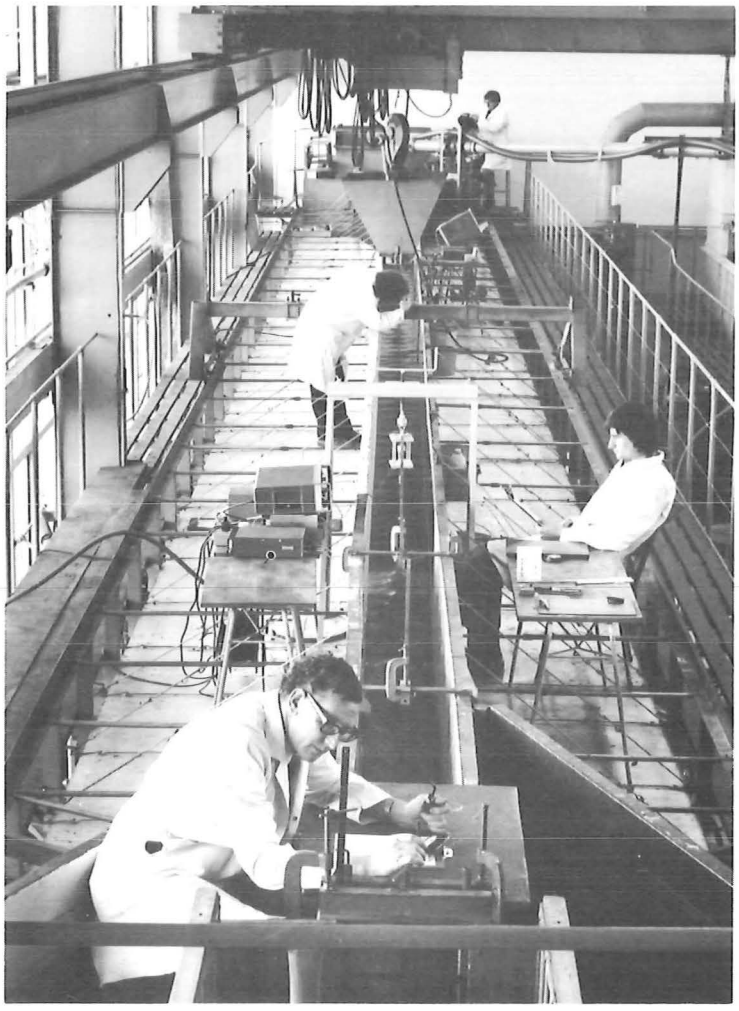

Plate 2– VIEWS FROM DOWNSTREAM OF FLUME DURING A SERIES III NON–STEADY EQUILIBRIUM TRANSPORT EXPERIMENT

CHAPTER 5

PRESENTATION AND DISCUSSION OF EXPERIMENTAL RESULTS

5.1 SYNOPSIS

This chapter is divided into four parts, each part describing a separate phase of the experimental program. For reasons given in Chapter 6 the majority of the results presented are from the Series III experiments. Criteria, formulae and background data are listed in Appendices D and E.

5.2 INITIAL MOTION

5.2.1 Observations of Grain Movement

The initial movement of grains was impulsive in nature and little warning of impending motion was given although in some cases the grains made small wobbling movements prior to an excursion. Strong turbulent bursts near the bed often precipitated the movement of three or four particles. Step lengths varied from a single overturning motion to a series of hops or a continuous rolling motion out of the test section. The penetration distances of the particles into the flow were no more than two or three diameters. At lower values of bed shear stress there were periods when no movement occurred. Presumably at these flows the turbulence intensity was less and there were fewer bursts of sufficient strength to move grains.

5.2.2 Beginning of Movement

Fig. 5 is a plot of the dimensionless erosion rate N, versus Shields entrainment function, Y. It is of the nature suggested by Neill [31] and can be described by the equation

$$\frac{nD^3}{u_*} = 1.15 \times 10^5 \left(\frac{\rho u_*^2}{\gamma_s D}\right)^{8.2} \qquad \text{where } \frac{u_* d}{\nu} > 70$$

There are several points of interest; first, for uniform grains it is practical to use an arbitrary value of N as an initial motion criterion; second, the actual number of grains moving per unit bed area per unit time can be easily calculated; third, the commonly quoted value of $Y = 0.06$ corresponds to $N \simeq 1 \times 10^{-5}$ as Neill and Yalin [30] predicted. Also plotted are several objective criteria put forward by various authors (D.(1)). It can be seen that the $N = 1 \times 10^{-6}$ criterion is reasonable and is associated, for these experiments, with a rate of 40 grains/m^2/min which is a very small amount of movement indeed. ($Y = 0.056 \simeq 270$ grains/m^2/min). If further tests yield similar results then it will be possible to design a bed of quasi-uniform stones where the actual amount of movement likely to occur can be prescribed quantitatively.

5.3 BEDLOAD TRANSPORT

5.3.1 Equilibrium Transport

A. Steady Flows.

(i) Nature of Bedload Motion.

The bed particles moved by hopping, sliding and rolling, the last being the prevalent type of motion. Step lengths varied, some stones made a single movement and others a number of consecutive movements with short intermediate rest periods. One case was observed of a particle at the upper end of the test section which, once entrained, passed out of the flume in one continual movement. The penetration distances of the particles into the flow were no more than two or three diameters and saltation was not observed. Coloured stones were placed on the bed both before and during experimental runs. Most were eroded, but travelled only a short distance thus supporting similar experiments by Einstein [15].

(ii) Amount of Bedload Transport.

Ten runs were completed for a range of water discharges (E.2). Fig. 6(a) includes the results of the experiments and the

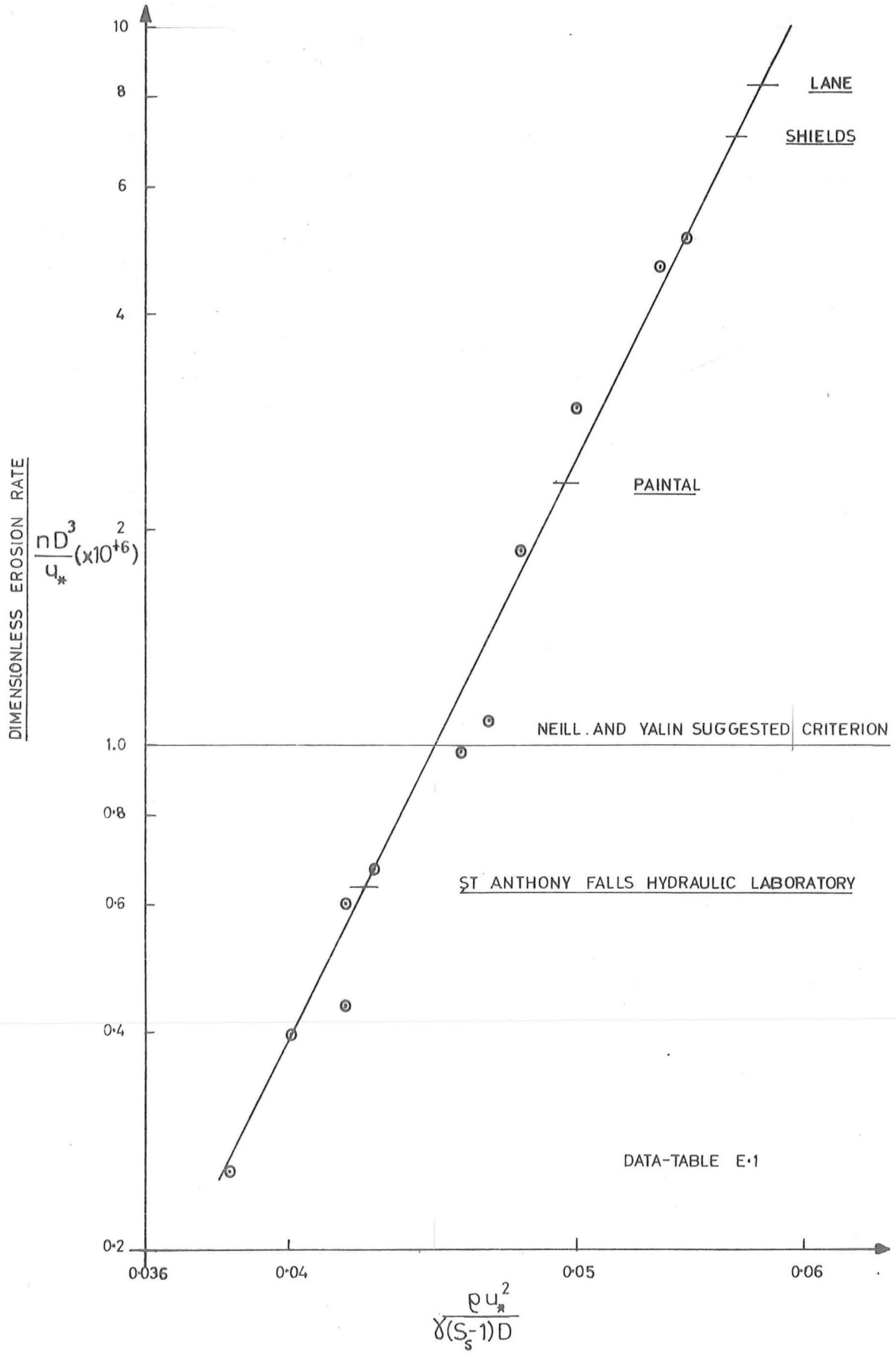

Fig. 5 – RELATIONSHIP BETWEEN DIMENSIONLESS EROSION RATE AND SHIELDS ENTRAINMENT FUNCTION

predicted values of various equilibrium bedload transport formulae (D.2). The performance of these is, as a rule, poor for reasons already given (3.3.2).

An equation of the form

$$g_s = a\, q^b \qquad g_s \ (N/s/m)$$

where $a = 7.75$, $b = 2.6$ $\qquad q \ (m^3/s/m)$

approximates the results. The best general agreement with the data (Fig. 6(a)) is given by the Einstein Bedload Function and the closest slope match by the Einstein-Brown (E-B) formula. If this latter formula was adjusted magnitude wise, that is an adjustment in the value of the constant "a", excellent agreement with the flume data would be obtained. A method of adjustment based on physical reasoning, as opposed to an arbitrary shift of the Einstein-Brown rating (Fig. 6(a)), is given below. The method relies on the fact that the E - B rating must satisfy known initial motion transport conditions. This fact is used later in determining the sediment discharge rating on a non-rated reach where initial motion conditions can be calculated.

Both bedload formulae and alluvial channel data - plotted as sediment rating relationships - show an increase in slope as critical transport conditions are approached. The reason is that $g_s \to 0$ at finite values of q . Consequently an assumption in the method is that the formula ratings may be approximated by two or more straight lines.

Fig. 6(b) illustrates the magnitude adjustment technique applied to the flume data and the E - B rating of Fig. 6(a).

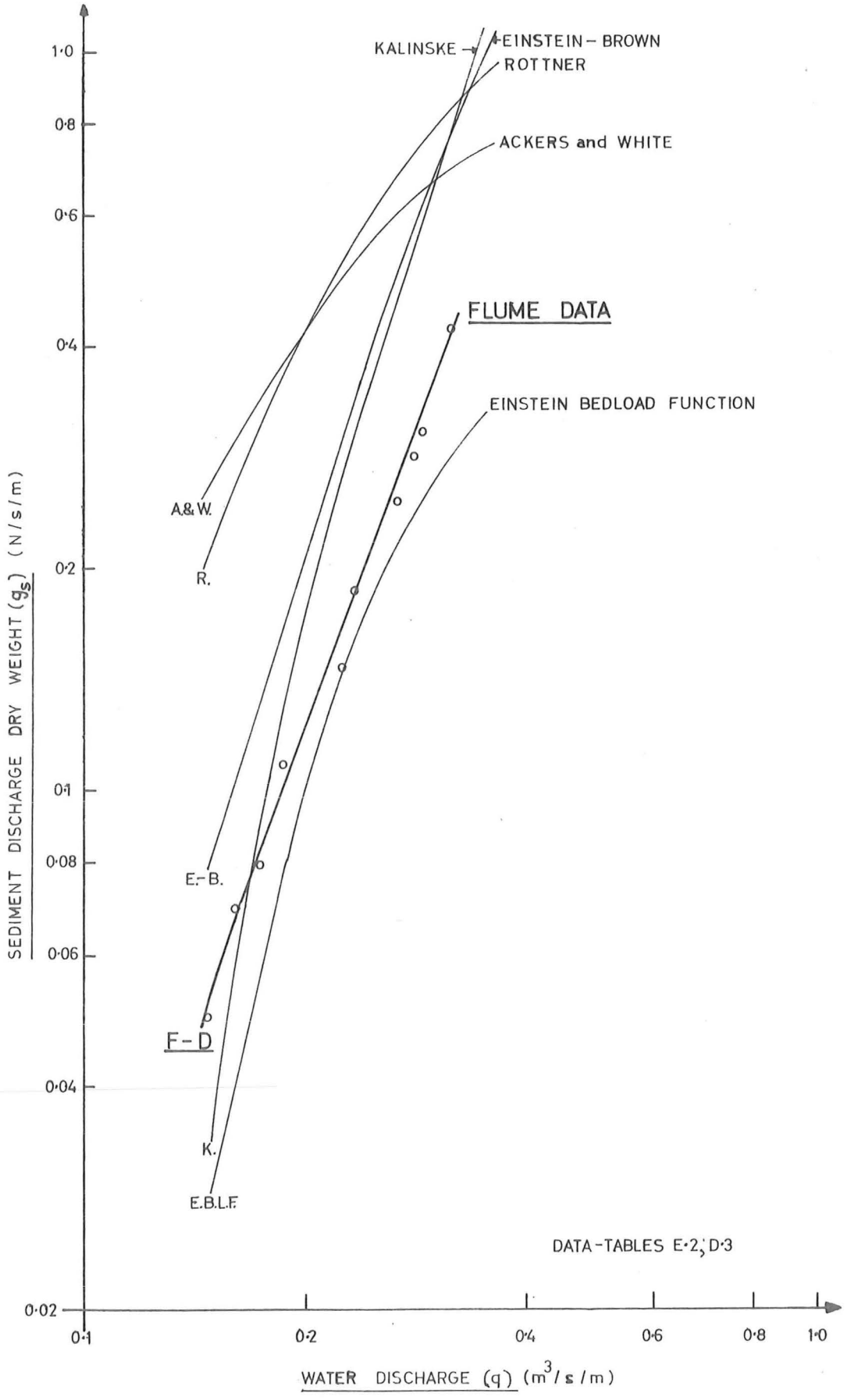

Fig. 6a– CALCULATED AND MEASURED STEADY EQUILIBRIUM TRANSPORT RATING CURVES

Listed stepwise the method is:

Step (1) : From the experimentally determined dimensionless erosion rate versus Shields' entrainment function relation (N v Y)(Fig. 5) choose values of N and note the corresponding values of Y . (The N v Y relation is used because it is extremely difficult to measure transport rates at low bed shear stresses).

Step (2) : Since ρ, D, γ_s and the bedslope S are known and

$$Y = \frac{\rho u_*^2}{\gamma_s D}$$

$$= \frac{\rho g y S}{\gamma_s D}$$

the value of u_* and the flow depth y may be calculated in each case.

Step (3) : From the values of N chosen in Step (1) find the associated values of n (number of grains moving per square metre per second). That is, from

$$N = \frac{nD^3}{u_*} \rightarrow n = \frac{Nu_*}{D^3}$$

where u_* is known in each case from Step (2).

Now

$$g_s = n \times \ell \times wg$$

wg = average dry weight of a grain

ℓ = average step length of a grain $\simeq$ 100 D

g_s values may therefore be found for each chosen value of N .

Step (4) : From the known depth-discharge relation determine the values of q corresponding to the values of y obtained in Step (2) and plot $g_s = f(q)$ thus extending the experimental curve.

Step (5) : Use the E - B formula and the values of u_* , D, γ_s (Step (2)) to calculate values of g_s and plot the rating g_s v q .

Step (6) : The ratings of Fig. 6(a) have now been extended into the initial motion region and may be approximated by straight lines of the general form

$$g_s = a q^b$$

Step (7) : An appropriate offset may be chosen and applied so that the E - B rating matches the flume data. The equations of the adjusted lines can now be determined.

This procedure is capable of general extension. For instance, suppose that on river A the sediment v water discharge, the depth v water-discharge and the quantitative initial motion conditions are known, i.e. the relations

g_s v q	Fig. 6(a)
(y - z) v q	Fig. 15(a)
N v y	Fig. 5

Further suppose that the g_s v q relation is required on river B which has a different known slope and known bed material size but is otherwise similar to river A. If the (y - z) v q curve is known (it can be measured or calculated) then the sediment rating may be obtained by the following procedure. (Fig. 6(c)).

Step (1) : Choose values of N from the unique relation N v Y and note the corresponding values of Y .

Step (2) : Determine in each case the value of y from Y as in Step (2) above where D and S are river B values.

Step (3) : For the same values of N calculate the corresponding values of g_s for river A as in Step (3) previously. Thus at this point, for chosen values of N , y for river B and g_s for river A are known.

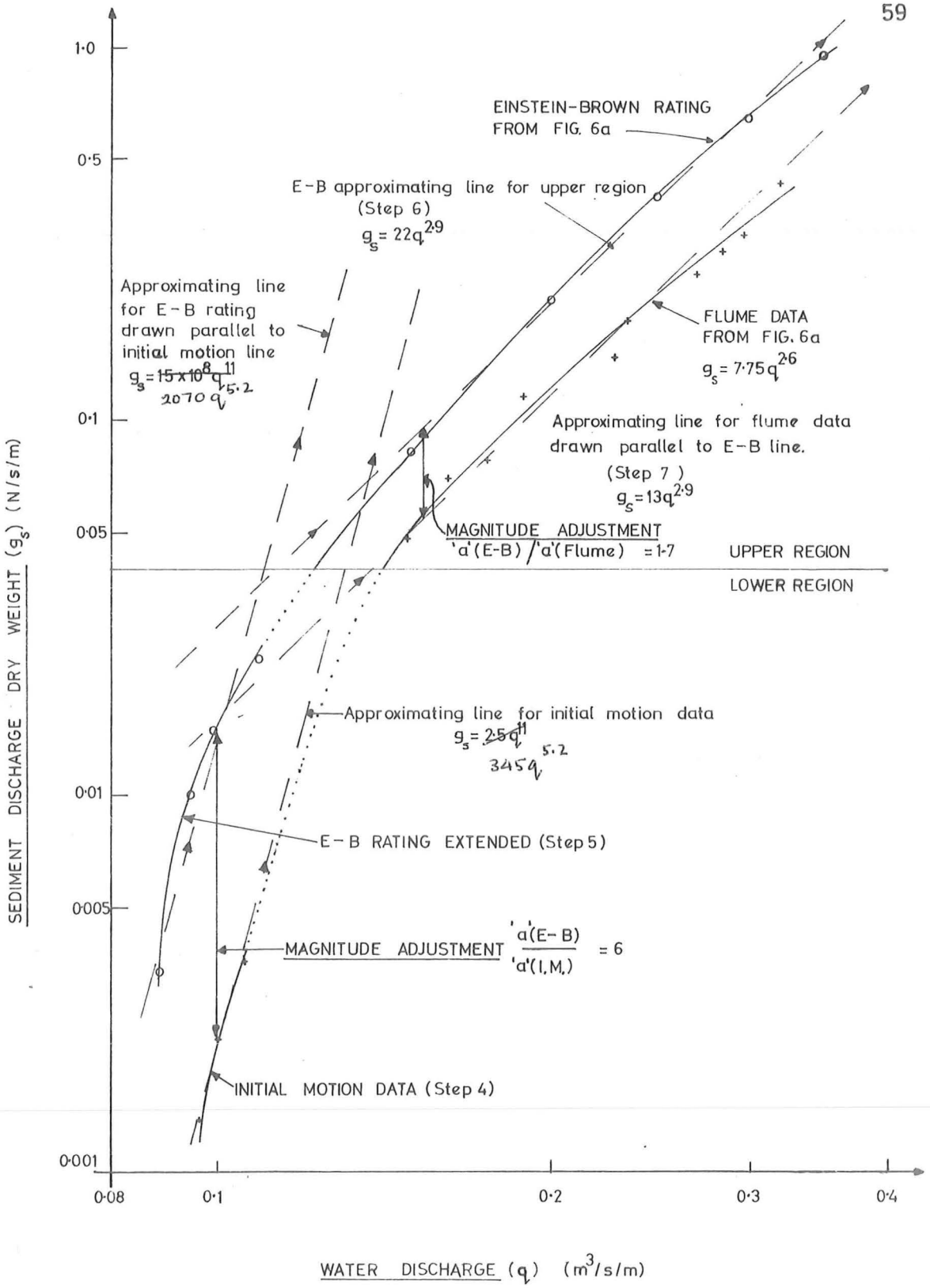

Fig. 6b - ADJUSTMENT OF CALCULATED RATING CURVE TO MATCH EXPERIMENTAL RESULTS

Step (4) : Since

$$g_s = n \times l \times wg$$

and $$N = \frac{nD^3}{u_*}$$

then $$\frac{g_s \text{ (river A)}}{g_s \text{ (river B)}} = \frac{(u_*D)_A}{(u_*D)_B}$$

Further, for any $N_A = N_B$

then $Y_A = Y_B$ N v Y unique

or $$\left(\frac{\rho u_*^2}{\gamma_s D}\right)_A = \left(\frac{\rho u_*^2}{\gamma_s D}\right)_B$$

then $$\frac{(u_*)A}{(u_*)B} = \left(\frac{D_A}{D_B}\right)^{1/2}$$

and so $$\frac{(g_s)_A}{(g_s)_B} = \left(\frac{D_A}{D_B}\right)^{3/2}$$ (a scaling relation)

$(g_s)_B$ may therefore be found for each of the $(g_s)_A$ values of Step (3).

Step (5) : From the known $(y - z)$ v q relation on river B, using the y values of Step (2) and the $(g_s)_B$ values of Step (4) plot the sediment rating for initial motion conditions (Fig. 6(c)).

Step (6) : Calculate and plot the g_s v q relation for river B from the $(y - z)$ v q curve by means of the E - B formula. It is presumed that the E - B formula gave the best slope match with the river A data.

Step (7) : Determine the magnitude adjustment or offset in the lower region. With this value and the adjustment values of river A find the magnitude adjustment for the upper region as shown (Fig. 6(c)). A parallel line may now be drawn at this offset in the upper region.

The adjustment procedure is now complete and a sediment discharge rating has been established for river B. Values of "a" and thus equations of the constructed lines may be found easily, by calculation or from the graph. These equations can then be used in the mathematical model (3.3.2. 1(b)(ii)). Although the procedure is approximate it should reduce the matching error (see Henderson [18] p.447) quite considerably.

B. Non-Steady Flows

(i) Nature of Bedload Motion

The bed particles moved in a similar manner to that described in the steady situation (5.3.1. A.(i)). However as the discharge of the translation wave increased the intensity of the bedload transport increased in a continuous fashion to the wave peak and then decreased. That is, the number of particles in motion increased and then decreased but no noticeable difference was observed in the step lengths or in the rest periods. Einstein's [15] experiments with coloured stones were repeated and gave the same results as in 5.3.1. A(i). Colby's [17] hypothesis (for sand bed streams) that the nett quantity of moving bedload if instantaneously deposited is equivalent to an average depth of deposit of a few hundredths of a foot was tested in the following way.
For a triangular water hydrograph the spatial distribution of the intensity of the bedload transport is essentially triangular. If G_T is the total bedload then

$$G_T = \frac{h' L_W B . B_C}{2} \qquad B_C = \text{flume width}$$

where h' is the depth of deposit under the peak, L_W is the wavelength and B is the bulk specific dry weight of sediment in the bed.

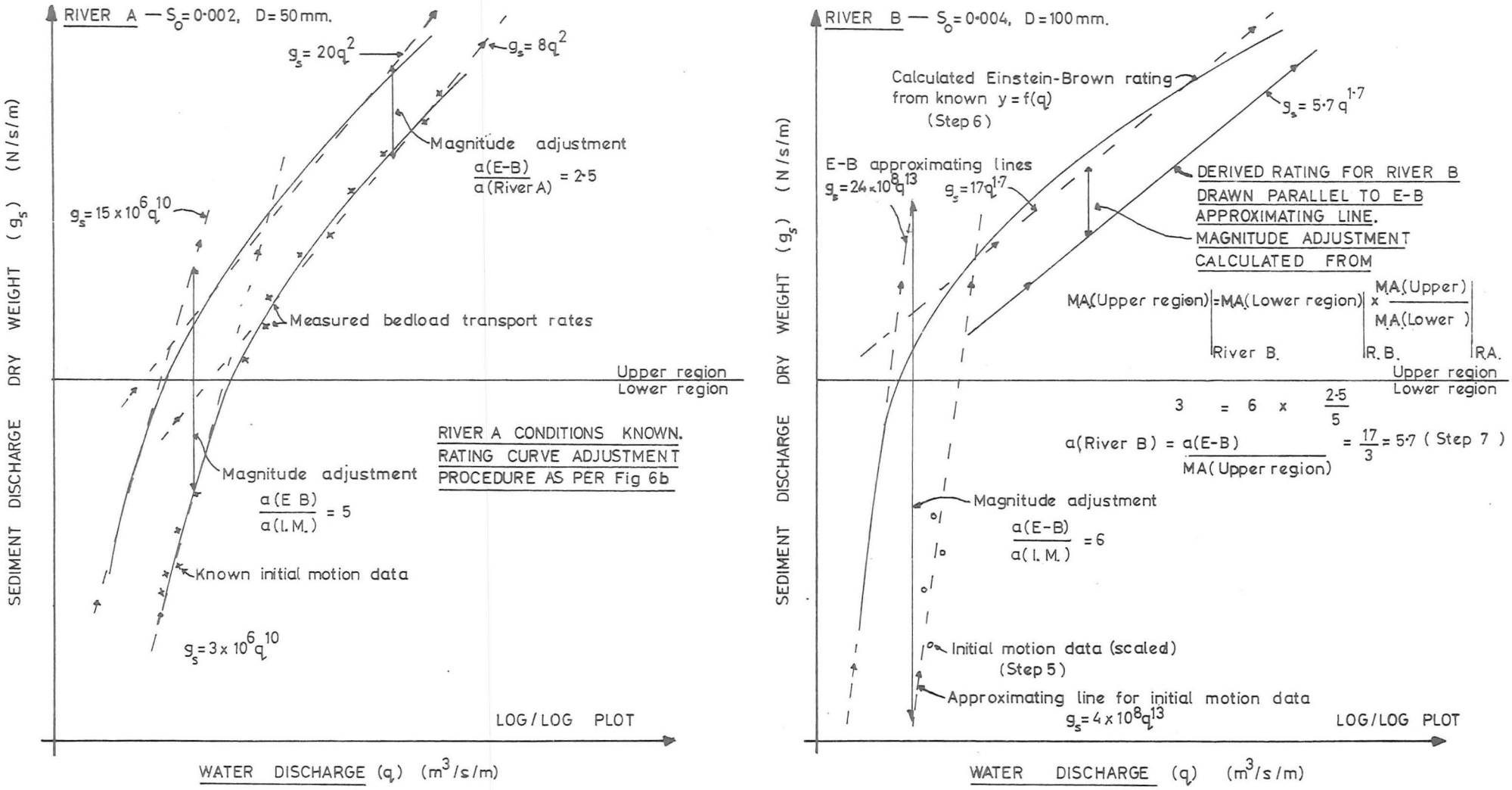

Fig. 6c – HYPOTHETICAL ADJUSTMENT OF RIVER B CALCULATED RATING CURVE USING INITIAL MOTION DATA AND RIVER A MAGNITUDE ADJUSTMENTS

Substitution of experimental values

$$B_c = 1 \text{ ft} \qquad L_W = 4500 \text{ ft} \qquad B = 107 \text{ lb/ft}^3 \qquad G_T = 18 \text{ lb.}$$

gives $$h' = 7.5 \times 10^{-5} \text{ ft}$$

$$= 2.3 \times 10^{-5} \text{ m.}$$

If suspended load was present then the value of the maximum depth would be increased. Notwithstanding this, Colby is correct in that the depth of deposit is very small. It is worth noting that it is less than a grain diameter (D = 4 mm was used in the experiments). This is reasonable because not all the surface particles were moving at the peak water discharge. Physical support is given by this observation to the results of 3.3.2. 1(b)(i) which show that the moving bedload has a negligible effect on the dynamics of the wave motion.

(ii) Distribution and Relative Amounts of Bedload Transport

Six triangular water hydrographs were routed through the flume (Fig. 15 (e)). Fig. 7 shows the principal result, being a plot of the measured instantaneous bedload transport rates and the comparable steady rates attained by the comparison procedure of 3.3.2. 1(b)(ii) as a function of time. The relevant plots and data are presented in E.3. Observations on these equilibrium transport results are set out below.

(1) The inflow and outflow sediment hydrographs were of similar shape in each experiment and between experiments. No temporal or spatial lags were observed between the peak water and sediment discharges.

(2) Transport capacities of the waves were satisfied as the inflow and outflow sediment hydrographs were approximately the same and the mean bed level increased only slightly in each case. This deposition indicates that the transport potential has been marginally overestimated.

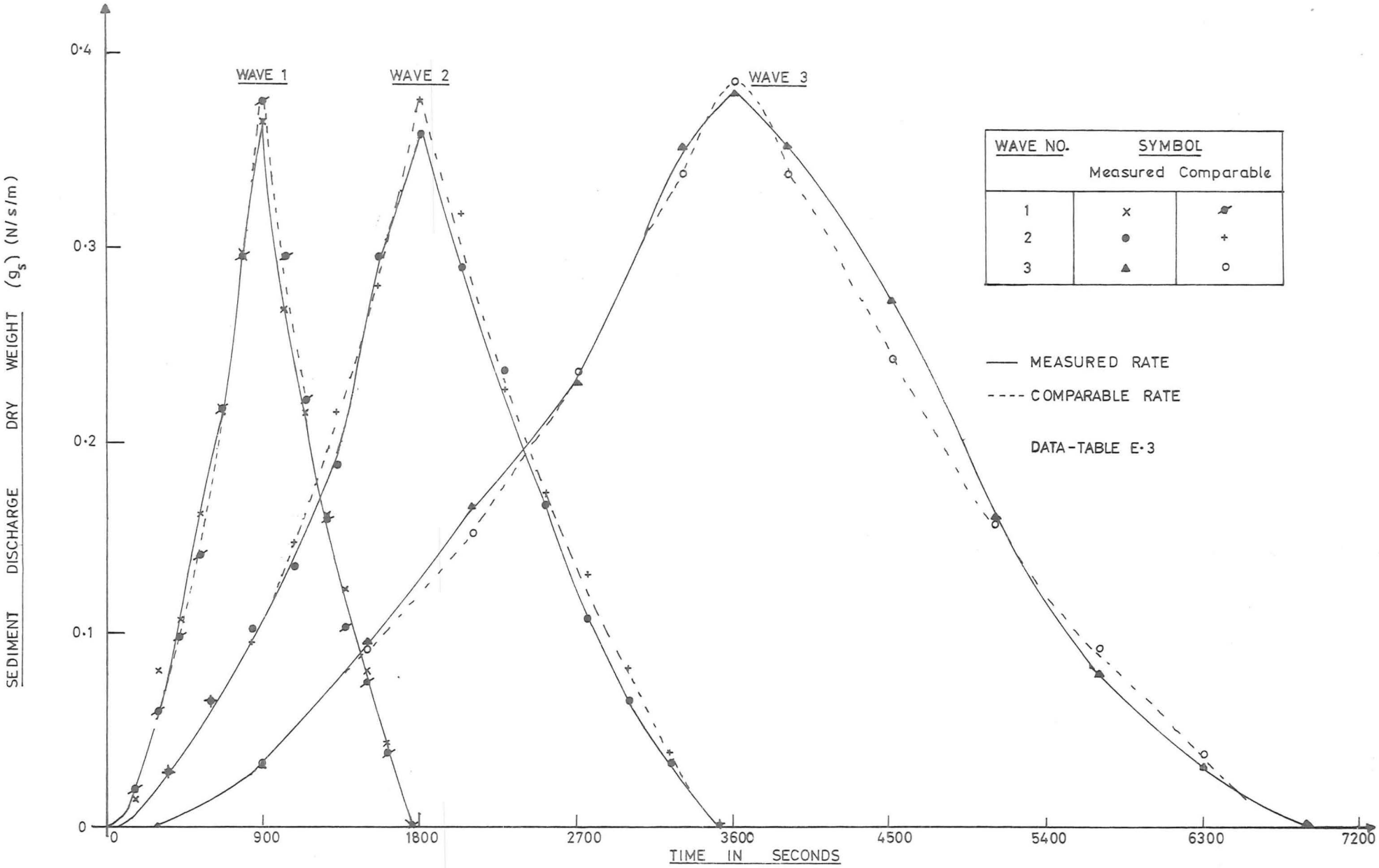

Fig. 7 – COMPARISON RESULTS (NON-STEADY EQUILIBRIUM TRANSPORT)

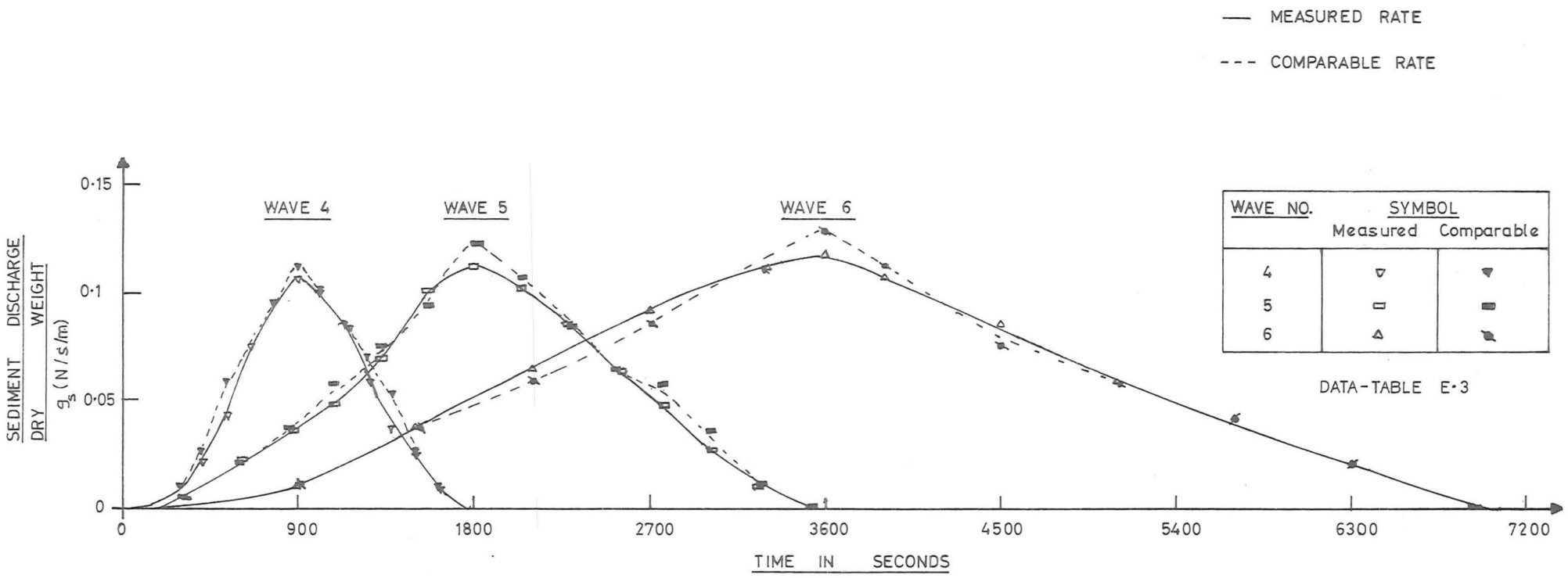

Fig. 7 (CONTINUED) – COMPARISON RESULTS (NON-STEADY EQUILIBRIUM TRANSPORT)

(3) As soon as the water discharge increased above the baseflow, which was the initial motion condition, continuous particle motion began. It ceased at the corresponding point on the tail of a wave. Thus no temporal or spatial lags existed between the changes in water discharge and the allied changes in sediment discharge at these points.

(4) As can be seen from Fig. 7 no difference, within experimental error, was found between measured bedload transport rates in non-steady flows and comparable steady rates obtained by the comparison process. As a rule the steady value at the wave peak was slightly greater than the non-steady value. There are two possible reasons for this; first, the wave peak corresponds to the point of inflection of a cumulative mass curve and it is difficult to measure the gradient precisely here; second, the water hydrograph was triangular and thus the position relates to an instantaneous peak with a sharp increase and decrease in inlet valve movement before and after. Error is thus introduced in the non-steady case.

(5) The comparison process Fig. 3(a) exhibits and then considerably reduces, by averaging, the effect of the water discharge loop rating thus allowing other effects such as lags (3.2.2. 1(b)) to become apparent. A reduction of about 50% in the loop size is achieved when a mean value of the comparable steady and non-steady water discharge is taken (Fig. 3(a), top left graph). The question arises as to what differences would occur between the measured non-steady sediment discharge hydrograph and the hydrograph derived by applying the steady state transport results directly to the non-steady outflow water hydrograph. That is, instead of taking a mean value of g_s (comparable steady)

(Fig. 3(a)) take the value corresponding to the loop water discharge. Unfortunately this question cannot be decided because the magnitude of the loop or the differences between the non-steady and steady stage - discharge relations are very small (Table E.3). Consequently the result would be indistinguishable from that of Fig. 7 - the comparison between comparable rates (mean value used) and measured rates.

Observation (4) states that $g_s(t)\big|_{md}$ (measured non-steady sediment outflow hydrograph) and $g_s(t)\big|_{cd}$ (comparable steady sediment outflow hydrograph) is, in all tested cases, the same function. This observation and the above point implies

$$g_s(t)\big|_{md} = g_s(t)\big|_{cd} = a\,(q(t))^b \qquad \text{[non-steady]}$$

measured hydrograph — comparable hydrograph — substitution hydrograph.

Hence the non-steady sediment outflow hydrograph may be derived from the non-steady water outflow hydrograph and the steady state transport rating.

But this is precisely what the mathematical model assumes (3.3.2. 1(b)(i)).

Therefore, for our experimental conditions the use of an equilibrium transport formula in the model is valid.

(6) If the average (Yield/Time) water and bedload discharges q_{av}, $g_{s_{av}}$ for a wave are computed and the steady water discharge q_s corresponding to this mean bedload discharge $(g_{s_{av}})$ is found from the steady bedload data, the result is that the water discharges are nearly equivalent. Moreover, this result is true for any time during the wave passage provided it exceeds the half period (Fig. 8(a) E.4). What this means is that the yield of a wave may be found if the steady state sediment transport

conditions are known. Symbolically

$$q_{av} = \frac{1}{T} \int_0^T q(t)\, dt$$

and $$g_{s_{av}} = \frac{1}{T} \int_0^T g_s(t)\, dt = {}^{G_T}/_{T}$$

where G_T is the sediment yield per unit width.

Substitution of $g_{s_{av}}$ in the steady state formula

$$g_s = a\, q_s^b$$

gives

$$q_s = \left(\frac{g_{s_{av}}}{a}\right)^{1}/_{b}$$

Then

$$\frac{q_{av}}{q_s} = \frac{q_{av}}{\left({}^{G_T}/_{Ta}\right)^{1}/_{b}} \simeq 1 \qquad t = T$$

and indeed for $t > {}^{T}/_{2}$

$$\frac{q_{av}}{q_s} = \frac{q_{av}}{\left({}^{G_T}/_{ta}\right)^{1}/_{b}} \simeq 1 \qquad \text{Fig. 8(a)}$$

Therefore the yield

$$G_T\Big|_t = ta\left(q_{av}\Big|_t\right)^b$$

can be determined from a knowledge of the non-steady water hydrograph and an applicable steady state equilibrium bedload transport formula.

Correlation is poor at $t = {}^{T}/4$. A possible reason is that throughout the triangular wave $\frac{\partial q}{\partial t}$ is constant whereas $\frac{\partial g_s}{\partial t}$ varies quite rapidly in the region

$$0 \leqslant t \leqslant {}^{T}/4 \quad , \quad {}^{3T}/4 \leqslant t \leqslant T$$

This coupled with the fact that the bulk of the sediment is transported in the intervening period suggests that variations in the value of q_{av}/q_s may occur. It is of interest to note that the best correlation occurs at $t = {}^{3T}/4$ as may be expected since beyond this point rapid variations in $\frac{\partial g_s}{\partial t}$ occur once more.

5.3.2 Non-Equilibrium Transport

A. Steady Flows

(i) General

Thirteen runs were completed for a range of water discharges (E.5). The nature of the bed particle motion was similar to that described previously (5.3.1.A(i)). Up to about 25% of the coloured particles introduced onto the flume bed remained in the same vicinity for the duration of a run even though the bed was degrading.

(ii) Scour

As no sediment was added to the flow the mean bed level decreased during the course of each experiment (E.5). A scour hole developed just below the upstream transition from the fixed to the mobile bed. At this point a rolling vortex existed, under which the bed reached its maximum depth of degradation. From here the scour hole extended downstream, its depth gradually decreasing to the point of intersection with the original bed. During a run this position migrated slowly downstream. Additional evidence for this observation can be seen in Fig. 16(c). Initially the bedload transport rate measured at the downstream end is close

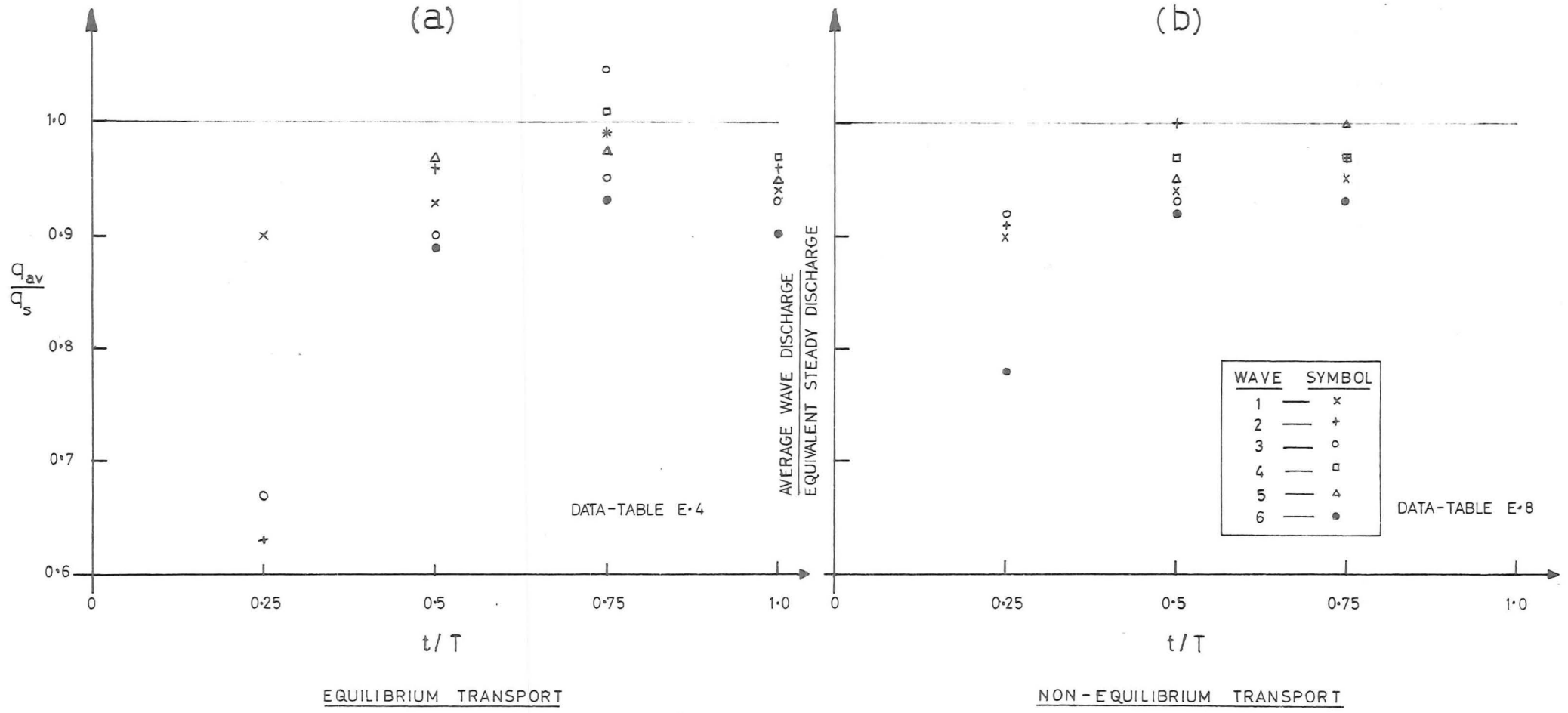

Fig. 8— CORRELATION BETWEEN EQUIVALENT STEADY AND AVERAGE WAVE DISCHARGE

to the equilibrium value; it begins to decrease when the length of the scour hole equals that of the test section (Fig. 16(c)). For low water discharges this effect did not occur because of the duration of the runs and as a consequence the bedload transport rate is approximately constant (Fig. 16(c)). The amount of sediment removed from the test section in all runs was small. This is reflected in the changes in the mean bed level and by the fact that the mean water surface level remained reasonably constant. (Within experimental error ± 5%).

B. Non-Steady Flows

(i) General

The six water hydrographs of 5.3.1.A(ii) were routed through the flume (Fig. 16(g)). Particle motion was similar to that described in 5.3.1. B(i). With each wave a scour hole formed. Small amounts of material were removed from the test section and with the small waves at no point was an equilibrium depth of scour reached.

(ii) Distribution and Relative Amounts of Bedload Transport

Fig. 9(a) is a plot of the principal results. It exhibits the relationship between the measured instantaneous bedload transport rates and the comparable steady rates obtained by the comparison procedure of 3.3.2. 1(b) as a function of time. Relevant plots and data are presented in E.6. General observations on this non-equilibrium transport follow below:

(1) The outflow sediment hydrographs are of similar general shape.

(2) No spatial or temporal lags (3.2.2. 1(b)) were observed between the water and sediment discharges either at the peaks or the tails of the waves.

(3) As can be seen from Fig. 9(a) differences occur between the measured bedload transport rates in the non-steady flows and the comparable steady rates. These differences increase and decrease with the water discharge the maximum discrepancy

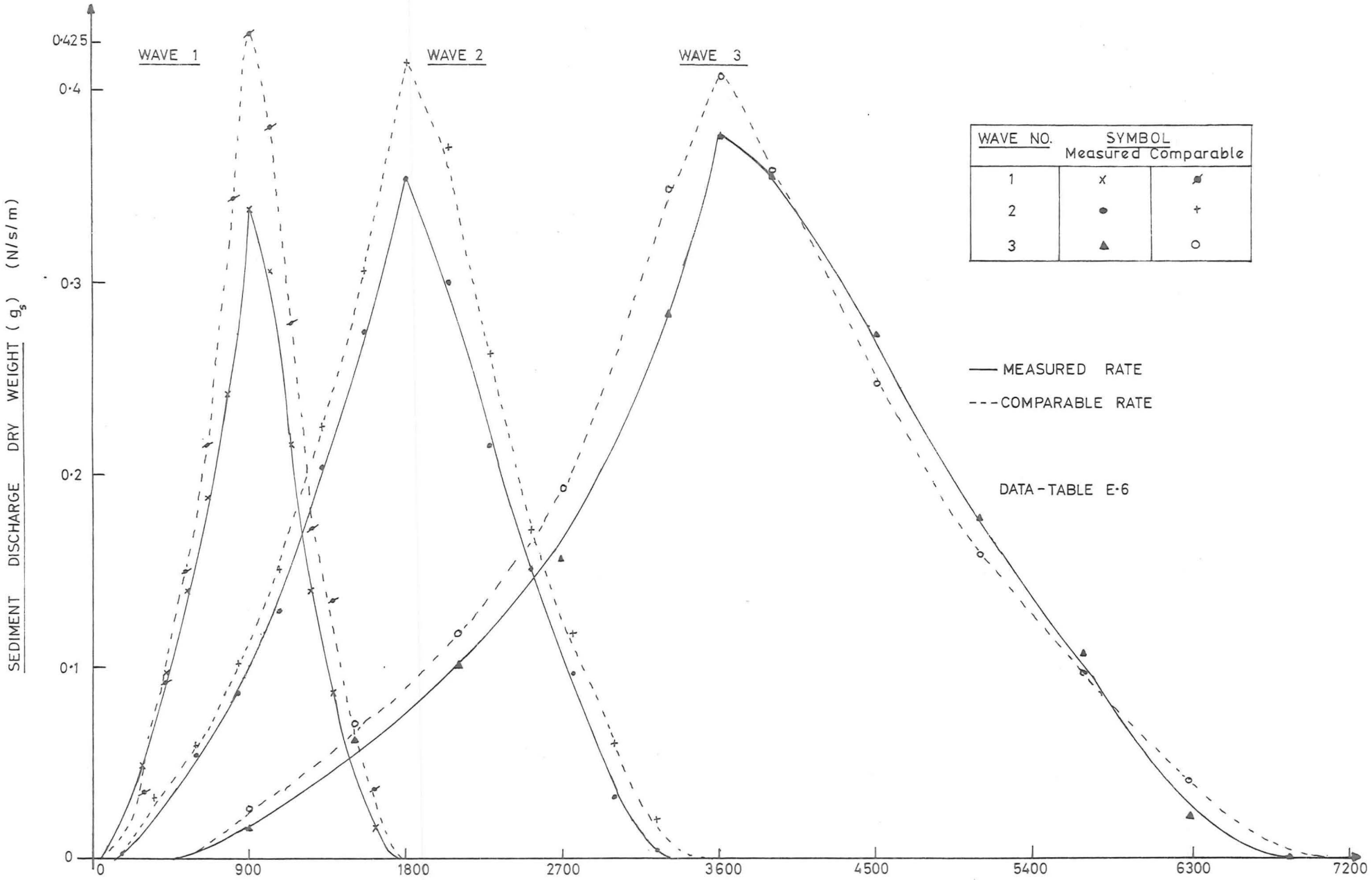

Fig. 9a- COMPARISON RESULTS (NON-STEADY NON-EQUILIBRIUM TRANSPORT)

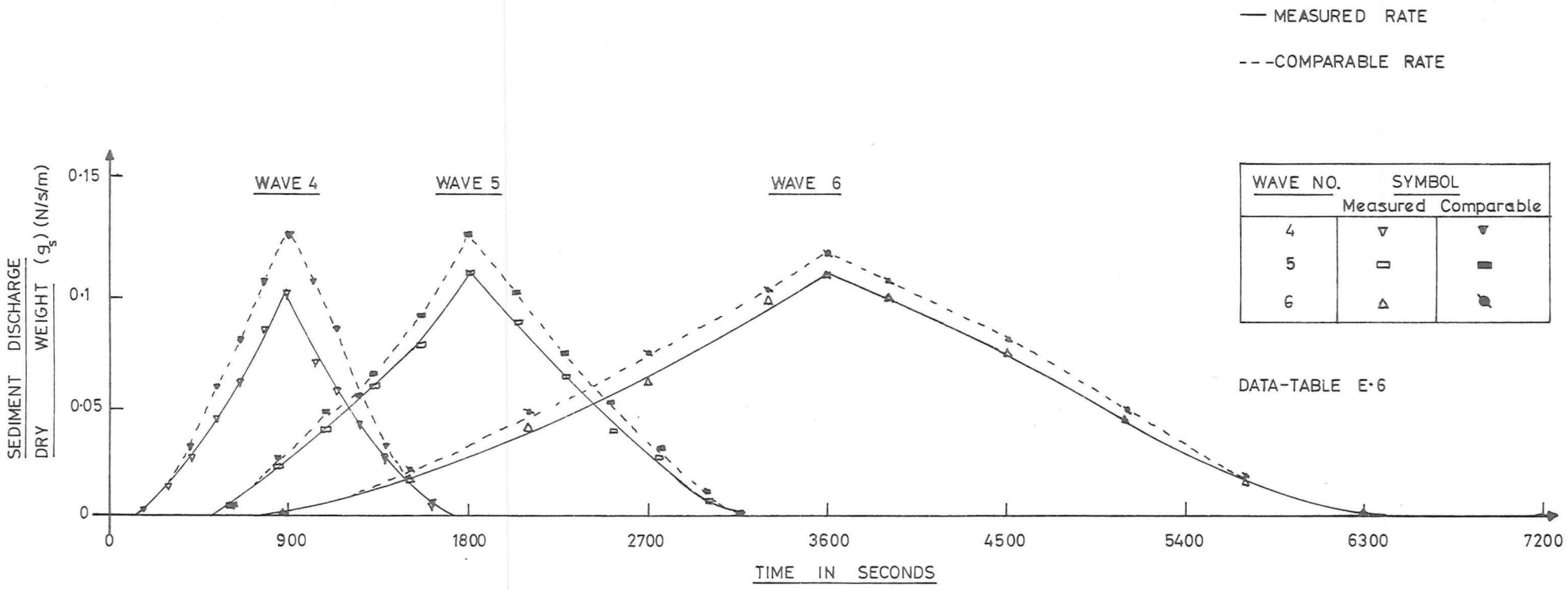

Fig. 9a (CONTINUED) - COMPARISON RESULTS (NON-STEADY NON-EQUILIBRIUM TRANSPORT)

occurring at the wave peak. For the same bedslope and sediment size faster rising waves are associated with greater differences. It appears that a bed response effect is involved. The bed does supply sediment as the transport capacity of the flow changes but the amount of material entrained falls below the transport potential. There is a finite time between a change in water discharge and the attainment of the corresponding transport rate. This magnitude lag (3.2.2. 1(b)) in response is more severe when the discharge is changing rapidly.

One point, which it is important to be clear about, is that the magnitude of the differences is a function of the sampling position within the region of scour. We assume that the region is of finite extent (3.2.3 (2b)). This implies that downstream of the scour hole the wave is in a state of non-steady equilibrium transport. The bed response effect is absent here as the flow and the bed are interchanging particles and the transport capacity of the flow is satisfied.

Corroboration for this argument can be gained by considering the passage of a clear water wave from a fixed to a mobile bed. If two sampling points are established one downstream of the other then, since the yield at the lower position will exceed that of the upper and the wave period is unique, the maximum transport rate must be higher at the downstream point. Now, as the sampler is moved towards the end of the scour region the observed and comparable transport rates must approach the equilibrium value. Therefore the difference between the former two must diminish. In other words the response effect decreases. This is in accordance with what was stated earlier since, as the wave travels downstream, the bed beneath a given point is continually

supplying material until, after a finite time, the fixed transport potential at this moving position is fulfilled. There is no conflict between these assertations and the observations herein, made at a specific point, as the observations are relative between waves and comparable conditions are involved.

Experimental results concerning the relative behaviour between waves at a point can be presented in dimensionless coordinates in the following manner.

The behaviour of the system is governed by the dimensionless parameters (3.3.4)

$$\frac{u_* T}{y} \quad , \quad \frac{\rho u_*^2}{\gamma_s D} \quad , \quad y/D$$

Since the baseflow in all cases was such that critical transport conditions obtained, it is pertinent to choose

$$y = y_{crit}$$

and

$$u_* = u_{*_{max}}$$

where u_{*max} is the shear velocity at the wave peak.

Now

$$D \propto y_{crit}\, S_o \quad \text{(Henderson [18]p.417)}$$

Therefore y/D may be replaced by S_o.

The parameter

$$\frac{\rho u_*^2}{\gamma_s D}$$

is a measure of the flow intensity (Einstein [15]) which is related to the transport rate. For a single wave this parameter has the same value for the measured non-steady and the comparable steady flow conditions. It does not therefore

reflect the transport rate differences caused by the bed response effect. However these may be represented by

$$\left(\int_0^T g_s(\text{steady})_{\text{comparable}}\, dt - \int_0^T g_s(\text{non-steady})_{\text{measured}}\, dt \right) \Big/ \int_0^T g_s(\text{non-steady})_{\text{measured}}\, dt$$

which is the proportional difference in sediment yield for a wave (ΔG_T)

Thus the experimental data may be described by the parameters

$$\frac{y_{crit}}{u_{* \max}{}^T} \quad , \quad \Delta G_T \quad , \quad S_o \qquad \text{(Table E.9)}$$

Fig. 9(b) (Table E.9) shows the relationship between these parameters. The set corresponding to $S_o = 0.0044$ is from the Series I experiments. Here the grain size was 2.18 mm.

It is not clear how the two lines (Fig. 9(b)) may be combined as there is insufficient data*. The plot (Fig. 9(b)) does show that faster rising waves (higher values of $\frac{y_{crit}}{u_{* \max}{}^T}$) are associated with greater differences between measured and comparable steady transport rates.

(4) The earlier observations (based on Series I experiments) [14] that slower rising waves of the same maximum discharge have smaller maximum transport rates and that less sediment is transported on the falling limb as compared to the rising limb of a wave, are not apparent. A possible explanation is as follows:

Far less material was removed from the test section in the Series III experiments. For example, the ratio of the reduction in mean bed level for two waves of approximately the same period and rate of rise, is

$$\Delta z_{(I)} / \Delta z_{(III)} \simeq 16$$

* The reach lengths were different in the two sets of experiments (I,III). For one effect of this see (4) in this section.

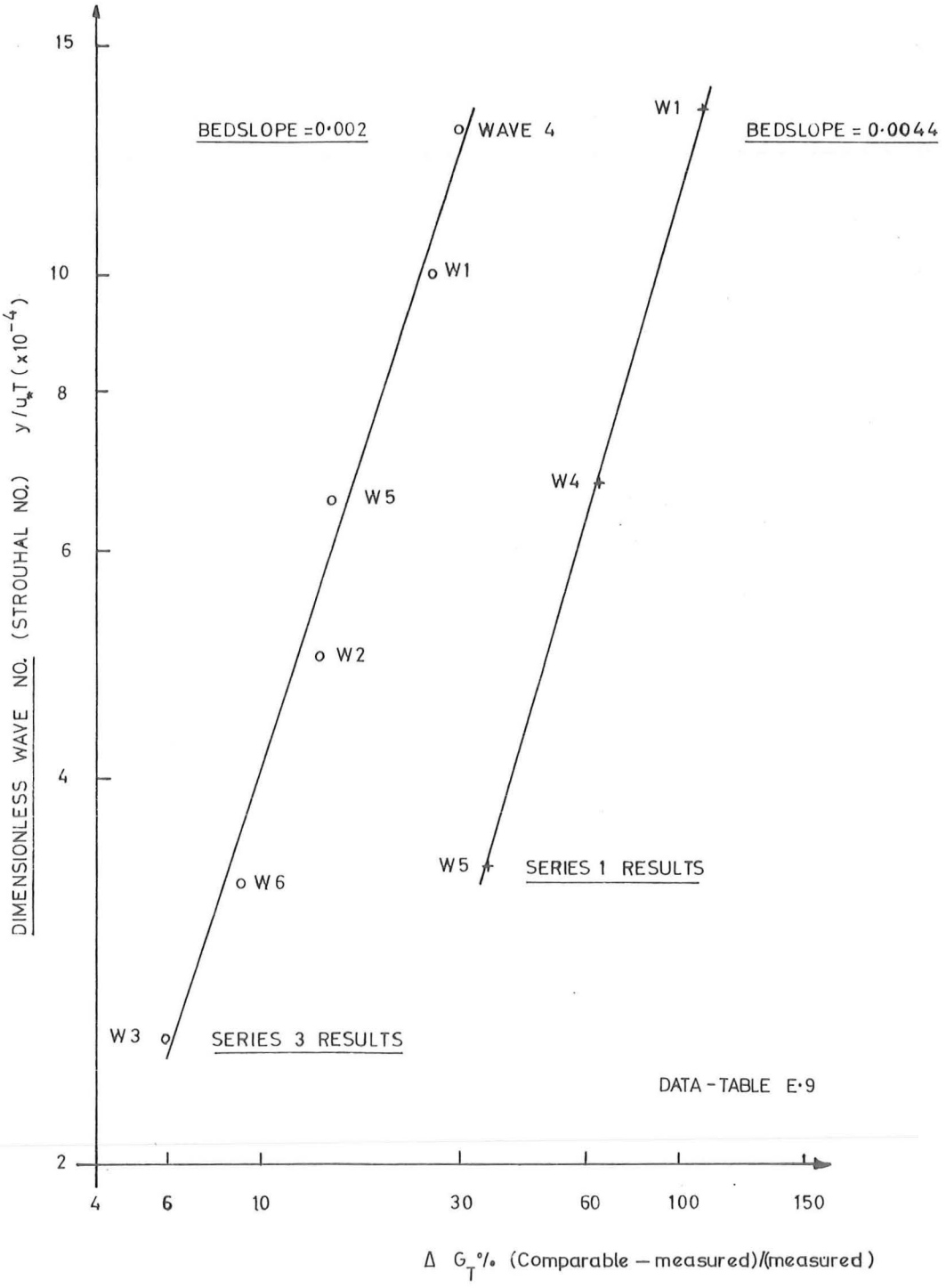

Fig.9b - SEDIMENT YIELD DIFFERENCES FOR SERIES 1,3 NON-EQUILIBRIUM TRANSPORT EXPERIMENTS

Consequently the falling limb of a Series III wave would not be presented with a deeply scoured bed when it entered the test reach. Therefore the transport capacity of this limb would be similar to that of the rising limb and the outflow sediment hydrograph would be moderately symmetrical. Furthermore the maximum bedload discharge of the waves would be similar. These characteristics are exhibited in Fig. 9(a).

(5) As in 5.3.1 B(ii)(6) an equivalent steady discharge q_s which produces the same yield in the same time as a wave can be defined. In the absence of a function of the type

$$g_s(t) = f(q,t)$$

for the steady non-equilibrium transport case an analytic expression for the determination process cannot be written as was done in 5.3.1 B(ii)(6). There the expression

$$g_s = a\,q^b$$

was used.

The value of q_s was worked out by calculating for any time t during the wave motion, the average wave discharge

$$q_{av} = \frac{1}{t}\int_o^t q(t)\,dt$$

Then the yield

$$G_T = \int_o^t g_s(t)\,dt = g_{s_{av}}\,t$$

was found from the experimental results and matched with the steady yield value G_{T_S}, on the plot (Fig. 16(c))

$$G_{T_S} = f(q,t) \qquad \text{(steady non-equilibrium case)}$$

where t has the same value throughout.

Then

$$G_T\Big|_t = G_{T_s}\Big|_t \quad \text{implies} \quad q = q_s$$

thus q_s was found and hence q_{av}/q_s .

To make the determination precise a graph was drawn of

$$G_{T_S} = G_{T_S}(q,t)$$

which had the form

$$G_{T_S} = C(t)\, q^d \qquad d, \text{ constant}$$

The results are presented in Fig. 8(b). These show that if q_{av} is known G_T may be found since $q_{av}/q_s \simeq 1$. As with the equilibrium case the correlation is poorest for $t = T/4$ Generally, faster rising waves give better results than the slower ones.

(6) Results of a similar nature have been obtained by Walker [42] who measured the scour depth, as a function of time, produced by the passage of a translation wave past a pier of circular section. Flow conditions throughout the wave were such that no bed motion occurred upstream of the pier. The scour hole was thus developed under clear water conditions. While the scouring process was active during the wave passage the measured scour depth was always less than that which would have occurred under comparable steady flow conditions. This magnitude lag (3.2.2.1(b)) increased as the wave steepness increased. Given sufficient time at the peak discharge the scour did develop to the comparable steady or equilibrium scour depth. This is analogous to the present experiments in which given sufficient length of bed the wave will attain equilibrium transport conditions. Walker [42] could also define a steady discharge which produced the same scour depth as a wave.

Herein (5.3.2. B(ii)(5)) it is the sediment yield of the wave that can be matched with an equivalent steady discharge.

5.4 BEDFORMS

5.4.1 Development

Dunes as defined by Simons and Richardson [32] were the only type of bedform which appeared during the course of the experiments. This was to be expected as the water flows were subcritical and the bed material was gravel size. When the discharge was above a certain value dunes developed downstream of a slight mound of sediment which had been built up on the bed from excavation of the scour hole at the fixed to movable bed transition. At such times most of the surface particles were moving and the remaining material tended to become imbricated. That is the longitudinal axes tended to become aligned in the flow direction. The first noticeable stage in the dune development was the appearance of longitudinal variations in the intensity of the bedload transport which occurred at regular intervals and seemed to be precipitated by the mound. Within a short period of time small dunes were observed. These grew rapidly into a steep faced, flat top shape with a long tail. Advancement was achieved by particles rolling over the top and down the front face of the dune. These reappeared on the bed surface when the bedform had passed the point of observation. Five or six dunes were normally present at any one time and they were out of phase with the surface waves.

5.4.2 Characteristics

With the steady flows dunes became noticeable for dicharges exceeding 230 ℓ/sec/m which corresponds to a flow depth y of 0.25 m and velocity $u = 0.92$ m/sec. The ratio of the dune length λ_d to the depth

$$\frac{\lambda_d}{y} \simeq 5$$

and the maximum height (A_d) and velocity of the bedforms was 0.02 m and 0.15 m/min. respectively.

General observations made during the non-steady equilibrium transport flows include

(1) Dunes formed by the same mechanism as that outlined in the steady flow case.

(2) For waves of the same peak water discharge the amplitude and wavelength of the bedforms increased as the rate of rise decreased. With the fastest rising wave (W_1) disturbances in the longitudinal intensity of the bedload transport culminated in very small dunes near the wave peak. Whereas, in the slowest rising case (W_3) dunes were readily apparent. For example the maximum development for W_1 was $A_d \simeq 0.01$, $\lambda_d < 1$ m and for W_3, $A_d \simeq 0.015$ m, $\lambda_d \simeq 1$ m.

(3) The maximum dune development occurred shortly after the wave peak. ($^T/2 + (5 \rightarrow 10\%)T$).

(4) Development was not as great as it was under comparable steady flows and began at higher discharges (240 → 260 ℓ/sec/m). For example the maximum development for W_3 was $A_d \simeq 0.015$ m, $\lambda_d \simeq 1$ m and for a comparable steady flow $A_d \simeq 0.2$ m, $\lambda_d \simeq 1.25$ m.

(5) Dunes were present for longer periods on the falling stage than on the rising stage. Furthermore their height decreased and their length increased during the destruction process.

The implications of these points are discussed in 5.5, 5.6.

5.5 FLOW RESISTANCE

In the non-steady equilibrium experiments variations in the longitudinal intensity of the bedload transport or developing dunes only appeared in the waves of the higher maximum discharge. Bedforms were most distinct in Wave 3 (Fig. 15(e)) so this was selected for study.

Variations in the flow resistance were expressed as percentage differences in the Manning's 'n' value (computed from the Manning formula) relative to the comparable steady flow value at selected inflow discharges. These were plotted against the dimensionless bedload transport rate

$$\phi = \frac{g_s}{\gamma_s}\left(\frac{\rho}{(\rho_s - \rho)gD^3}\right)^{1/2}$$

of Einstein [15].

The results are shown in Fig. 10(a).

It can be seen that the difference or relative resistance is less on the rising and greater on the falling stage of the wave. This variation is related to the dimensionless transport rate and persists to lower values of ϕ as the water discharge decreases. But this asymmetric behaviour is analogous to that of the bedforms. Therefore it is reasonable to suppose that the size of the dunes is changed by the bedload transport and that the resistance is proportional to the dune size.

5.6 STAGE - DISCHARGE RELATIONS

The stage discharge curve for Wave 3 (Fig. 15(e) Equilibrium Transport) at the downstream water level recording site and the steady flow relationship at this point are shown in Fig. 10(b). Its form reflects the dune and resistance behaviour. An explanation for this form may be that since the dune development lags the increasing discharge then so does the resistance. Consequently, for a given discharge, the depth is lower on the rising and greater on the falling stage of the wave than the steady flow value. Before the bedforms appear and after they disappear, plane bed conditions obtain and thus all depths correspond, i.e. the loop disappears (Fig. 10(b)). With faster rising waves of the same maximum water discharge a lesser degree of dune development was apparent (5.4.2 (2)).

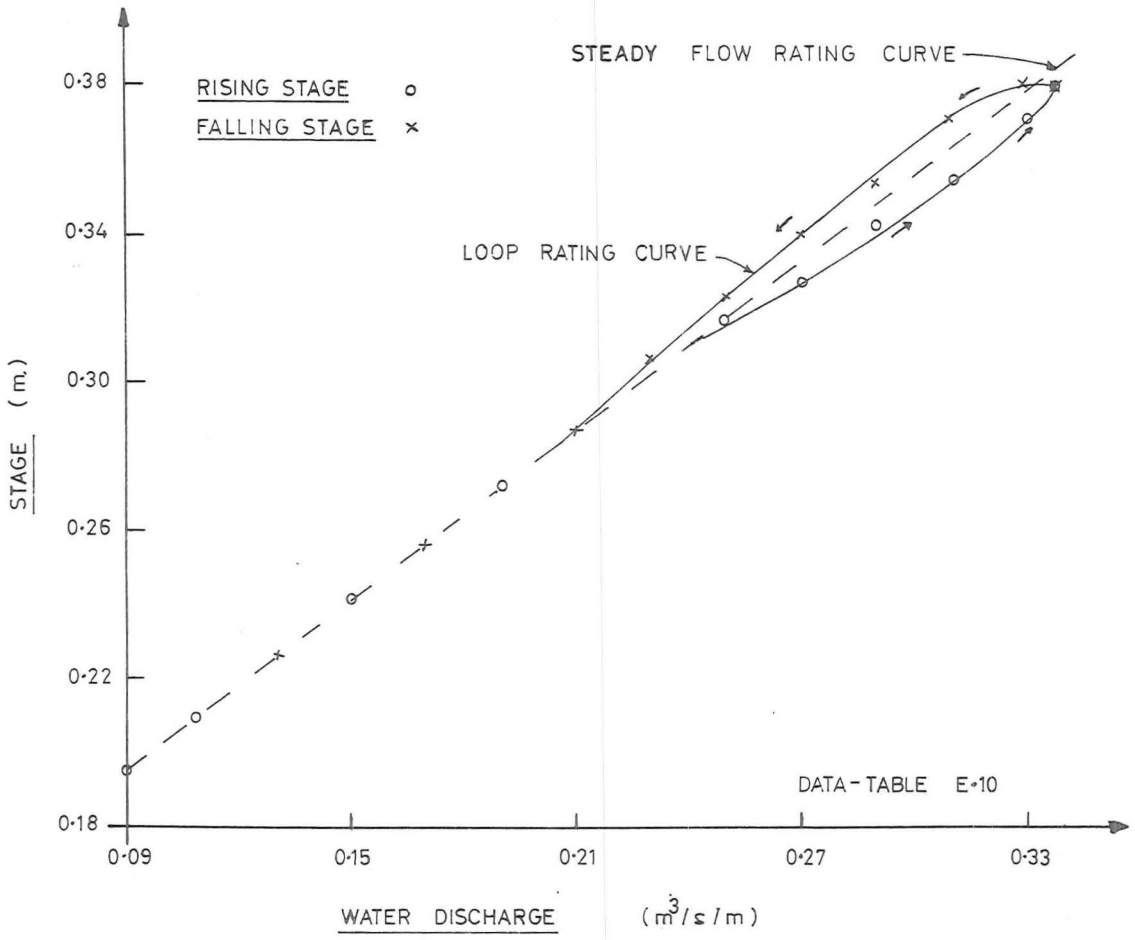

Fig.10(b) - STAGE-DISCHARGE RELATION FOR WAVE 3
(NON-STEADY EQUILIBRIUM TRANSPORT)

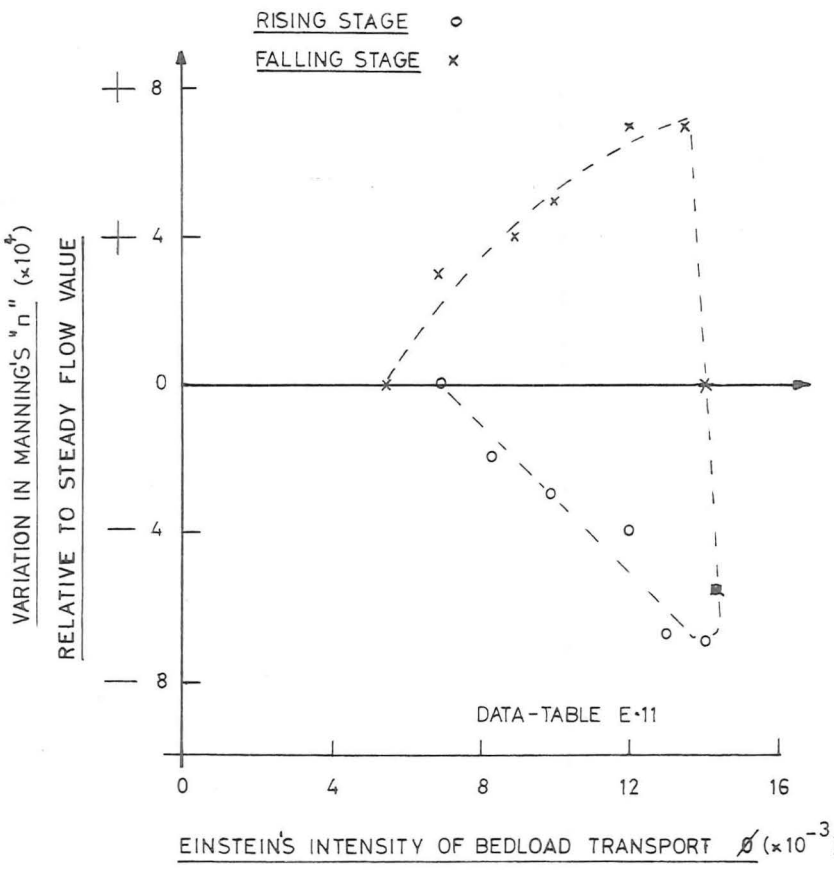

Fig.10(a) - RESISTANCE VARIATIONS FOR WAVE 3 (NON-STEADY EQUILIBRIUM TRANSPORT)

Possibly the variation in the resistance and the depth would be correspondingly larger relative to the uniform flow result.

5.7 GENERAL CONSEQUENCES

It is now pertinent to discuss the probable performance of the mathematical model.

(a) Non-steady Equilibrium Transport.

It has been shown that provided a steady equilibrium transport formula can be found to match the steady flow transport results then the non-steady flow behaviour can be predicted. However because of the resistance variations the St. Venant Equations will overestimate the stage on the rising and underestimate it on the falling limb of a wave. For the waves examined herein this will be more serious in the fast rising case and thus will have some small effect on the instantaneous bedload transport rates. In regard to the estimation of yield it can be ignored.
As a rule, the principal source of error will be in matching the transport formula. If this is successful then the performance of the model would be excellent. Moreover any simplification introduced in the St. Venant Equations would be reflected in the bedload transport results.

(b) Non-steady Non-equilibrium Transport.

The performance of the mathematical model at some point within the region of scour can be expected to be poor for two main reasons; first, an equilibrium transport equation is used and second; a bed response effect is apparent. Consequently the bedload transport rate will be overestimated but the degree will decrease as the downstream end of the hole is approached. By comparison, the contribution of roughness variations will be small.

CHAPTER 6

CONCLUSIONS AND RECOMMENDATIONS

6.1 SYNOPSIS

This chapter sets out the conclusions reached after carrying out the theoretical and experimental programs described in Chapters 3 to 6. It provides answers to the questions of Chapter 2. The performance of the apparatus, practical implications and further research needs are also discussed.

6.2 PERFORMANCE OF THE APPARATUS

During the course of the Series II experiments it became apparent that the frequency of bedload sampling was inadequate. This was increased but little improvement resulted because of the bedforms moving through the flume. The practice of sampling in the presence of bedforms and under non-steady flows was judged to be questionable as there is no criterion whereby the obtained mean value of the bedload transport rate can be checked. Thus the bedload data from Series II was rejected.

In order to avoid these difficulties a nearly continuous recording bedload collection device was installed in Series III.

With the exception of the sampler in Series II the equipment performed consistently.

The important observation to be made is that the general layout of the designed and adopted apparatus has proved to be satisfactory and will be useful in future studies of alluvial bed behaviour under non-steady flows.

6.3 CONCLUSIONS BASED ON THE RESULTS OF THIS THESIS

Both general conclusions and answers to the questions of 2.3 are presented. The relevant question number is noted beside each answer. Two answers may appear to the same question - one for the equilibrium transport situation and one for the non-equilibrium situation.

6.3.1 Initial Motion

(1) The initial movement of grains was impulsive and random in nature and seemed to be initiated by strong turbulent bursts near the bed.

(2) The suggested form of the relation between the dimensionless erosion rate N and Shields' entrainment function Y was confirmed. QUESTION 1

(3) The relation N v Y shows that for a wide channel, turbulent flow and uniform stones, a quantitative estimate may be made of the point of initial motion. However, the particular value of N and thus the estimate is arbitrary. Once this is decided the actual number of stones likely to move on unit bed area in unit time can be easily determined.

(4) The grain movement associated with the criteria of many other authors can be estimated. Therefore a uniform bed may be designed, for example by Shields' criterion, and the number of grains likely to move in a given area in a given time may be found.

6.3.2 Equilibrium Bedload Transport

A. Steady Water Flows

(1) The predominant form of grain movement was surface rolling. Vertical displacements did not exceed three grain diameters. Step lengths were, on average, short and rest periods were long compared with periods of movement. The majority of coloured particles introduced into the flow remained in the test section.

(2) Of those tried the equilibrium transport formula which most closely matched the flume data was the Einstein Bedload Function. The Einstein - Brown bedload formula gave the best fit slopewise.

QUESTION 2

(3) A transport formula, expressed as a rating, can be adjusted magnitude wise if its slope matches the data slope and if the formula can be approximated by straight lines. The method of adjustment is based on the fact that the formula must satisfy the rating conditions associated with initial motion.

(4) Conclusion (3) allows the possibility of calculating a sediment rating on a similar but non-rated reach by the scaling of quantitative initial motion conditions (6.3.1 (3)) and the magnitude adjustment of the matched bedload formula of (3) above.

B. Non-Steady Water Flows (Triangular Translation Waves)

QUESTION 3

(1) There is no difference in the nature of the bedload motion between translation waves and comparable steady flows. (See conclusion A(1)).

(2) If the moving bedload under a wave was instantaneously deposited then the resulting average depth of aggradation would be very small.

QUESTION 4

(3) An equilibrium transport rate can be associated with a wave. When a wave passes through an alluvial reach and there is no nett gain or loss of sediment under the wave and the mean bed level of the reach remains unchanged, then the wave is in a state of non-steady equilibrium transport. The intensity of interchange of the bed particles varies as the transport capacity varies from segment to segment. The maximum intensity occurs at the wave peak.

QUESTION 5

(4) The sediment motion itself has a negligible effect on the dynamics of the wave motion. It has a tendency to increase the diffusion of the wave and, if bedforms develop, then the resulting change in resistance enhances subsidence effects in non-kinematic waves.

QUESTION 6

(5) The inflow and outflow water and sediment hydrographs were of similar general shape. There was a closer resemblance between hydrographs of the same phase.

QUESTION 7

(6) No temporal and/or spatial lags (3.2.2. 1(b)) were observed between the water and sediment discharges.

QUESTION 8

(7) With equilibrium waves no differences or magnitude lags were observed between the measured outflow sediment hydrographs and the derived comparable (3.3.2. 1(b)(ii)) steady flow hydrographs.

QUESTION 9

(8) Provided an equilibrium transport formula can be found and adjusted to fit the steady flow rates then it may be applied directly to the wave outflow hydrograph. The resulting calculated sediment hydrograph will be approximately the same as the measured outflow sediment hydrograph.

QUESTION 10

(9) An equivalent steady discharge can be defined which produces the same yield as a wave. It is equal to the average wave discharge (Water Yield/Time) and by means of an appropriate steady flow sediment rating, the wave yield may be found. This wave yield estimation procedure may be carried out at any time for a wave passing a fixed point. More accurate results pertain if it is attempted after the peak has passed.

(10) With the proviso of conclusion (8) the use of an equilibrium transport formula in the mathematical model is justified.

6.3.3 Non-equilibrium Bedload Transport

A. Steady Water Flows

QUESTION 11

(1) If the sediment inflow to an equilibrium state in an alluvial reach is halted then a scour hole will develop from the upper end of the reach. Presume the reach length is infinite; then in an infinite period of time so will be the length of the scour hole. The depth of this excavation will be such that initial transport conditions obtain on its base. At any given time the region downstream of the scour hole will be in a state of steady equilibrium transport.

(2) If an equilibrium transport formula is used in a mathematical model of the situation, the extent of scour in a given period of time will be overestimated.

B. Non-Steady Water Flows (Triangular Translation Waves)

QUESTION 4

(1) A state of non-equilibrium transport ensues when a wave, capable of transporting sediment, passes from a fixed to a movable bed. (We assume here that the wave is superimposed on a steady base flow at critical transport conditions). As the wave moves downstream a scour hole of finite length develops. To an order of magnitude the length of the hole is one thousandth of the wave length. Beyond the scour region the wave is in a state of non-steady equilibrium transport as in conclusion 6.3.2. (B)(3). It can then be associated with an equilibrium transport rate.

The amount of bedload in transport by the wave is proportional to the volume of the scour hole.

QUESTION 6

(2) Inflow and outflow water hydrographs were of similar shape but the corresponding sediment hydrographs need not be. The reason is that the rising limb of a wave, in satisfying its transport capacity, removes material from the bed. Consequently the falling limb meets an increase in depth and thus has a reduced transport capacity. As a result the outflow sediment hydrograph from the scour region may not be symmetrical.

QUESTION 7

(3) No temporal and/or spatial lags were observed.

QUESTION 8

(4) Magnitude lags were observed. That is, differences in magnitude occurred at a point between the measured outflow sediment hydrograph and the derived comparable (3.3.2. 1(b)(ii)) steady hydrograph - the maximum discrepancy being at the wave peak. Faster rising waves were associated with greater differences. It is thought by the writer that a bed response mechanism is responsible. This involves a finite time between a change in discharge and the attainment of the corresponding transport rate. The magnitude of the differences will decrease, for a given wave, as the downstream end of the associated scour hole is approached.

QUESTION 9

(5) If an equilibrium formula is used to estimate the sediment discharge at some point within the scour region then considerable error will be involved (see Conclusion (3) above). The magnitude of the error will decrease as the estimation point is moved toward the downstream end of this region.

QUESTION 11

(6) An equivalent steady discharge, which produces the same yield as a wave, can be defined as in Conclusion (6.3.3. (B)(9)). However the comparable steady flow non-equilibrium transport conditions

must be known.

(7) Walker [42] studied the scour hole development produced by a clear water translation wave moving past a circular pier. He observed a magnitude lag (3.2.2. 1(b)) between the non-steady measured and comparable steady scour depths. An equivalent steady discharge which produced the same scour depth as a wave could also be defined. There appears to be an analogy between his observations and the earlier experiments of Sutherland and Griffiths [14] and those presented herein.

6.3.4 Bedforms and Flow Resistance

A. Bedforms

QUESTION 12

(1) Dunes, in the sense of Simons and Richardson [32], were the only type of bedform observed. They are thought, by the writer, to develop from longitudinal variations in the intensity of the bedload transport initiated by a non-uniformity in the bed surface. On the rising stage of a wave dune development lags both temporally and in magnitude similar development in comparable (3.3.2. 1(b)(ii)) steady flows. On the falling stage dunes persist for longer periods than on the rising stage.

B. Flow Resistance

QUESTION 13

(1) Variations in the resistance are related to the changing dimensions of the bedforms under a wave. The bedload transport provides the mechanism for these changes.

6.3.5 Stage-Discharge Relations

QUESTION 14

(1) The changes in the bedforms and flow resistance are reflected in these relations by the production of a loop around the steady flow rating. Such a loop is not symmetrical - it persists longer on the falling than on the rising stage - and the magnitude of the difference

between the two stages increases with the rate of rise of the waves. Dynamic wave effects also contribute toward loop development. For the conditions herein this contribution was small.

6.3.6 General

QUESTION 15

(1) A mathematical model comprising the St. Venant Equations, a sediment continuity equation and a steady flow sediment rating relation may be used to predict the reach response to non-steady water and sediment inflows. If the sediment inflow is an equilibrium one (see Conclusion 6.3.2. B (3)) and a rating can be found (see Conclusion 6.3.2. B (8)) then the performance of the model will be good. The steady flow resistance expression will overestimate the resistance on the rising and underestimate it on the falling limb of a wave (a result of 6.3.5. (1)). However this effect will be small in comparison to the error involved in matching a sediment rating curve (6.3.2. B (8)).

QUESTION 16

(2) The natural channel cannot be modelled exactly as all the scaling relations cannot be satisfied simultaneously (Yalin [26]). A two-dimensional model is possible without distortion, that is a geometrically similar model, for restricted conditions. The sort of restrictions required are those which pertain in the experimental work herein. These include the prescription that ρ and ρ_s must be the same in model and prototype and that

$$\lambda_\ell > \simeq \left[\frac{70}{\frac{u_* k_s}{\nu}}\right]^{2/3}$$

6.4 PRACTICAL IMPLICATIONS

The essential contribution of this thesis, in a practical sense, is a set of indications of general physical behaviour in what was previously an unexplored field. Conditions treated herein are quite severe especially as regards the rate of rise of the flood waves. Therefore for lesser rates of rise and/or lesser bedslopes it is reasonable to suppose that the obtained results will hold and that errors such as those due to bed response effects will be reduced. Possible applications of the work are given below.

The initial motion results may prove useful in the design of nearly uniform bed channels, outflow sections downstream of culverts and similar structures, and in other works where scour is to be prevented. As flood routing procedures are reasonably successful in rivers there is hope that so may be sediment routing. It has been shown that provided a steady flow sediment rating relationship can be found then non-steady flows present no real problem unless the downstream station is within the upper portion of the scour region associated with a wave's passage. Normally some bedload inflow occurs in a river reach. Therefore if the length of the reach of interest is, say, at least one tenth of a wavelength, which is longer than the wave scour hole, then the non-equilibrium situation is not important.

Since it is very difficult to measure bedload transport rates in the larger New Zealand rivers the routing problem may be attacked as follows. A long, reasonably uniform reach in a smaller river should be selected and a bedload transport formula calibrated for a series of steady flows by means of measurements obtained at the downstream end. These should be near equilibrium transport values. The mathematical model may be applied to the uniform section of interest where the inflow sediment hydrograph is assumed to be an equilibrium one - the inflow water hydrograph being known.

Then the model or a simplification thereof may predict the outflow water and sediment discharge hydrographs. Application of the model may be made to similar reaches on other rivers where no data is available - the bedload equation being adjusted by initial motion criteria.
With further work it should be possible to account for such factors as changes in slope, width and bed material.

Another major application is that of the sediment yield determination method. Here again, an adjusted bedload equation is required. As a rule of thumb the method may be useful in determining the relative loads of various floods. Such information would be valuable, for example, in estimating changes in mean bed level and thus flood protection work heights in a region of aggradation. The method could also be important in degradation problems associated with the non-steady release of water from reservoirs.

6.5 RECOMMENDATIONS FOR FUTURE RESEARCH

The scope for further work is vast, not only in the laboratory but also in the field. What are considered as the more important lines in the various aspects of this study are set out below;

(1) Initial Motion

Additional experimental data for a range of slopes and sediment sizes is required to extend or curtail the applicability of the quantitative definition of initial movement.

(2) Steady and Non-steady Equilibrium Bedload Transport

The wave characteristics, wave type, bedslope and bed sediment size all need to be varied with a view to finding the limits within which the non-steady processes can be approximated by steady ones. If a long flume, say 100 m, was available, it would be interesting to contain a whole wave within the

flume at one time in contradistinction to the situation in this study. Of course the wave would necessarily be steep but a rather better physical picture would be gained.

(3) Steady and Non-steady Non-equilibrium Bedload Transport

As a first step theoretical work is required to derive a non-steady bedload formula which applies in quasi-steady water flows.

The bed response phenomenom needs further attention, in particular, because it may be related to any lags between changes in discharge and changes in bedforms.

If a wave is contained within a long flume, as above, then it would be possible to ascertain the scour hole length and to check if equilibrium conditions obtain downstream of this region.

(4) Resistance, Bedforms and Stage Discharge Curves

The relationship between changing bedforms, resistance and flow depths is known only in outline. Conditions need to be varied as in (2), especially in regard to the bedform development under various rates of rise of the waves. Also, as yet, no theoretical work has been forthcoming.

(5) General

The mathematical model remains to be tested against actual data derived from a range of sediment sizes and bed slopes. Clearly much further work is needed before the problem of bedload transport by translation waves can be fully understood.

REFERENCES

1. Bennett, J.P., "Concepts of Mathematical Modelling of Sediment Yield", Water Resources Research, Vol. 10, No. 3, June 1974, p.489.

2. Henderson, F.M., "Report on the 1960 Improvement Scheme, Waimakariri River", North Canterbury Catchment Board, Christchurch, N.Z., 1960, p.25.

3. Shen, H.W., (Ed.), "River Mechanics", Vol. 1,2, Colorado State University, Fort Collins, 1971.

4. Graf, W.H., "Hydraulics of Sediment Transport", McGraw-Hill, New York, 1971.

5. Yalin, M.S., "Mechanics of Sediment Transport", Pergamon, Oxford, 1972.

6. Gessler, J., "Aggradation and Degradation", Chapter 8 of River Mechanics Vol. 1, (Ed. Shen), Colorado State University, Fort Collins, 1971, p.8-1.

7. de Vries, M., "Considerations about Non-Steady Bed-Load Transport in Open Channels", International Association of Hydraulic Research, 11th Congress, Leningrad 1965, Paper 3.8(2).

8. de Vries, M., "Solving River Problems by Hydraulic and Mathematical Models", Conf., Jablonna, Poland (Publ. Delft Hydr. Lab. No. 76-II), 1969.

9. de Vries, M., "River-Bed Variations - Aggradation and Degradation", International Association of Hydraulic Research, Seminar on Hydraulics of Alluvial Streams, New Delhi, 1973.

10. Wu, C.M., "Unsteady Flow in Open Channel with Movable Bed", Proc. I.A.H.R. - I.A.T., International Symposium on River Mechanics, Vol. 3, Paper C-40, Bangkok, 1973.

11. Chang, F.M., "Computer Simulation of Riverbed Degradation and Aggradation by the Method of Characteristics", International Association for Hydraulic Research, 13th Congress, Kyoto, 1969, Paper A37.

12. Miloradov, M., Muskatirovic, D., "Calculation of River Bed Deformation in Unsteady Flow", International Association for Hydraulic Research, 14th Congress, Paris, 1971, Paper C-22.

13. Sakhan, K.S., Riley, J.P., Renard, K.G., "Hybrid Computer Simulation of Sediment Transport with Stochastic Transfer at the Stream Bed", Sedimentation, (Symposium to Honour Prof. H.A. Einstein), Ed., Shen, Colorado State University, Fort Collins, 1972, p.21-1.

14. Sutherland, A.J., Griffiths, G.A., "Non-Steady Bedload Transport by Translation Waves", International Association for Hydraulic Research, 16th Congress, Sao Paulo, 1975, Paper B25.

15. Einstein, H.A., "The Bedload Function for Sediment Transportation in Open Channel Flows", U.S. Dept. Agric., Soil Conserv. Serv., Tech Bull., No. 1026, 1950.

16. Shen, H.W., "Hans A. Einstein's Contributions in Sedimentation", Jnl. Hyd. Div. ASCE, Vol. 101, No. HY5, Proc. Paper 11290, May 1975, pp.469-488.

17. Colby, B.R., "Scour and Fill in Sand-Bed Streams", U.S. Geol. Surv., Prof. Paper 462-D, 1964, 32p.

18. Henderson, F.M., "Open Channel Flow", Macmillan, London, 1966, p.383.

19. Hill, I.K., "Fluvial Sediment Transport at a Large Bed Shear Stress", Ph.D. Thesis, Univ. of Canterbury, N.Z., 1967, 238p.

20. White, W.R., Milli, H., Crabbe, A.D., "Sediment Transport:An Appraisal of Available Methods", Hyd. Res. Station, Wallingford, 2 Vols, Report No. INT 119, 1973.

21. Gunaratnam, D.J., Perkins, F.E., "Numerical Solutions of Unsteady Flow in Open Channels", M.I.T., Dept. Civil Eng., Hydrodynamics Lab. Report No. 127, 1970.

22. Henderson, F.M., "Flood Waves in Prismatic Channels", Jnl. Hyd. Div. ASCE, Vol. 89, No. HY4, Proc. Paper 3568, July 1963, pp.39-67.

23. Komura, S., Simons, D.B., "River-Bed Degradation Below Dams", Jnl. Hyd. Div. ASCE, Vol. 93, No. HY4, Proc. Paper 5335, July 1967, pp.1-13.

24. Tinney, E.R., "The Progress of Channel Degradation", Jnl. Hyd. Research, Vol. 67, No. 4, 1962.

25. Newton, C.T., "An Experimental Investigation of Bed Degradation in an Open Channel", Trans. of Boston Society of Civil Engineers, 1951.

26. Yalin, M.S., "Theory of Hydraulic Models", Macmillan, London, 1971, p.229.

27. Shields, A., "Application of Similarity Principles and Turbulence Research to Bed-load Movement", Berlin, 1936, English translation by W.P. Ott and J.C. van Uchelen, Caltech. publication 167.

28. Paintal, A.S., "Concept of Critical Shear Stress in Loose Boundary Open Channels", Jnl. Hyd. Research, Vol. 9, No. 1, 1971.

29. Vanoni, V.A., (et al) Closure to Discussion, Jnl. Hyd. Div. ASCE, Vol. 93, No. HY5, September 1967, pp.297-302.

30. Neill, C.R., Yalin, S.M., "Quantitative Definition of Beginning of Bed Movement", Jnl. Hyd. Div. ASCE, Vol. 95, No. HYl, January 1969, pp.585-587.

31. Neill, C.R., "A Re-examination of the Beginning of Movement for Coarse Granular Bed Materials", Unpublished report, Hyd. Res. Station, Wallingford, 1968.

32. Simons, D.B., Richardson, E.V., "Forms of Bed Roughness in Alluvial Channels", Jnl Hyd. Div. ASCE, Vol. 87, No. HY3, Proc. Paper 2816, May 1961, pp.87-105.

33. Znamenskaya, N.S., In Graf (4), p.285.

34. Simons, D.B., Richardson, E.V., "Flow in Alluvial Sand Channels", Chapter 9 of River Mechanics Vol. 1., (Ed. Shen), Colorado State University, Fort Collins, 1971, p.9-5.

35. Gee, D.M., "Bed Form Response to Nonsteady Flows", Jnl. Hyd. Div. ASCE, Vol. 101, No. HY3, Proc. Paper 11195, March 1975, pp.437-449.

36. Jensen, P.D., "Dune Formation under Nonsteady Conditions", Int. Assoc. Hyd. Research, 15th Congress, Paper A23, Turkey, 1973.

37. Simons, D.B., Richardson, E.V., "Stage Discharge Relations in Sand Channels", Int. Assoc. Hyd. Research, 15th Congress, Paper Al7, Turkey, 1973.

38. Sediment Transportation Mechanics: F, "Hydraulic Relations for Alluvial Streams", Jnl. Hyd. Div. ASCE, Vol. 97, No. HYl, Proc. Paper 7786, January 1971, pp.101-141.

39. Simons, D.B., Stevens, M.A., Duke, J.H., "Predicting Stages on Sand-Bed Rivers", Jnl. Waterways, Harbours and Coastal Eng. Div. ASCE, Vol. 90, No. WW2, Proc. Paper 9731, May 1973, pp.231-243.

40. Santos-Cayade, J., Simons, D.B., "River Response", Chapter 1 of Environmental Impact on Rivers, Ed. Shen, Colorado State University, Fort Collins, 1973.

41. Simons, D.B., Richardson, E.V., Hausild, W.L., "Depth Discharge Relations in Alluvial Channels", Jnl. Hyd. Div. ASCE, Vol. 88, No. HY5, Proc. Paper 3263, 1962, pp.57-72.

42. Walker, B.F.G., Scour at a Cylindrical Pier by Translation Waves", M.E. Thesis, Univ. of Canterbury, N.Z., 1975, 142p.

43. Chow, V.T., "Open Channel Hydraulics", McGraw-Hill, New York, 680p., 1959.

44. Keulegan, G.H., Patterson, G.W., "Mathematical Theory of Irrotational Translation Waves", Jnl. of Research, N.B. Standards, Vol. 30, No. 1, R.P. 1544, 1943.

45. Strelkoff, T., "One-Dimensional Equations of Open Channel Flow", Jnl. Hyd. Div. ASCE, Vol. 95, No. HY3, Proc. Paper 6557, May 1969, pp.861-876.

46. Strelkoff, T., "Numerical Solution of Saint-Venant Equations", Jnl. Hyd. Div. ASCE, Vol. 96, No. HYl, Proc. Paper 7043, January 1970, pp.223-252.

47. Grace, R.A., Eagleson, P.S., "Similarity Criteria in the Surface Runoff Process", M.I.T., Dept. Civil Eng., Hydrodynamics Lab. Report No. 77, 1965, p.2.

48. Brutsaert, W., "Review of Green's Functions for Linear Open Channel", Jnl. Eng. Mech. Div. ASCE, Vol. 99, No. EM12, Proc. Paper 10236, January 1973, pp.1247-1257.

49. Dooge, J.C.I., Harley, B.M., "Linear Routing in Uniform Open Channels", Int. Hydrology Symposium, Fort Collins, Paper 8, September 1967, pp.57-64.

50. Folk, R.L., "Petrology of Sedimentary Rocks", Hemphills, Texas, 1968, 170p.

51. Schlichting, H., "Boundary Layer Theory", McGraw-Hill, Verlag G. Braun (6th Edition), 1968.

52. Kamphuis, J.W., "Determination of Sand Roughness for Fixed Beds", Jnl. Hyd. Research, Vol. 12, No. 2, 1974.

53. Lane, E.W., Design of Stable Channels", Trans. ASCE, Vol. 120, 1955, pp.1234-1279.

54. Williams, G.P., "Flume Width and Water Depth Effects in Sediment-Transport Experiments", U.S. Geol. Surv., Prof. Paper 562-H, 1970, 37p.

APPENDIX A

THEORETICAL

A.1 DEFINITION AND BASIC PROPERTIES OF TRANSLATION WAVES

Translation waves belong to the non-steady flow regime (Chow [43]). Therein the depth and mean velocity of the flow vary both temporally and spatially.

Translation waves are gravity waves which have the particular property that the motion of all the fluid particles in a cross-section is sensibly the same at any given instant. As a translation wave passes, the liquid particles are displaced by an amount proportional to the volume of the wave. As far as open channels are concerned two extreme cases may be cited. Where the effect of friction is negligible and the volume and length of the wave is small, the disturbance is termed an irrotational translation wave. Examples include the solitary wave and surges produced by abrupt changes in flow at either end of an open channel.

In contradistinction to this is the case where the effect of friction is predominant, the effect of weight and inertia being small. This is the type of translation wave dealt with in this thesis. It is commonly known as a flood wave.

The mathematical theory of flood waves and other waves of translation has been presented by Keulegan [44]. Henderson [22] and Strelkoff [45], [46] consider more practical aspects, the latter author giving a comprehensive reference list.

A.2 GOVERNING EQUATIONS AND ASSUMPTIONS

A.2.1 Fluid Flow

The propagation process of long waves in open channels is described by the St. Venant Equations. These represent the conservation of mass

and momentum of fluid flow. Fundamental assumptions made in their derivation include:

(a) The flow is assumed to be one-dimensional thus centrifugal effects due to channel curvature and Coriolis effects are neglected.

(b) The pressure is assumed to be hydrostatic, i.e., vertical accelerations are neglected and the fluid density is presumed to be homogeneous.

(c) The effects of boundary friction and turbulence can be described by empirical resistance equations.

Many authors, for example, Keulegan [44] and Strelkoff [45] have derived these equations; it is not intended to rederive them here. However a definition sketch of their formulation for the special case of a wide uniform channel of constant slope with no lateral inflow is given below:

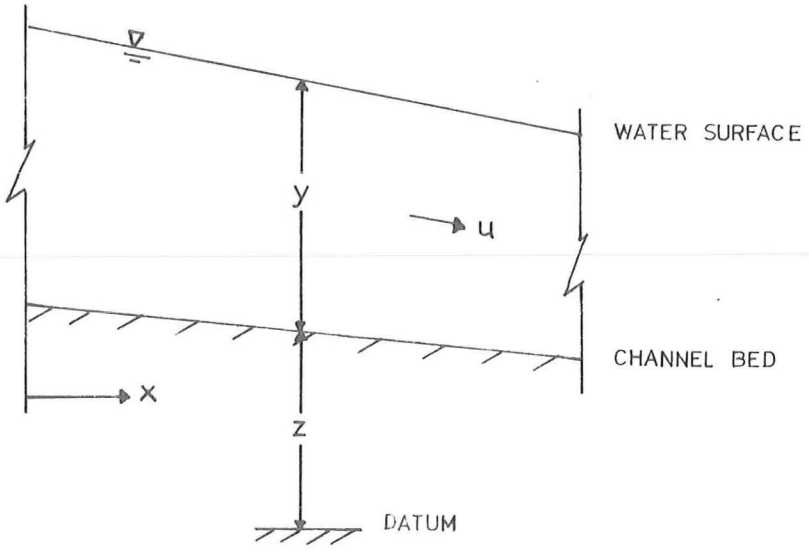

Fig.11 - DEFINITION SKETCH FOR THE MATHEMATICAL MODEL

Momentum Equation

$$\frac{\partial u}{\partial t} + u\frac{\partial u}{\partial x} + g\frac{\partial y}{\partial x} = g(S_o - S_f)$$

$$= g\left(\frac{\partial z}{\partial x} - \frac{u^2}{C^2 y}\right)$$

where the bed slope $S_o = -\frac{\partial z}{\partial x}$ and the friction slope $S_f = \frac{u^2}{C^2 y}$

using the Chezy Equation.

Alternatively, in terms of the discharge per unit width $q = uy$,

$$\frac{\partial q}{\partial t} + 2u\frac{\partial q}{\partial x} + \frac{\partial y}{\partial x}(gy - u^2) = gy\left[\frac{\partial z}{\partial x} - \frac{u^2}{C^2 y}\right] \quad \ldots (A.1)$$

Continuity Equation

$$u\frac{\partial y}{\partial x} + y\frac{\partial u}{\partial x} + \frac{\partial y}{\partial t} = 0$$

or

$$\frac{\partial q}{\partial x} + \frac{\partial y}{\partial t} = 0 \quad \ldots (A.2)$$

A.2.2 Sediment Flow

The sediment motion may be described by the Exner Erosion Equation (a continuity equation) and, in the absence of a momentum equation, an empirical steady flow equilibrium transport formula is used. In terms of the definition sketch these are:

Continuity Equation

$$\frac{\partial g_s}{\partial x} + B\frac{\partial z}{\partial t} = 0 \quad \ldots (A.3)$$

where g_s is the sediment discharge per unit width in dry weight and B = bulk specific dry weight of bed sediment, which expressed in terms of the bed porosity p becomes

$$B = \gamma S_s (1 - p)$$

Equilibrium Transport Equation

Written as a rating relation this is

$$g_s = a q^b \qquad \ldots (A.4)$$

where a , b are constants.

The role of the various terms is as follows:

$\frac{\partial u}{\partial t}$ - acceleration due to time variation in velocity

$u \frac{\partial u}{\partial x}$ - acceleration due to spatial variation in velocity

$g \frac{\partial y}{\partial x}$ - pressure force term

$g \frac{\partial z}{\partial x}$ - gravity body force due to bed slope

$g \frac{u^2}{C^2 y}$ - frictional force effects

$\frac{\partial y}{\partial t}$ - rate of rise term which gives storage changes due to water surface elevation changes with time

$y \frac{\partial u}{\partial x}$, $u \frac{\partial y}{\partial x}$ - wedge storage term due to areal variations in velocity.

$B \frac{\partial z}{\partial t}$ - rate of rise term which gives storage changes due to bed elevation changes with time

$\frac{\partial g_s}{\partial x}$ - storage term due to areal variations in sediment discharge

The set of equations (A.1) to (A.4) constitute a mathematical description of non-steady, gradually varying two phase flow in a wide, uniform open channel of constant slope.

A.3 SIMILARITY PARAMETERS

If the partial differential equations governing the system of 3.2.2. Case 1(b) are normalized with respect to appropriate reference parameters then the resulting coefficients are the similarity parameters. (Grace and Eagleson [47]).

The equation set (A.1) to (A.4) of A.2.1,2 can be rewritten more conveniently as follows:

$$\frac{\partial u}{\partial t} + u\frac{\partial u}{\partial x} + g\frac{\partial y}{\partial x} = g\left(\frac{\partial z}{\partial x} - \frac{\tau}{\gamma y}\right)$$

$$\frac{\partial y}{\partial t} + u\frac{\partial y}{\partial x} + y\frac{\partial u}{\partial x} = 0$$

$$\frac{\partial z}{\partial t} + \frac{1}{B}\frac{\partial g_s}{\partial x} = 0$$

Definition of the dimensionless variables

$$V_* = \frac{u}{U}\ ,\quad z^* = \frac{z}{D}\ ,\quad y_* = \frac{y}{Y}\ ,\quad \tau_* = \frac{\tau}{\tau_o}\ ,\quad g_{s_*} = \frac{g_s}{g_{so}}$$

$$x_* = \frac{x}{L} \qquad t_* = \frac{t}{T}$$

where U, D, Y, τ_o, g_{so}, L, T are reference parameters and substitution into the above set of equations gives

$$\frac{\partial V}{\partial t_*} + \left(\frac{TU}{L}\right) V_* \frac{\partial V_*}{\partial x_*} + \left(\frac{TgY}{UL}\right)\frac{\partial y_*}{\partial x_*} = \left(\frac{TgD}{LU}\right)\frac{\partial z_*}{\partial x_*} - \left(\frac{T\tau_o}{\rho YU}\right)\frac{\tau_*}{y_*}$$

$$\frac{\partial y_*}{\partial t_*} + \left(\frac{TU}{L}\right)\frac{\partial y_*}{\partial x_*} + \left(\frac{TU}{L}\right)\frac{\partial v_*}{\partial x_*} = 0$$

$$\frac{\partial z_*}{\partial t_*} + \left[\frac{Tg_{so}}{DLB}\right]\frac{\partial g_{s_*}}{\partial x_*} = 0$$

Then the similarity parameters are

$$\left(\frac{UT}{L}\right) \quad , \quad \left(\frac{TgY}{LU}\right) \quad , \quad \left(\frac{TgD}{LU}\right) \quad , \quad \left(\frac{T\tau_o}{\rho YU}\right) \quad , \quad \left(\frac{Tg_{so}}{DLB}\right)$$

The reference parameter scales are therefore

$$\lambda_u = \frac{\lambda_L}{\lambda_T}$$

$$\lambda_y = \frac{\lambda_u \lambda_L}{\lambda_T}$$

$$\lambda_L = \frac{\lambda_T \lambda_D}{\lambda_u}$$

$$\lambda_T = \frac{\lambda_y \lambda_u}{\lambda_{\tau_o}}$$

$$\lambda_D = \frac{\lambda_T \lambda_{g_{so}}}{\lambda_L}$$

As geometric similarity has been provided (3.3.4)

$$\lambda_D = \lambda_Y = \lambda_L$$

and the scaling relationships become

$$\lambda_u = \sqrt{\lambda_L}$$

$$\lambda_T = \sqrt{\lambda_L}$$

$$\lambda_{\tau_o} = \lambda_L$$

$$\lambda_{g_{so}} = (\lambda_L)^{1.5}$$

A.4 PROPERTIES OF LINEARISED GOVERNING EQUATIONS

A.4.1 Linearisation

The governing equations expressed in terms of the water discharge per unit width are:

$$\frac{\partial q}{\partial t} + 2u \frac{\partial q}{\partial x} + \frac{\partial y}{\partial x}(gy - u^2) = gy\left(\frac{\partial z}{\partial x} - \frac{q^2}{C^2 y^3}\right) \quad \ldots (A.5)$$

$$\frac{\partial q}{\partial x} + \frac{\partial y}{\partial t} = 0 \quad \ldots (A.6)$$

$$\frac{\partial g_s}{\partial x} + B \frac{\partial z}{\partial t} = 0 \quad \ldots (A.7)$$

$$g_s = a q^b \qquad a,b \text{ constant} \quad \ldots (A.8)$$

Equations (A.7) and (A.8) combined give

$$b a q^{b-1} \frac{\partial q}{\partial x} + B \frac{\partial z}{\partial t} = 0 \quad \ldots (A.9)$$

These equations may be linearised by the method of small perturbations, i.e. the variables are written as

$$q = q_o + q' \ , \quad y = y_o + y' \ , \quad u = u_o + u' \ , \quad z = z_o + z'$$

where the subscripts indicate reference parameters and the superscripts small variations. Substitution of these relations into (A.5), (A.6) and (A.9) yields, after dropping powers and products of the primed variables and their differentials as second order quantities

$$\frac{\partial q'}{\partial t} + 2u_o \frac{\partial q'}{\partial x} + (gy_o - u_o^2) \frac{\partial y'}{\partial x} = gy_o \left[\frac{\partial z'}{\partial x} - \frac{-\frac{\partial z_o}{\partial x} - \frac{q_o^2}{C^2 y_o^3}}{\left(1 + 3\frac{y'}{y_o}\right)}\left(1 + \frac{2q'}{q_o}\right)\right] \quad \ldots (A.10)$$

$$\frac{\partial q'}{\partial x} + \frac{\partial y'}{\partial t} = 0 \qquad \ldots (A.11)$$

$$G_o \frac{\partial q'}{\partial x} + B \frac{\partial z'}{\partial t} = 0 \qquad \ldots (A.12)$$

where $G_o = b\, a\, q_o^{b-1}$

Differentiation of equations (A.11) and (A.12) with respect to x gives

$$\frac{\partial y'}{\partial x \partial t} = - \frac{\partial^2 q'}{\partial x^2} \qquad \ldots (A.13)$$

$$\frac{\partial z'}{\partial x \partial t} = - \frac{G_o}{B} \frac{\partial^2 q'}{\partial x^2} \qquad \ldots (A.14)$$

Equation (A.10) after differentiation with respect to t and substitution of (A.13) and (A.14) becomes

$$\frac{\partial^2 q'}{\partial t^2} + 2u_o \frac{\partial^2 q'}{\partial x \partial t} - \left[gy_o \left[1 + \frac{G_o}{B}\right] - u_o^2 \right] \frac{\partial^2 q'}{\partial x^2}$$

$$= - \frac{g q_o^2}{C^2 y_o^2} \left[\frac{2}{q_o} \frac{\partial q'}{\partial t} - \frac{3}{y_o} \frac{\partial y'}{\partial t} \right] \qquad \ldots (A.15)$$

Writing $C^2 = \dfrac{u_o^2}{y_o S_o}$ and substituting for $\dfrac{\partial y'}{\partial t}$ from (A.11) transforms (A.15) to

$$\left[gy_o \left(1 + \frac{G_o}{B}\right) - u_o^2 \right] \frac{\partial^2 q}{\partial x^2} - 2u_o \frac{\partial^2 q}{\partial x \partial t} - \frac{\partial^2 q}{\partial t^2} - 3gS_o \frac{\partial q}{\partial x} - \frac{2gS_o}{u_o} \frac{\partial q}{\partial t} = 0 \qquad \ldots (A.16)$$

where the prime notation is omitted for convenience.

(A.16) is a linear, second order, homogeneous, hyperbolic partial differential equation.

A.4.2 Effect of Sediment on Wave Motion

A systems engineering approach may be used to solve this problem. That is, since Eq. (A.16) is linear it is only necessary to determine the solution for a delta function input. For any other inflow, it is only necessary to convolute the impulse response with the actual inflow. Dooge and Harley [49] solved a similar equation to (A.16) - it differed only in the coefficients. The first and second moments of their solution, modified for this case, are

$$M_1 = \frac{x}{1.5u_o}$$

$$M_2 = {}^2/_3 \left(1 - \frac{Fr_s^2}{4}\right)\left(\frac{y_o}{S_o x}\right)\left(\frac{x}{1.5u_o}\right)^2$$

M_1 is the average speed of propagation of the disturbance and is unaffected by the presence of moving sediment. M_2 indicates that the spread or diffusion of the disturbance will be altered by the term Fr_s^2.

Now $$Fr^2 = \frac{u_o^2}{gy_o}$$

and $$Fr_s^2 = \frac{u_o^2}{gy_o(1 + \frac{G_o}{B})}$$

so $$\frac{M_2(\text{mobile bed})}{M_2(\text{fixed bed})} = \frac{(1 - Fr_s^2/4)}{(1 - Fr^2/4)} < 1\ \% \qquad \ldots (A.17)$$

since $\frac{G_o}{B} << 1$.

where typical natural river values $Fr^2 \simeq 0.4$ $B = 0[10^4]$ $G_o = 0[10^1]$ are taken.

The result indicates that the presence of moving bedload has a negligible effect on the dynamics of the wave motion. It follows from this that the velocity of the dynamic forerunner is also reduced only very slightly. This velocity, co_1, is given by Dooge and Harley [49] as

$$co_1 = u + (gy)^{1/2}$$

which modified for the movable bed situation becomes

$$co_1 = u + \left(gy\,(1 + \frac{G_o}{B})\right)^{1/2}$$

The above result (A.17) implies that

$$\frac{co_1(\text{mobile})}{co_1(\text{fixed})} < 1\,\%$$

When bedforms are present the flow resistance is increased. This has the effect of reducing the wave speed and enhancing subsidence in the crest region of non-kinematic waves. Henderson [22] expresses the subsidence equation in general form as

$$\frac{\partial y}{\partial x} = \frac{y_o}{2p_o S_o c_o^2} \frac{\partial^2 y}{\partial t^2} \left(1 - \frac{Fr^2}{4}\right) \qquad \ldots \text{(A.18)}$$

p_o constant

and the resistance equation as

$$v = C R^j S^{\frac{1}{2}} \qquad \ldots \text{(A.19)}$$

j constant

Now the value of the Chezy C may be 52 in the fixed bed case and 33 if bedforms are present (Eqs. 11.91, 11.94 Graf [4] p.317). Since y_o, c_o, Fr are functions of C, it is clear that the effect is considerable.

For example, if a wave passes from a fixed to a movable bed of the same slope in the ideal test reach then if the discharge near the wave peak remains approximately constant the resistance equation (A.19) implies

f = fixed bed

m = movable bed

$$\frac{ym}{yf} = \left(\frac{Cf}{Cm}\right)^{\frac{2}{3}} \qquad R^j = y^{1/2}$$

and $$\frac{uf}{um} = \left(\frac{Cf}{Cm}\right)^{\frac{2}{3}}$$

Assume that (Henderson [22]) $c_o = \frac{3}{2} u \{1 + \frac{1}{3r^2}\}$

$r = S_w/S_o$

c_o = wave velocity

$$\simeq \frac{3}{2} u \quad \text{since } r > 10$$

then $$\frac{uf}{um} \simeq \frac{c_{o_f}}{c_{o_m}}$$

The relative subsidence is, from (A.18)

$$\frac{\left(\frac{dy}{dx}\right)_m}{\left(\frac{dy}{dx}\right)_f} \simeq \frac{ym}{yf} \left(\frac{uf}{um}\right)^2$$

since $Fr^2 < 0.5$

If the aforementioned values of C are introduced

$$\frac{\left(\frac{dy}{dx}\right)_m}{\left(\frac{dy}{dx}\right)_f} \simeq \left(\frac{Cf}{Cm}\right)^{\frac{2}{3}} \left(\frac{Cf}{Cm}\right)^{\frac{4}{3}} = \left(\frac{Cf}{Cm}\right)^2 \simeq 2.5$$

That is $c_{o_m} < c_{o_f}$ and $\left(\frac{dy}{dx}\right)_m > \left(\frac{dy}{dx}\right)_f$.

APPENDIX B

APPARATUS

B.1 THE FLUME

The flume has been described in detail by Hill [19]. It consists, in essentials, of a flat steel plate deck, 27.5 m in length, with a working section of 20 m. Adjustable side walls which form the channel allow a maximum width of 2.6 m. These are constructed of steel plate except for a 7 m section of 19 mm thick plate glass located 8 m downstream from the inlet. Slope changes may be made by the use of screw jacks at the midpoint and upper end of the flume, the downstream support being freely hinged.

B.2 SEDIMENT HOPPER (FIG. 12, PLATE 4)

In order that sediment could be added to the flow at both constant and variable rates a dispensing hopper was designed and built. It was constructed in stainless steel in the shape of a four sided truncated pyramid. Principal features were;

1) A variable width, screw operated, sliding gate with attached scale.
2) A lug mounted constant speed Sinex rotary electric vibrator (A. Series) affixed to the base of the hopper. This machine ensured that the flow rate was constant for a particular gate setting.

Extensive calibration tests were carried out. It was found that the relationship between outflow rate (gm/sec) and gate opening was linear and independent of the falling shingle head until the hopper was nearly empty. Furthermore a triangular hydrograph could be generated successfully by small step changes in the sediment discharge.

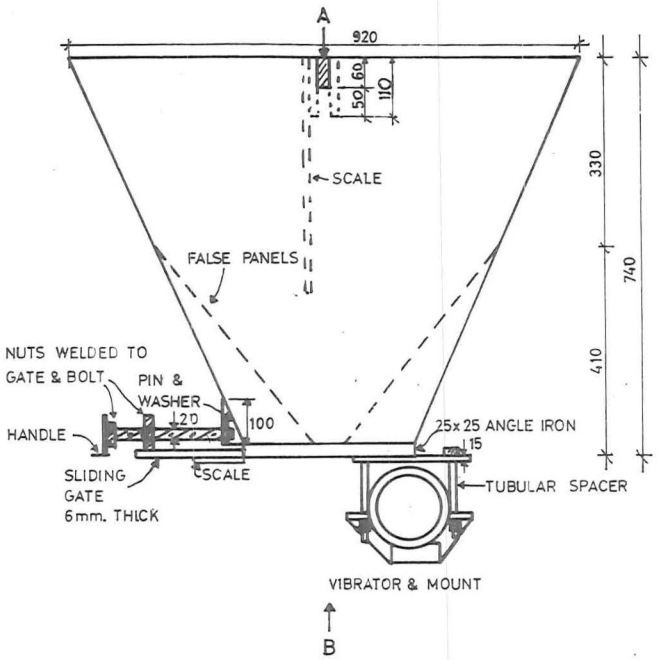

SIDE ELEVATION

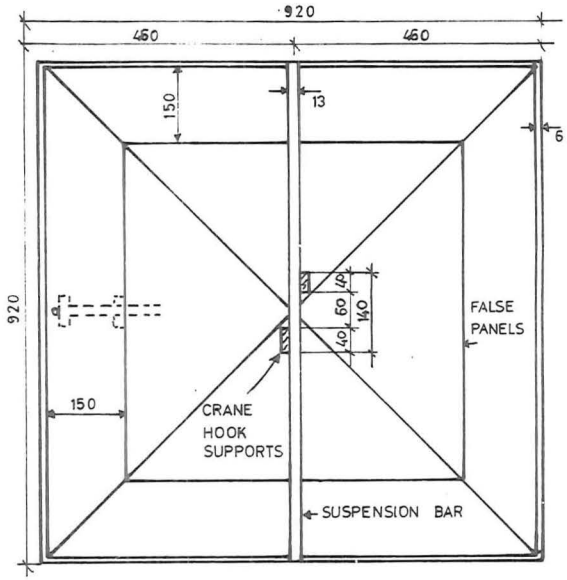

VIEW A

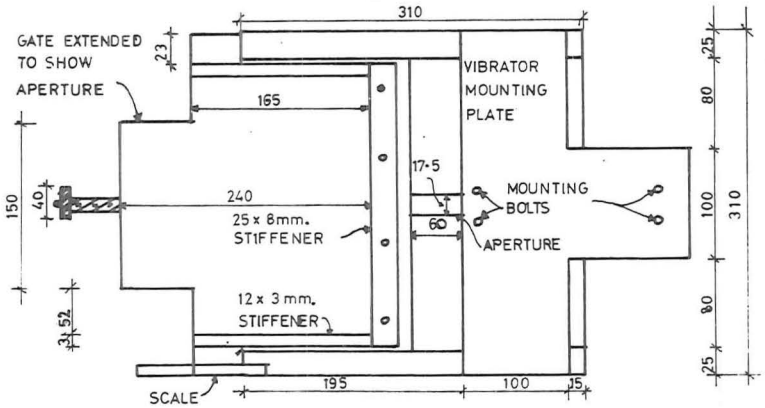

VIEW B

CONSTRUCTION DETAILS

MATERIAL - Mild steel

CONNECTIONS - Welded unless otherwise shown

VIBRATOR - SINEX SERIES "A"
2860 rpm, 50 cycles, constant speed.

DIMENSIONS IN MILLIMETRES

Fig.12 - SEDIMENT DISPENSING HOPPER

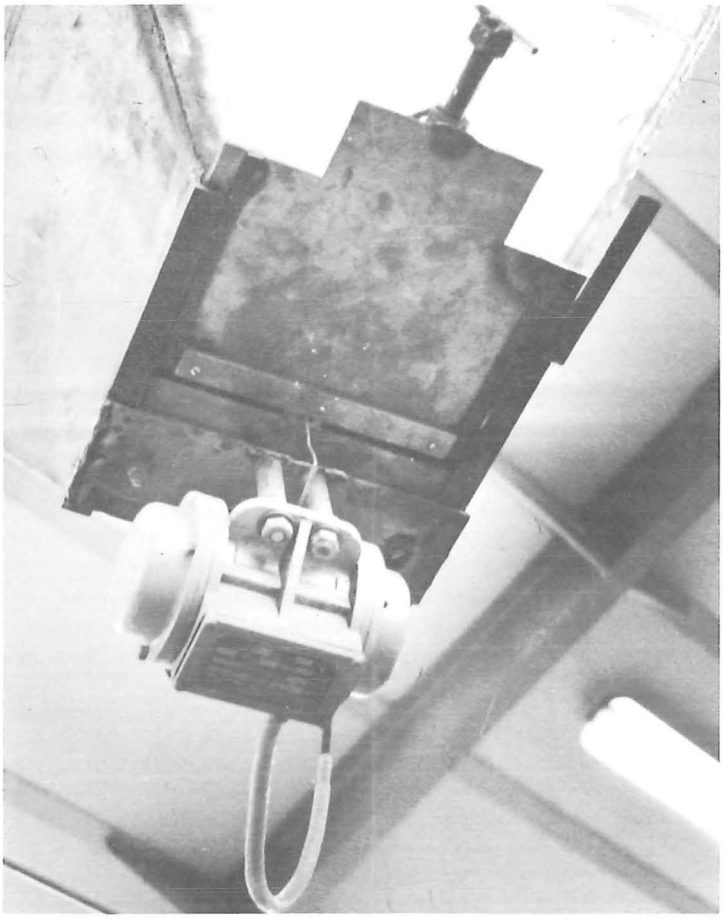

Plate 4 - VIEW FROM BELOW OF SEDIMENT DISPENSING HOPPER

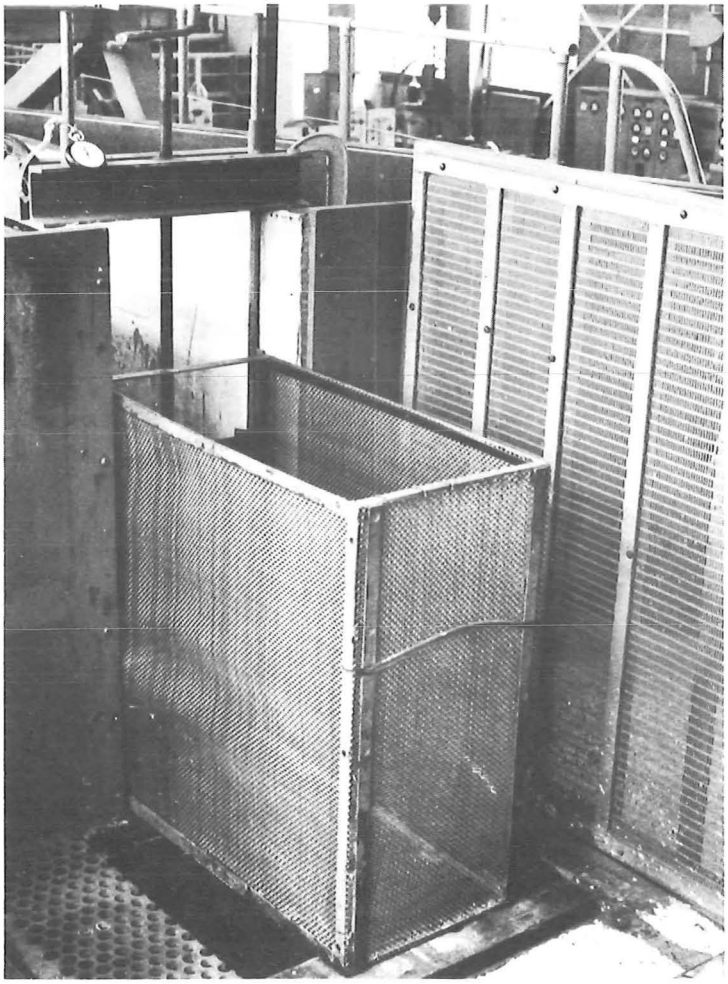

Plate 5 – VIEW FROM DOWNSTREAM OF SERIES II BEDLOAD SAMPLING DEVICE

Specifications and hopper design are presented in Fig. 12 and Plate 4.

B.3 SEDIMENT MEASURING DEVICES

Different devices were used for the two series of experiments.

B.3.1 Bedload Sampler (Series II) (Fig. 4, Plate 5)

This consists of a steel frame (0.61 x 0.61 x 0.29 m) enclosed on the base and three sides by 3 mm mesh. Handles were attached midway down the rear closed side and in top front. It was placed adjacent to the downstream side of the underflow gate (B.5.1). Water issued from the flume (0.15 m high), in the form of a free overfall, through the base of the sampler and into the outflow water hopper and settling tank (Fig. 4). Sediment was retained by the mesh. (Plate 5).

B.3.2 Continuous Bedload Recorder (Series III)(Fig. 13, Plate 3)

A continuous cumulative weight recording device was designed and constructed using the load cell principle. It was positioned immediately downstream of the test section. Here a rectangular hole was cut in the flume deck and an enclosed steel box was bolted onto the underside so as to cover the opening. Suspended within this box by high tensile cables and rod was a mesh basket. Above the opening was placed a steel plate grid consisting of transverse members only. This was mounted on legs to bring it to the level of the raised gravel bed, its purpose being to provide commensurate roughness and to entrain the sediment into the basket by virtue of the vortices existing between the grid members. A piece of galvanised steel was laid over the upstream half of the grid so as to direct the sediment into the centre section of the basket. Thus the collected material formed a cone shape which kept the basket balanced and prevented it from skewing and touching the walls or base of the trap. Spacings for the grid members and the length of the galvanised steel was determined by trial and error; the dimensions of the trap being dictated by the estimated bedload and structural constraints imposed by the flume.

The suspending rod was attached by way of a universal joint to a shaft which passed through the hollow centre section of a cylindrical strain gauge and was restrained vertically by being bolted to a circular steel disc covering the top of the gauge. The gauge itself therefore bore the weight of the sediment basket and bedload. It was mounted on the base plate of a rectangular steel frame which was supported by a universal joint and screw to a gantry, the legs of which were bolted to the deck on either side of the channel. Output from the gauge, after amplification, was displayed as a voltage by a digital voltmeter. At the completion of a run the sediment basket was lowered to the floor of the trap, the suspending rod was uncoupled and the galvanised steel and grating were removed. The laboratory crane was used to lift the basket which, after emptying, was replaced and the device was reassembled in reverse order.

Calibration tests showed that;

1) The relationship between the immersed weight of the basket and the output voltage was linear.
2) The motion of the water in the channel did not effect the stability of the basket nor the recordings.
3) Almost all the bedload dropped into the centre portion of the basket over the downstream edge of the galvanised plate, a negligible amount overpassing the trap completely.
4) The strain gauge was sensitive to a mass change of 35 gm.
5) The accuracy of the device was determined by repeated tests and found to be $\pm$ 0.001 volts = $\pm$ 0.035 kg. This applies to any measurement and consequently the percentage error was greater when the basket contained little sediment. However this was of small importance as relative weight was the parameter of interest.

The specifications and layout of the recorder are given in Fig. 13 and Plate 3.

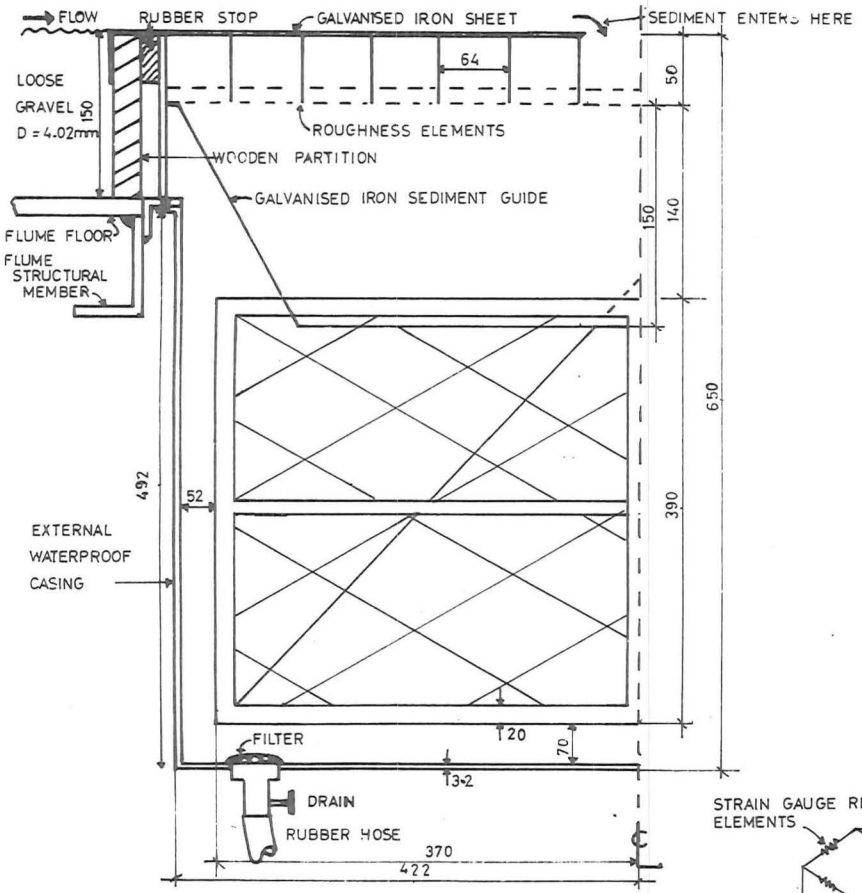

ELEVATION

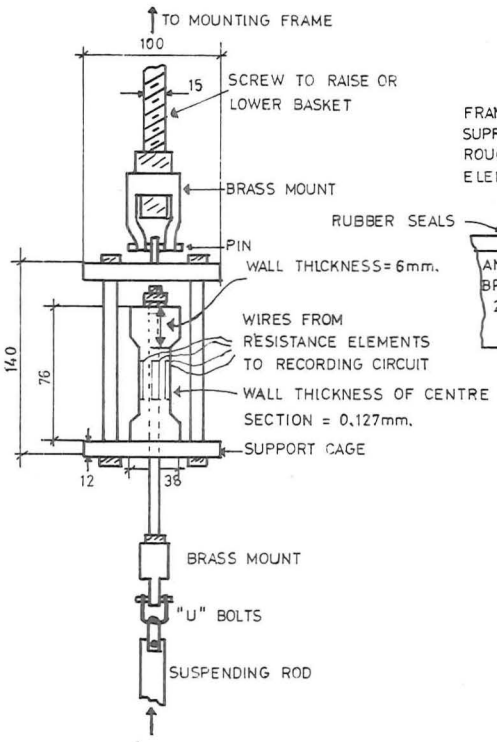

DETAIL
STRAIN GAUGE UNIT

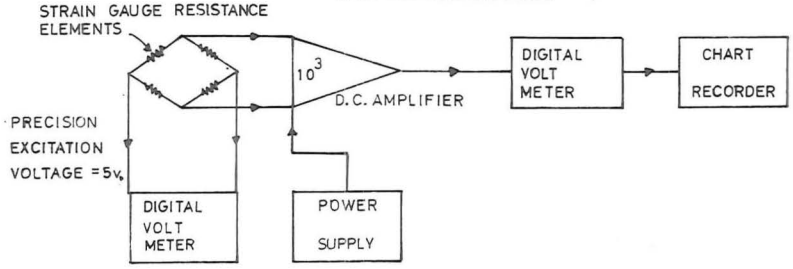

CIRCUIT DIAGRAM

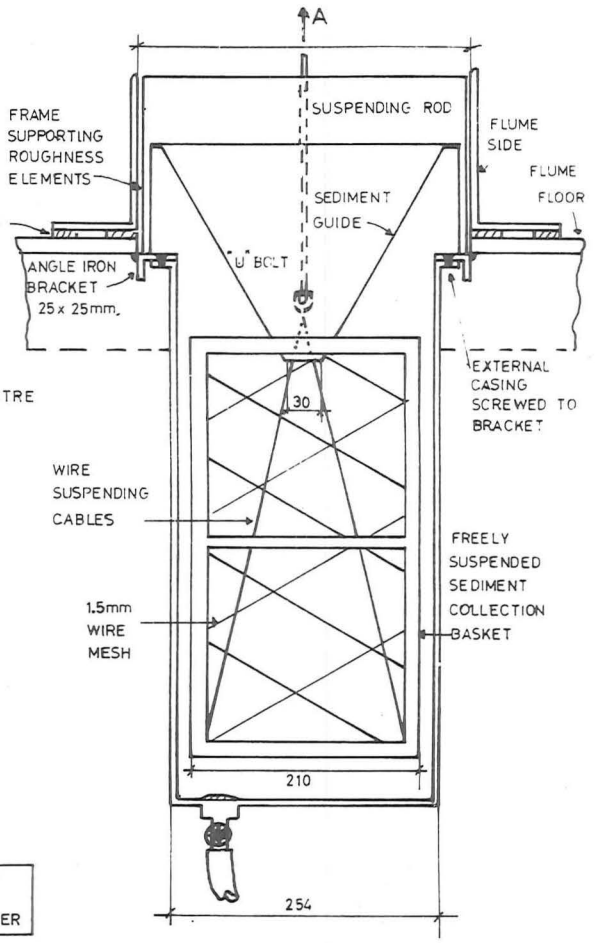

END ELEVATION

CONSTRUCTION DETAILS

MATERIAL - Mild steel unless otherwise shown

CONNECTIONS - Welded " " "

DIMENSIONS IN MILLIMETRES

Fig.13 - CONTINUOUS RECORDING BEDLOAD COLLECTOR

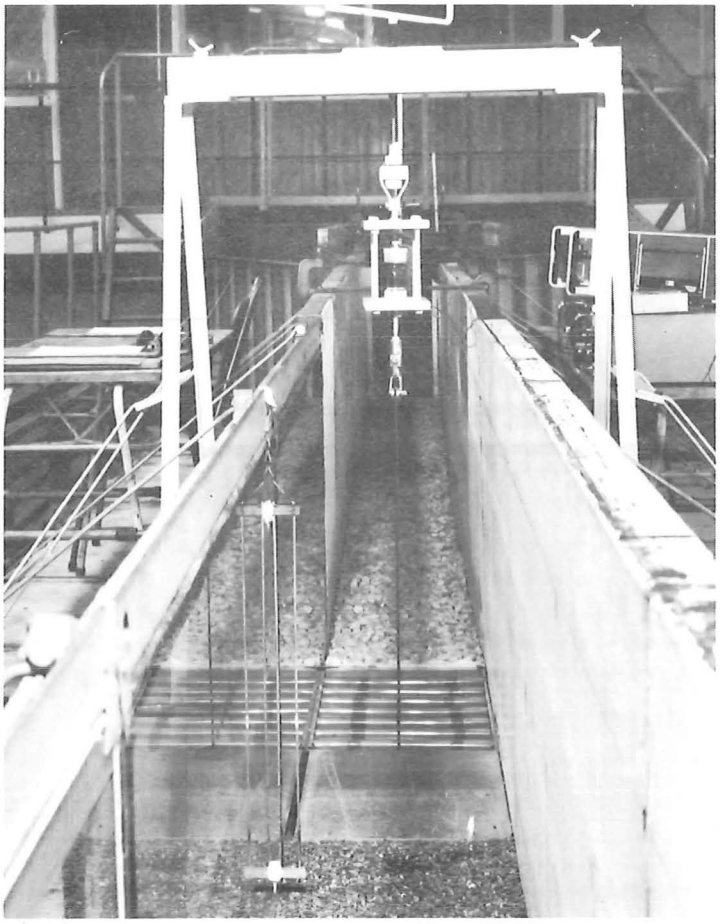

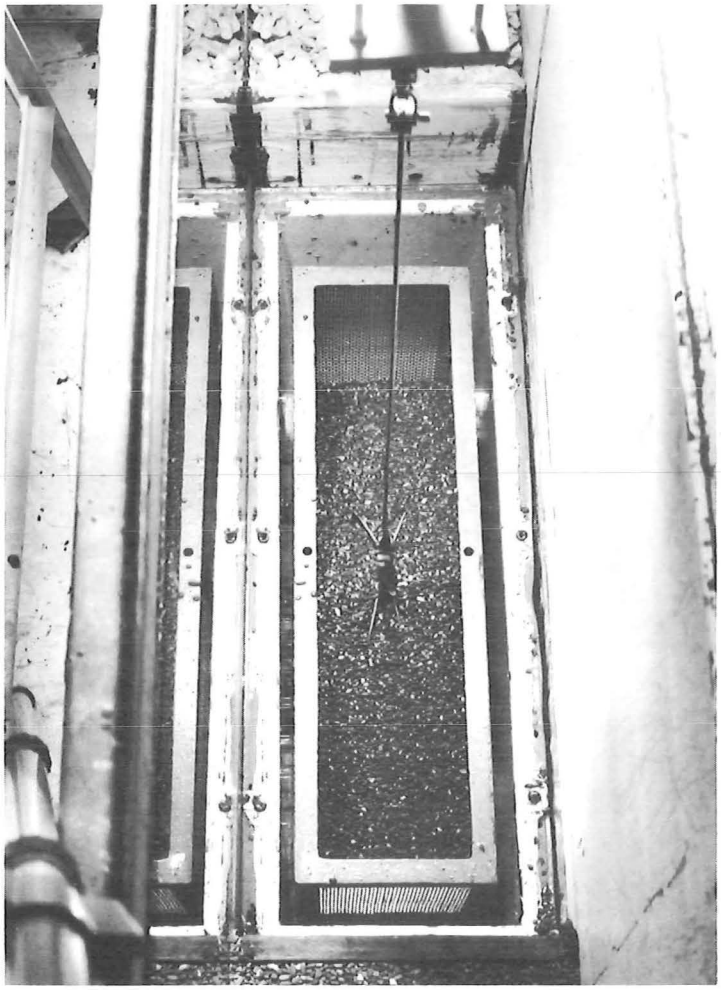

Plate 3 - VIEW FROM UPSTREAM (Top plate) AND ABOVE (Bottom plate)

OF CONTINUOUS RECORDING BEDLOAD COLLECTION DEVICE

B.4 WATER LEVEL RECORDERS (FIG. 4, PLATE 6)

Two recorders were constructed. Each consisted of two 3.18 mm diameter stainless steel rods 0.455 m long anchored at both ends in rectangular perspex blocks and spaced about a distance of 26 mm. They were attached with glue to the flume walls with the 26 mm spacing at right angles to the flow. Only the lower block was submerged, it having been given an aerofoil shape to reduce flow disturbance. The rods of a particular recorder were connected to a circuit which measured the impedance between them as they became immersed in water and transmitted the results as a voltage to a Hewlett-Packard chart recorder. Unfortunately this output was non-linear so a calibration scale had to be constructed. However this disadvantage was offset by the fact that the depth could be measured continuously (Fig. 4, Plate 6).

B.5 ADJUSTABLE TAILGATE AND WEIR

B.5.1 Tailgate (Series II) (Plate 8)

A standard underflow gate was built. Two channel sections (420 x 75 x 38 mm) were bolted together and secured by two cylindrical spacers welded between them 0.27 m apart. Two (0.915 m x 16 mm (D)) steel rods passed vertically through the spacers and were attached to a (0.3 m x 0.3 m x 4 mm) blade. Movement of the blade was controlled by a centrally mounted screw and handle. A scale was etched on one of the support rods and the device was affixed across the top of the channel walls and was restrained by screw clamps.

B.5.2 Weir (Series III) (Plate 9)

This was of the submerged knife-edge type and was constructed simply by modifying the tailgate. The controlling screw mounting was shifted from the reduced blade (0.155 x 0.3 m) to a horizontal strut welded between the support rods 0.49 m above the blade.

Plate 6 - CONTINUOUS DEPTH RECORDING PROBE

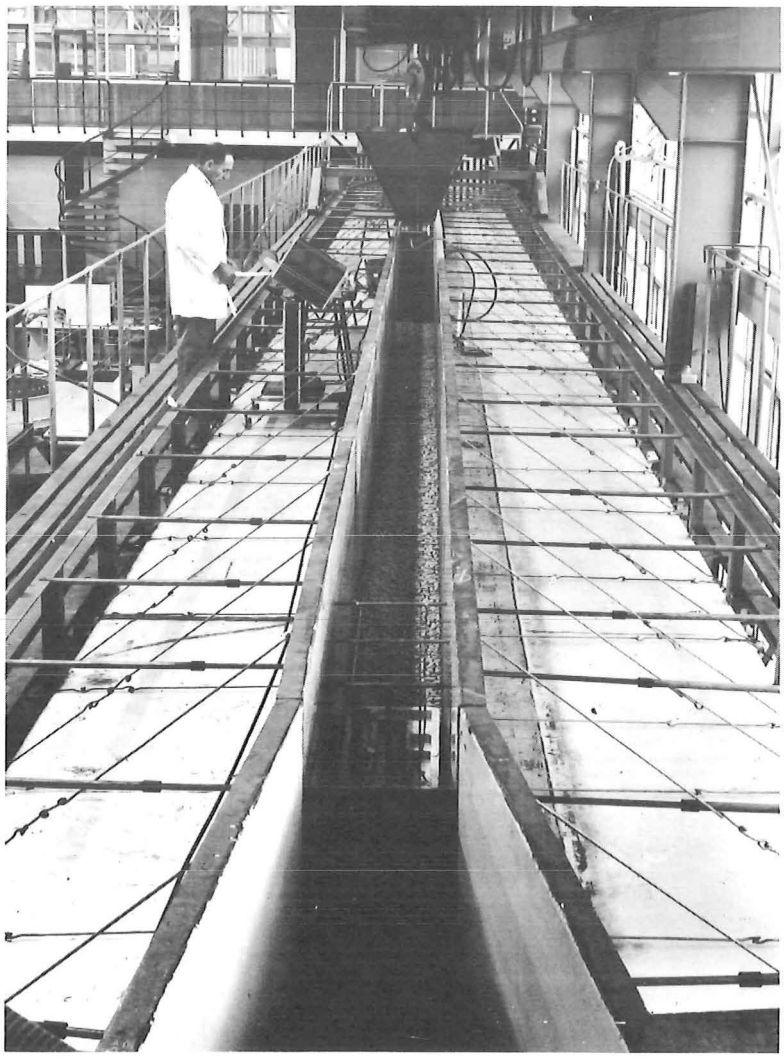

Plate 7 – VIEW FROM UPSTREAM OF FIXED BED AND INLET STRUCTURES

Plate 8 - VIEW FROM DOWNSTREAM OF UNDERFLOW TAILGATE

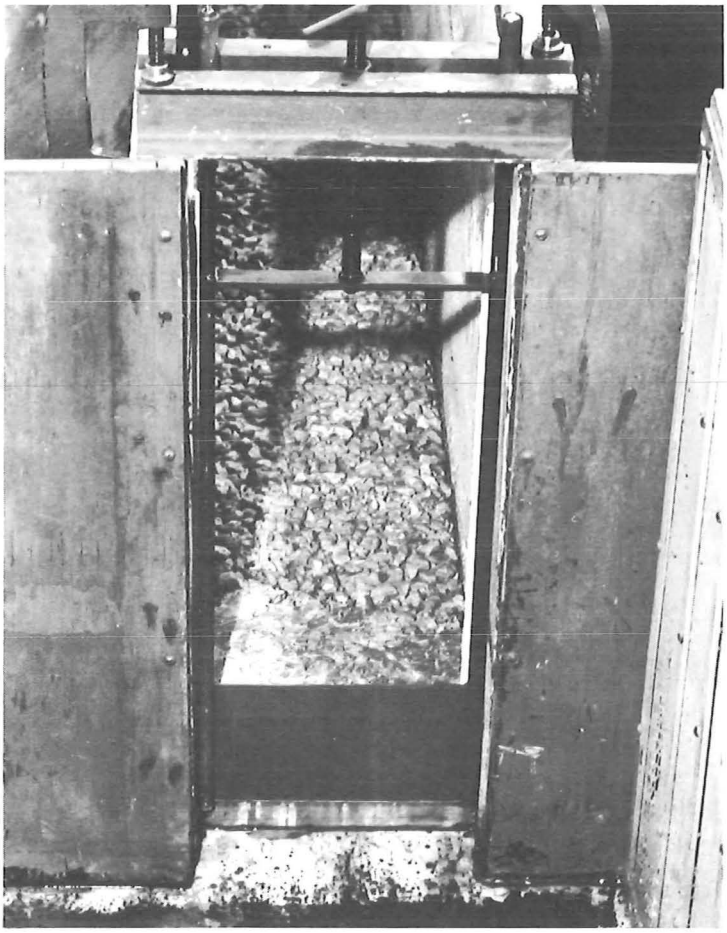

Plate 9 - VIEW FROM DOWNSTREAM OF SUBMERGED WEIR

When the weir was in position in the flume quarter-round wooden beading was fixed to the flume walls on the upstream side of the exposed lateral rods to reduce flow disturbance. (Plate 9.)

B.6 WATER INFLOW SMOOTHING AND ALIGNING DEVICE (FIG. 4, PLATE 7)

Three devices were used to smooth the water surface and align the flow after it entered the storage area at the upper end of the flume. A coarse screen was placed at the transition point between this area and the channel. The flow alignment device consisted of three 0.6 m x 0.6 m x 4 mm mild steel plates welded at 78 mm spacings to a base plate. This, with a weight on top, was positioned 0.55 m downstream of the screen in the channel itself. Disturbances of the water surface were removed - although they developed again downstream for a different reason* - by a float board of dimensions 0.5 m x 0.3 m x 20 mm which was placed on the water surface 0.3 m downstream of the 'flow straightener'. The float was restrained in this position by two guy wires (Fig. 4, Plate 7).

B.7 PROPERTIES OF THE BED SEDIMENT (FIG. 14, PLATE 10)

The bed sediment was obtained locally from a Late Pleistocene beach deposit termed the 'Kaiapoi Grit'. It was sieved to within 3 - 5 mm limits. Two random samples of 1 kg each were subjected to size analysis by standard procedures (Folk [50]). No significant difference was found between the samples and results are given in Fig. 14. Relevant properties of the sediment include:

A) Petrology	% Composition
1) Light grey, very well indurated, rounded to well rounded, very fine to fine sand size, submature feldsarenite	66%

* due to slight irregularities on the flume walls, and the transition from fixed to movable bed

2) As in 1) but containing quartz and/or prehnite veins	20%
3) As in 1) but fine sand size	12%
4) Chert	2%
	100%

+ trace of shell fragments

where the Powers and Wentworth scales are used.

B) Size

Sediment size was log normally distributed

D_{50} = 4.02 mm (pebble size gravel)

G.S.D. = 1.16

C) Shape Factor

0.21 < S.F. < 0.75

S.F. (mean) = 0.54

D) Specific Gravity

S_s = 2.65 ± 0.01

E) Surface Texture

S.T. = smooth

F) Fall Velocity

W(mean) = 0.24 m/sec.

(Plate 10.)

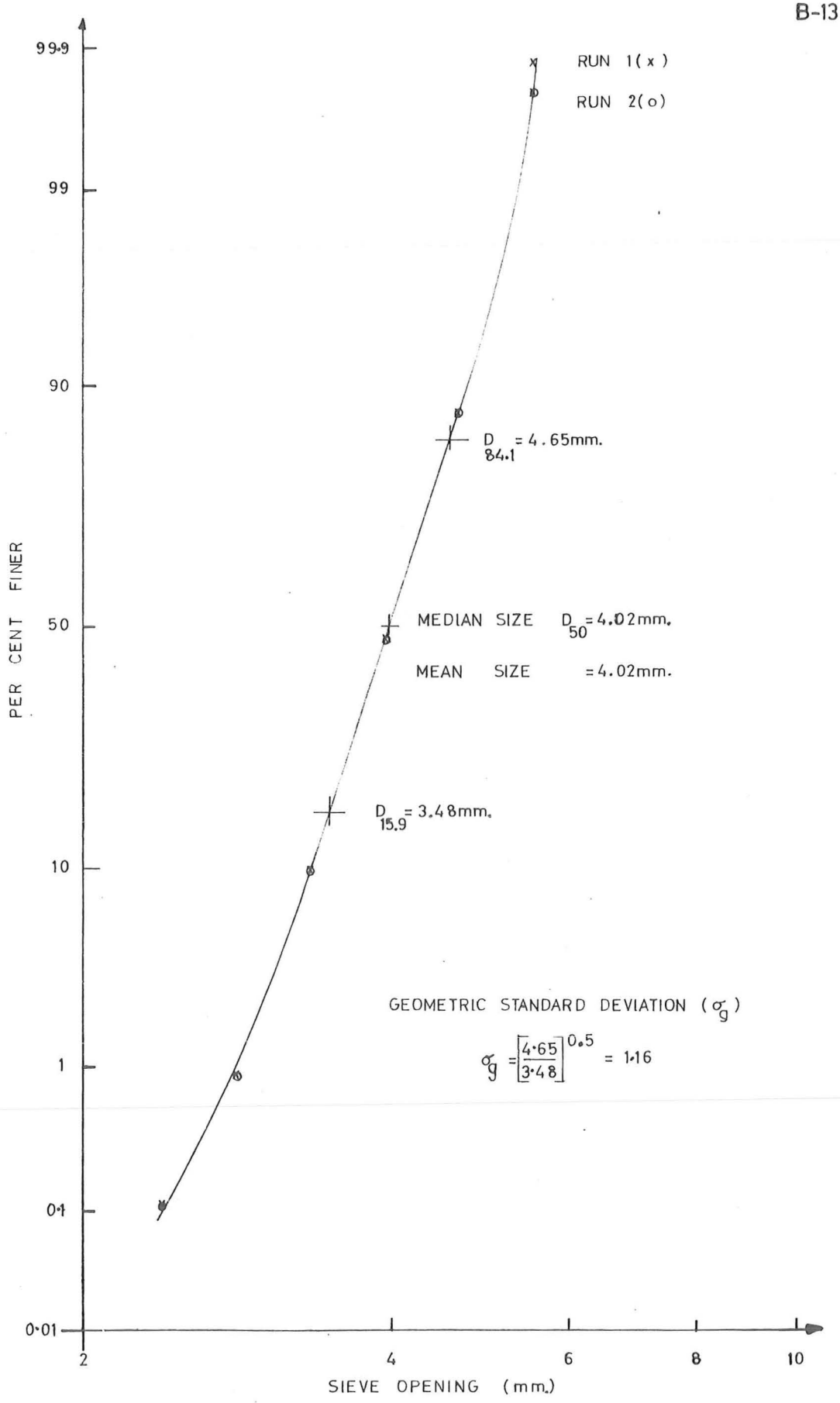

Fig.14 – CUMULATIVE LOGARITHMIC – PROBABILTY SIZE FREQUENCY GRAPH FOR BED MATERIAL

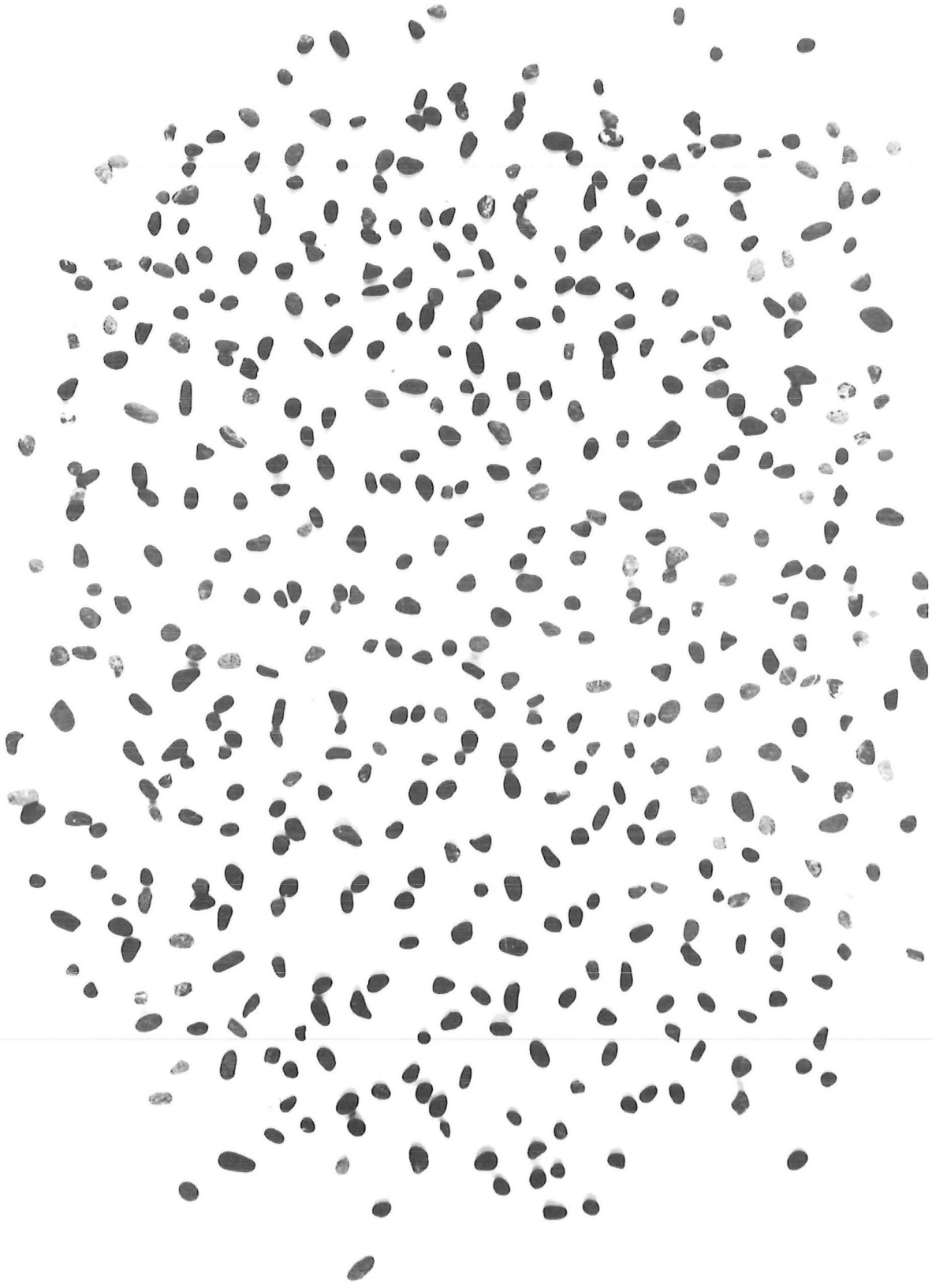

Plate 10– PARTICLE SHAPE (D = 4·02 mm)

APPENDIX C

EXPERIMENTAL DESIGN AND MEASUREMENTS

C.1 FIXED BED LENGTHS AND ROUGHNESS VARIATIONS

C.1.1 Fixed Bed Lengths

The surface of the gravel bed placed in the flume was fixed in the upper region where the turbulent boundary layer developed and in the lower region where backwater effects associated with the outflow occurred. Therefore these and other non-uniformities in the flow were separated from the test section. A fluid mixture of cement and water was lightly sprayed over the 22 mm gravel chip composing the upper bed layers in these areas. After hardening it proved to be a durable seal coat. Fixed bed lengths were determined as follows;

a) Inflow Region

The analogy of the turbulent boundary layer development on a uniformly rough plate is taken. For a given depth of flow y and Nikuradse sand roughness k_s we require to know the distance from the leading edge x where the boundary layer thickness δ equals the flow depth. Schlichting [51] expresses the local coefficient of total skin-friction drag as

$$c_f' = (2.87 + 1.58 \log {}^{x}/_{k_s})^{-2.5} \qquad \ldots (C.1)$$

where $$c_f' = \frac{\tau_o}{\frac{1}{2}\rho u_\infty^2} = 2\left(\frac{u_*}{u_\infty}\right)^2 \qquad \ldots (C.2)$$

since $\tau_o = \rho u_*^2$

The universal velocity distribution for a completely rough region with sand grain roughness is given by

$$\frac{u}{u_*} = 5.75 \log {}^{y}/_{k_s} + 8.5 \qquad \ldots (C.3)$$

(C.1), (C.3) may be equated where (C.3) is subject to the boundary condition

$$u = u_\infty , \quad y = \delta$$

to yield

$$\frac{1}{2}\left[5.75 \log {}^{\delta}/_{k_s} + 8.5\right]^2 = \left[2.87 + 1.58 \log {}^{x}/_{k_s}\right]^{2.5} \quad \ldots (C.4)$$

Now, the boundary layer fills the channel where $\delta = y$.

After substitution of this condition (C.4) can be written as

$$x = 0.0152 k_s \exp \{2.3 [\log(30.1 \frac{y}{k_s})]^{0.8}\} \quad \ldots (C.5)$$

In the experiments $y_{max} \simeq 0.4$ m and $k_s \simeq D_{50} = 0.004$ m.

For these values (C.5) gives

$$x = 7.6 \text{ m.}$$

Kamphuis [52] showed that for rough turbulent conditions

$$k_s \simeq 2D_{90}$$

which implies that $x = 6.2$ m.

The more conservative estimate was used and the velocity profile was checked near the end of the fixed bed with a Pitot Tube. It showed that the turbulent boundary layer was fully developed.

b) Outflow Region

The point where the water issued from the flume into the settling tank was a free overfall. In order to reduce the length of the back water curve in this area an adjustable tailgate (B.5.1) was installed. (Series II). By introducing the bottom edge of the gate a short distance

into the flow the curve was confined to the immediate region of the control. During non-steady runs the gate was raised and lowered at a rate dictated by calibration with steady flows. That is, the known inflow water hydrograph was approximated as a series of small step changes in discharge; the corresponding gate settings being determined by interpolation from a steady state plot.

It was found that the gate had a tendency to wash out, that is the water outflow detached itself from the bottom edge, so, in Series III, it was replaced by a submerged knife-edge adjustable weir. This was operated in a similar manner.

The length of fixed bed which had to be greater than the maximum backwater length was determined by trial and error in Series II and was dictated by the position of the sediment collection device in Series III.

C.1.2 Roughness Variations

A fixed plane bed has a constant roughness which may be estimated by, for example, a value of Manning's 'n' obtained from the Manning-Strickler formula

$$n = 0.041 D^{1/6} \qquad D \text{ in metres}$$

In our case this yields $n = 0.022$ for the sealed bed and $n = 0.016$ for the movable bed. The effect of this difference in roughness was observed as a change in water surface level at the transitions. At high discharges such changes were not apparent for two reasons, first because of the wavy nature of the water surface and second, because the roughness of the loose bed region had increased owing to the presence of bedforms and bed-material diffused into the flow.

C.2 WATER SUPPLY AND DISCHARGE MEASUREMENT

C.2.1 Water Supply

Water was supplied from a constant head tank to the flume by means of two pipelines (diameters 152 mm, 76 mm). With a head of 10 m the maximum available discharges were 110 ℓ/sec and 25 ℓ/sec. respectively. The smaller pipe supplied the baseflow for non-steady runs. A valve in each pipe regulated the flow rate.

Prescribed inflow hydrographs, superimposed upon the baseflow, were achieved by opening and closing the valve in the 152 mm line. As with the tailgate a hydrograph was approximated as a series of small step changes in discharge; the corresponding settings being determined by interpolation from a steady state plot. In practice the valve was nearly continuously moved.

C.2.2 Discharge Measurement

A calibrated pit, situated between the flume outflow and the storage sump (4.3.2.A) was used to measure the flow rate of the baseflow and all steady flows. (Error = $\pm$ 0.5%). For non-steady flows, a commercial (Annubar) Pitot Tube type meter was installed in the 152 mm pipe. It was calibrated during steady runs and the output from a pressure transducer, displayed visually by a needle scale, was recorded manually. (Error = $\pm$ 3%)

C.3 SEDIMENT SUPPLY AND DISCHARGE MEASUREMENT

C.3.1 Sediment Supply

When appropriate, sediment was supplied by the 'drop in' feed method from a hopper (B.2) suspended just upstream of the movable bed. The calibration plot for the hopper was linear and inflow sediment hydrographs were achieved by the step change method (C.2.1). (Error = $\pm$ 4%).

C.3.2 Sediment Discharge Measurement

The water-sediment mixture leaving the flume passed through a sediment collection box (B.3.1) the sediment being retained. (Series II). Periodically the box was removed from its position and weighed. This value, divided by the collection time gave the bedload transport rate for wet gravel. A calibration chart gave the equivalent dry weight. Problems arose with this sampling method because of the high fluctuations of the transport rate which occurred when bedforms were present. It was evident that continuous measurement was desirable. Consequently in Series III a collection device capable of this was designed and used (B.3.2). Cumulative weight, linearly related to the visual display of a digital volt meter was recorded manually as a function of time - the device having been calibrated with dry gravel. Instantaneous rates were obtained from the relevant slopes of the cumulative weight v time plots.

The positioning of this collector at the downstream end of the movable bed eliminated backwater problems. (Error - see B.3).

C.4 WATER AND BED SURFACE ELEVATIONS

For steady flows elevations of the water and bed surfaces were measured to the nearest 3 mm with point gauges (a 30 mm square plate was attached to the bedlevel gauge). These were mounted, at a position corresponding to the centreline of the channel, on a four wheeled carriage that travelled on rails attached on either side of the flume. Measurements were recorded at stations as shown in Fig. 4. Elevations were plotted and straight lines of best fit by eye were drawn through the points for each surface. In the initial motion and equilibrium transport runs the lines were parallel for all sets of readings (equilibrium having been attained) and the elevation difference normal to the lines gave the mean depth as a function of time. With the

non-equilibrium runs the variation with respect to time of the mean water surface and bedlevel was recorded. (Error $\pm$ 5%).

Two resistance probes (B.4) placed as shown in Fig. 4 recorded the change in stage during the non-steady flows. (Error $\pm$ 5%).

C.5 WATER SURFACE AND BED SLOPES

The water surface slope is the sum of the flume slope (measured with a level) and the water surface slope relative to the flume (obtained from graphs of the water surface elevation (C.4).) Bed slopes were computed in a similar manner from the bed elevation graphs. (Error $\pm$ 5%).

C.6 BED CONFIGURATION

General bed configuration was noted visually. The length, height and velocity of the bedforms were evaluated by;

1) Observations through the glass side panels marked by a grid.
2) Observations in the centre of the flume by the point gauge with the plate attachment. (Error $\pm$ 10%).

C.7 WATER TEMPERATURE

The water temperature was measured to the nearest half of a degree centigrade with a mercury thermometer. Variations were small as the water was recirculated through the whole laboratory system. (Error $\pm$ 3%).

APPENDIX D

FORMULAE AND CRITERIA

D.1 INITIAL MOTION CRITERIA

(a) Shields

The value of the entrainment function

$$Y = \frac{\rho u_*^2}{\gamma(S_s - 1)D}$$

was determined from Shields diagram in Graf [4]p.96 by iteration.

(b) Paintal

Paintal [28] considered that the point of intersection of his curves

$$g_s^* = (6.56 \times 10^{18}) F_s^{16}$$

and $$g_s^* = 13 F_s^{2.5}$$

may be satisfactorily taken as the initiation point. The intersection occurs at

$$F_s = Y = 0.05 \qquad g_s^* = 10^{-2}$$

(c) St. Anthony Falls Hydraulic Laboratory

The critical value of the bed shear stress is that which removes 3% of the surface particles every hour.

For these experiments this can be determined as below;

$$N = \frac{nD^3}{u_*} \quad \text{and} \quad n = \frac{m}{AT}$$

where m = number of grains moving

A = area of test section

T = period of observation.

$$\text{So} \quad n = \frac{3}{100} \times A/D^2 \times \frac{1}{3600} \quad (m^2 sec)^{-1}$$

which value when matched with experimental values yields N

(d) Lane [53]

The critical bed shear stress τ_c is given by

$$\tau_c = 0.0164 \; d_{75}$$

where d_{75} is in millimetres and τ_c in lb/ft^2.

whence $$Y = \frac{\tau}{\gamma(S_s - 1)D}$$

D.2 STEADY STATE EQUILIBRIUM FORMULAE

The following values were used to determine the equilibrium transport rate by the methods given below;

Table D.2 - Equilibrium Formulae Data

q (Experimental) ℓ/sec/m	y (Experimental) m	u (Calculated) m/sec	τ_o (Calculated) N/m^2	u_* (Calculated) m/sec
150	.185	.811	3.70	.060
200	.225	.889	4.50	.066
250	.264	.947	5.28	.072
300	.303	.990	6.06	.077
350	.342	1.02	6.84	.082

$S_s = 2.65$ $S_o = 0.002$ $D = 4.02$ mm $\rho = 1000 \; kg/m^3$

Method A - Kalinske

Formula is detailed in White, Milli and Crabbe [20], p.4.

Method B - Einstein - Brown [1950],

Ref. [20], p.17.

Method C - Rottner

Ref. [20], p.28

Method D - Einstein Bed Load [1950]

Since mean velocities were available the following procedure was used to estimate u_*'

$$(u_*')^2 = g\, y'\, S_o$$

and $$u_*^2 = g\, y\, S_o$$

Hence $$y' = y \frac{(u_*')^2}{u_*^2}$$

Thus Einstein [15] p.10 Eq. 9 becomes

$$\frac{u}{u_*'} = 5.75 \log_{10} \left(12.27 \frac{(u_*')^2}{u_*^2} \cdot x\right)$$

where $R' = y'$ and $x = 1.00$ since $D/\delta' > 10$

From this equation u_*' was determined by iteration and the calculation then proceeded as in Einstein [15].

Method E - Ackers and White Total Load Formula

Ref. [20], p.41

The results of these formulae applied to the data of Table D.2 are as follows;

Table D.3 - Calculated Equilibrium Transport Rates

q ℓ/sec/m	g_s Kalinske N/sec/m	g_s Einstein-Brown N/sec/m	g_s Einstein N/sec/m	g_s Rottner N/sec/m	g_s Ackers and White N/sec/m
150	0.036	0.082	0.029	0.212	0.252
200	1.157	0.207	0.099	0.415	0.418
250	0.367	0.393	0.187	0.619	0.557
300	0.650	0.643	0.253	0.799	0.661
350	1.010	0.969	0.320	0.934	0.722

APPENDIX E

EXPERIMENTAL RESULTS

E.1 INITIAL MOTION

No sidewall correction procedure was carried out as the walls were smooth compared with the bed and the correction to the bed shear stress or slope amounted, using the Williams [54] formula, to less than 3%.

Table E.1 - Results of Initial Motions Runs

q	y	Θ	$u_* = (\sqrt{gyS_o})$	n	$\frac{nD^3}{u_*} \times 10^{-6}$	$\frac{\rho u_*^2}{\gamma_s D}$
ℓ/sec/m.	cm	°C	m/sec	$(m^2/sec)^{-1}$	.	.
69.0	11.7	16.2	.051	.310	.395	.040
85.2	13.2	17.3	.055	.820	.969	.046
94.7	14.1	17.5	.056	1.60	1.86	.048
108.6	15.2	17.8	.059	4.19	4.61	.054
88.8	13.4	16.1	.055	.915	1.08	.047
99.9	14.3	16.4	.057	2.55	2.91	.050
74.6	11.9	16.4	.052	.345	.431	.042
68.2	11.2	17.0	.050	.195	.253	.038
79.0	12.2	16.9	.052	.480	.600	.042
80.5	12.6	16.9	.053	.540	.662	.043
116.1	15.9	16.8	.060	4.68	5.06	.055

where $D = 4.02$ mm $\qquad S_o = 0.00203 = S_f$

E.2 STEADY STATE EQUILIBRIUM TRANSPORT

Table E.2 - Results of Steady Equilibrium Runs

q	y	Θ	g_s (input)	g_s (output)	$\bar{z}$ (initial)	$\bar{z}$ (final)
ℓ/sec/m	cm	°C	N/m/sec	N/m/sec	cm	cm
189	21.6	16.4	.108	.108	5.63	5.63
228	24.9	17.8	.157	.147	5.4	5.60
162	19.3	16.7	.078	.069	5.62	5.83
270	28.0	15.2	.235	.245	5.70	5.70
321	31.9	16.2	.432	.422	5.57	5.73
294	29.8	15.9	.314	.304	5.57	5.67
148	18.2	15.0	.059	.049	5.72	5.82
236	25.2	16.9	.186	.186	6.00	6.07
285	28.8	16.1	.275	.284	5.75	5.68
173	20.2	15.0	.981	.079	5.52	5.83

All values are mean values.

$S_o \simeq S_f = 0.002$, $D = 4.02$ mm.

E.3 NON-STEADY EQUILIBRIUM TRANSPORT - COMPARISON RESULTS

The method described in 3.3.2.1(b) and illustrated in Fig. 3(a) was applied. Fig. 15 is a composite plot showing the form of the various relationships. A table of results for selected times during wave passages at which the process was performed follows below. (Table E.3).

A measure of the error involved in matching flow conditions is given by the difference between the non-steady and steady discharges. This proved to be small and a mean value of q was taken.

E.4 YIELD AND EQUIVALENT STEADY DISCHARGE DETERMINATION

Table E.4 sets out the results of the process described in 5.3.1. B(ii)(6).

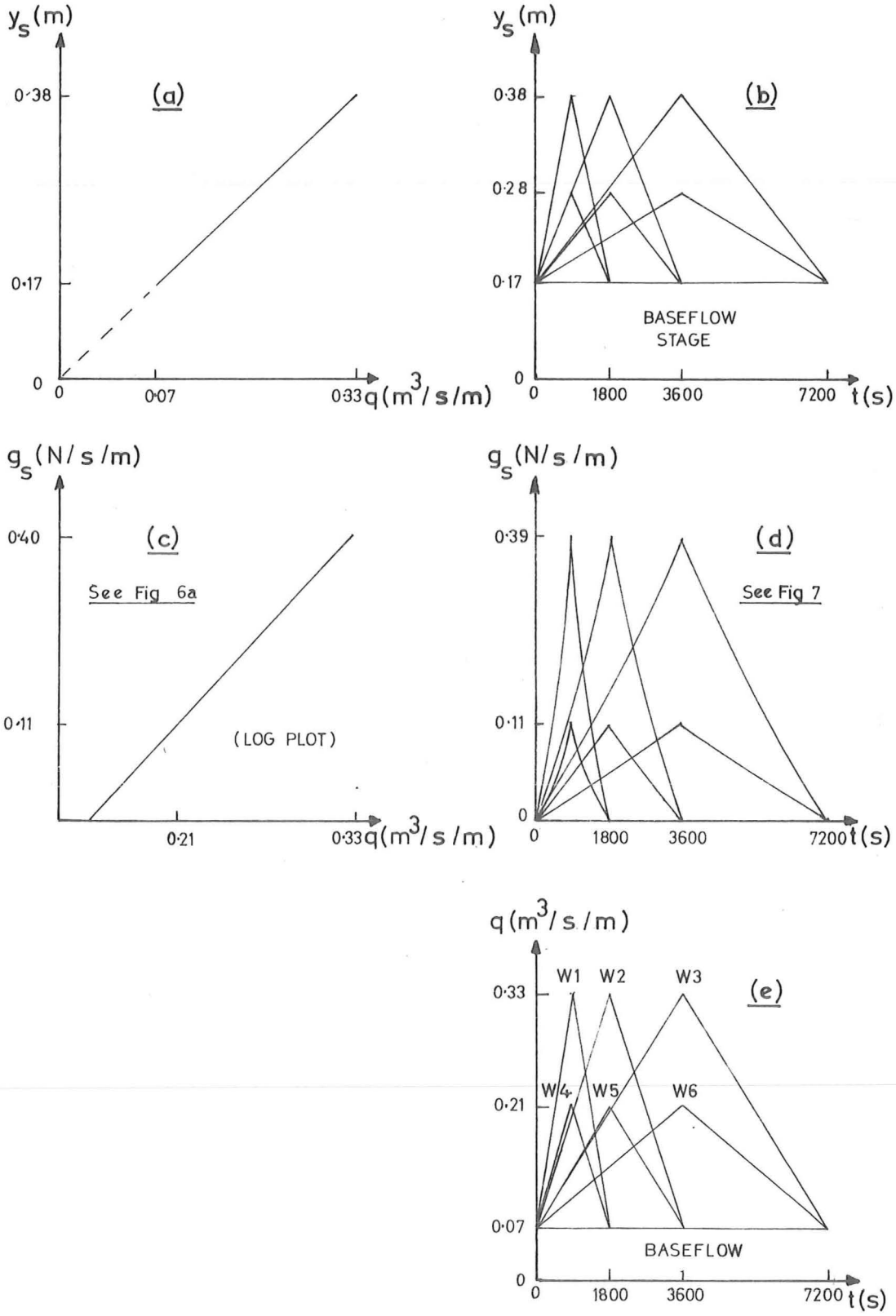

STEADY

NON-STEADY

Fig. 15 - FORM OF PLOTS USED IN THE EQUILIBRIUM TRANSPORT COMPARISON PROCESS (Refer to Fig 3a)

Table E.3 - Results of Bedload Transport Comparison Procedure

t	g_s	y_s	q	q	g_s
mins	N/m/sec	cm	ℓ/sec/m	ℓ/sec/m	N/m/sec
Selected	← Non-steady		Measured →	← Steady	Derived →
WAVE 1 (q_{max} = 330ℓ/sec/m , T = 30 mins)					
1	-	19.4	86	90	-
3	.014	21.2	118	114	-
5	.08	24.0	150	148	.016
7	.107	26.5	186	180	.059
9	.161	29.2	220	215	.096
11	.215	32.0	254	250	.215
13	.295	35.3	290	290	.295
15	.365	38.0	330	320	.386
17	.268	35.4	296	296	.295
19	.215	32.8	260	260	.220
21	.161	30.2	226	228	.161
23	.124	27.6	190	194	.102
25	.08	25.2	155	160	.076
27	.043	22.8	124	130	.037
29	-	20.0	90	96	-
WAVE 2 (q_{max} = 330 /sec/m , T = 60 mins)					
2	-	19.6	86	92	-
6	.026	21.4	120	115	.026
10	.065	24.4	155	154	.065
14	.102	27.0	190	186	.096
18	.134	29.6	222	220	.145
22	.187	32.4	260	256	.215
26	.295	35.0	294	288	.279
30	.359	37.8	330	326	.376
34	.289	35.4	300	294	.316
38	.236	33.0	270	264	.226
42	.166	30.6	240	234	.172
46	.107	28.2	210	212	.129
50	.065	26.0	178	174	.080
54	.032	23.5	148	142	.037
58	-	21.0	110	110	-
WAVE 3 (q_{max} = 380ℓ/sec/m , T = 120 mins)					
5	.003	19.8	90	96	-
15	.032	22.2	132	126	.032
25	.096	25.6	176	172	.091
35	.166	29.0	218	214	.145
45	.231	32.4	260	256	.226
55	.354	35.8	306	298	.337

60	.381	37.6	326	322	.387
65	.354	36.0	304	304	.338
75	.274	33.0	264	270	.241
85	.161	29.8	224	224	.156
95	.080	26.6	183	182	.091
105	.032	23.5	144	142	.037
115	-	19.8	98	94	-

WAVE 4 (q_{max} = 210 ℓ/sec/m , T = 30 mins)

1	-	18	78	74	-
3	.001	19.4	98	90	-
5	.006	20.8	116	110	.011
7	.022	22.2	136	126	.026
9	.043	23.8	154	148	.059
11	.076	25.2	174	164	.076
13	.096	26.6	192	186	.096
15	.107	28.0	208	200	.113
17	.102	27.0	194	188	.102
19	.085	26.0	178	174	.085
21	.059	25.0	164	162	.070
23	.037	23.8	148	148	.054
25	.027	22.8	133	134	.027
27	.011	21.4	118	116	.011
29	-	19.0	90	85	-

WAVE 5 (q_{max} = 210 ℓ/sec/m , T = 30 mins)

2	-	19	78	82	-
6	.004	19.6	96	92	-
10	.022	21.2	114	114	.022
14	.032	22.6	133	132	.032
18	.048	24.2	150	154	.059
22	.070	25.8	170	172	.076
26	.102	27.2	188	180	.096
30	.113	28.7	208	208	.124
34	.102	27.6	196	194	.107
38	.085	26.5	183	180	.085
42	.065	25.5	170	168	.076
46	.048	24.4	156	154	.059
50	.026	23.2	142	138	.037
54	.011	22.2	128	128	.016
58	-	21	110	110	-

WAVE 6 (q_{max} = 210 ℓ/sec/m , T = 120 mins)

5	.005	19.2	80	88	.005
15	.008	20.2	104	100	.010
25	.037	22.2	127	126	.037
35	.065	24.2	150	152	.059
45	.091	26.2	174	176	.085
55	.113	28.2	196	204	.113
60	.118	29.1	208	212	.129
65	.107	28.2	198	204	.113
75	.076	26.4	176	180	.085
85	.059	24.5	154	155	.059
95	.043	22.6	132	132	.043
105	.021	20.8	110	108	.022
115	-	18.8	88	84	-

Table E.4 - Non-Steady Average/Equivalent Steady Water Discharge

WAVES	W_1	W_2	W_3	W_4	W_5	W_6
T (mins)	30	60	120	30	60	120
q_{av} (ℓ/sec/m)	200	200	200	140	140	140
G_T (N/m)	260	499	1094	80.5	164	409
$g_{s_{av}}$ (N/m/sec)	.145	.138	.152	.045	.046	.057
q_s (ℓ/sec/m)	212	208	215	144	148	155
q_{av}/q_s	0.94	0.96	0.93	0.97	0.95	0.90
$\frac{1}{2}$ T	15	30	60	15	30	60
q_{av}	200	200	200	140	140	140
G_T	138	245	586	32	77	225
$g_{s_{av}}$	.893	.135	.163	.010	.043	.063
q_s	215	208	222	-	144	158
q_{av}/q_s	.93	.96	.90	-	.97	.89
$\frac{1}{4}$ T	7.5	15	30	7.5	15	30
q_{av}	135	135	135	105	105	105
G_T	23	135	241	3.2	13	29
$g_{s_{av}}$	.050	.150	.134	.007	.015	.016
q_s	150	215	205	-	-	-
q_{av}/q_s	0.9	.63	.67	-	-	-
$\frac{3}{4}$ T	22.5	45	90	22.5	45	90
q_{av}	222	222	222	152	152	152
G_T	232	457	1011	71	155	370
$g_{s_{av}}$	.172	.170	.187	.052	.057	.069
q_s	225	225	235	150	155	163
q_{av}/q_s	.99	.99	.95	1.01	.98	.93

E.5 STEADY STATE NON-EQUILIBRIUM TRANSPORT

Table E.5 - Results of Steady Non-Equilibrium Runs

RUN NO.	q	y_s	Θ
	ℓ/sec/m	cm	°C
1	186	26.8	17.2
2	149	24.0	14.6
3	231	30.9	16.5
4	209	29.1	17.6
5	163	25.3	17.4
6	114	21.7	18.2
7	252	32.6	18.0
8	273	34.1	18.7
9	294	35.5	17.7
10	230	30.9	18.4
11	207	28.9	16.0
12	315	37.1	15.3
13	321	37.5	15.9

$\bar{z}(t)$ (cms) (mean bed levels)

RUN NO.	t = 0 (mins)	15	30	45	60	75	90	105	120
1	5.67	5.01	4.89	4.86	4.69	4.76	4.71	4.69	4.64
2	5.83	5.40	5.31	5.17	5.10	5.10	5.11	5.07	5.01
3	5.81	5.26	5.07	4.99	5.03	4.84	4.74	4.66	4.61
4	5.97	5.31	5.26	5.10	5.19	5.07	4.83	4.67	4.78
5	6.06	5.53	5.46	5.44	5.29	5.30	5.14	5.09	5.06
6	5.98	5.63	5.60	5.60	-	5.53	-	-	5.50
7	5.89	5.36	5.21	5.23	5.09	5.01	4.78	4.80	4.44
8	5.94	5.10	4.87	4.69	4.53	4.34	4.34	4.36	4.29
9	5.73	5.10	4.89	4.78	4.53	4.23	4.20	3.91	4.09
10	5.66	5.43	5.36	5.26	5.06	4.93	4.99	4.93	4.57
11	5.76	5.33	5.29	5.21	5.10	5.07	5.04	4.78	4.76
12	5.64	5.01	4.40	4.46	4.21	3.69	3.83	-	-
13	5.74	5.01	4.59	4.04	4.00	3.94	3.66	3.74	3.40

Table E.5 (Continued)

$g_s(t)$ (N/m/sec) (Bedload transport rate)

RUN NO.	t = 5 (mins)	15	25	35	45	55	65	75	85	95	105	115
6	.002											.002
2	.043			.032								.032
5	.070	.045			.043							.043
1	.096	.076										.076
11	.118	.108										.108
7	.196	.177								.147		.147
8	.265	.245					.196			.186		.186
9	.324	.314						.245				.245
12	.402					.333						.275
13	.422					.373			.333			.334

All values are mean values

S_o = 0.002 (initial bed slope)

D = 4.02 mm.

E.6 NON-STEADY NON-EQUILIBRIUM TRANSPORT - COMPARISON RESULTS

The method described in 3.3.3. 2(b) and illustrated in Fig. 3(b) applied exceptthat a plot of $G_T(t)$ v q was used in place of the $\bar{z}$ (mean bed level)(t) v q . (Note: $G_T = \bar{z}$ x constants). Fig. 16 is a composite plot showing the form of the various relationships. A table of results follows below (Table E.6). A measure of the error involved in matching flow conditions is given by the differences between the non-steady and steady discharges. The non-steady values were taken from the non-steady (q v t) plot. It turned out that the discrepancies were very small and a mean value of q was taken and used in the $G_T(t)$ v q graph.

E.7 YIELD AND EQUIVALENT STEADY DISCHARGE DETERMINATION

Table E.7 sets out the results of the process described in 5.3.2. B(ii)(5).

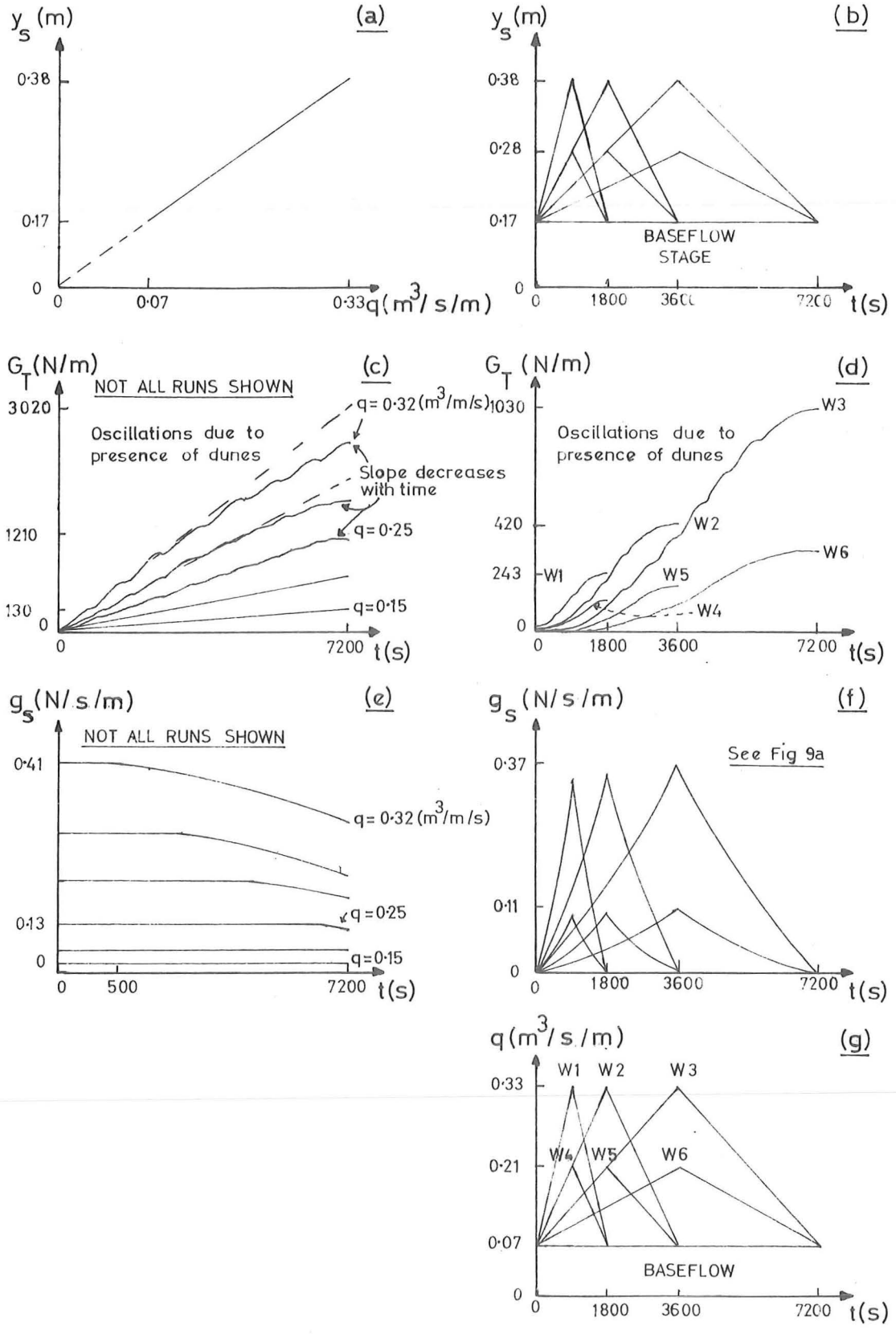

Fig.16 - FORM OF PLOTS USED IN THE NON-EQUILIBRIUM TRANSPORT COMPARISON PROCESS (Refer to Fig 3b)

Table E.6 - Results of Bedload Transport Comparison Procedure

t	g_s	G_T	y_s	q	q	t	g_s
mins	N/m/sec	N/m	cm	ℓ/sec/m	ℓ/sec/m	(mins)	N/m/sec.
Selected	← Non-steady		Measured →		← Steady		Derived →
WAVE 1 (q_{max} = 330 ℓ/sec/m , T = 30 mins)							
1	-	0	18.6	86	82	0	-
3	.003	0	21.4	120	115	1-	-
5	.048	2.25	24.4	155	152	1-	.054
7	.096	12.6	27.0	190	184	2-	.096
9	.139	29.9	30.4	226	226	4	.150
11	.187	48.3	33.2	260	260	4	.215
13	.241	70.8	36.0	296	298	4	.343
15	.338	109	39.0	330	340	5	.429
17	.306	145	37.2	304	310	8	.381
19	.215	190	34.8	276	280	10	.279
21	.142	212	32.4	248	250	23	.172
23	.085	219	30.0	218	220	29	.134
25	.054	225	27.2	190	186	55	.054
27	.016	232	24.8	160	156	115	.037
29	-	235	19.0	90	86	-	-
WAVE 2 (q_{max} = 330 ℓ/sec/m , T = 60 mins)							
2	-	0	18.6	88	82	0	-
6	.032	0	22	120	122	0	-
10	.054	3.54	24.8	154	158	5-	.059
14	.085	13.8	27.8	190	194	5-	.102
18	.129	33.2	30.6	224	228	5-	.150
22	.204	59.9	33.6	260	266	5-	.226
26	.274	97.5	36.4	295	302	10-	.306
30	.354	161	39.3	330	330	10-	.413
34	.300	245	37	304	306	10-	.370
38	.215	286	34.6	274	278	20	.263
42	.150	357	32	244	246	40	.172
46	.096	396	29.6	214	216	70	.118
50	.032	406	27.2	184	186	105	.076
54	.005	412	24.6	155	155	-	.021
58	-	412	22.4	116	120	-	-

Table E.6 (Continued)

WAVE 3 (q_{max} = 330 ℓ/sec/m , T = 120 mins)							
5	-	0	19	90	90	0	-
15	.016	7.08	22.6	132	132	10-	.027
25	.062	27.7	26	176	172	10-	.070
35	.102	77.2	29.6	220	218	10-	.118
45	.155	151	33	264	258	10-	.193
55	.285	322	36.6	306	308	15-	.348
60	.376	398	38.2	325	330	15	.407
65	.359	502	36.4	310	306	25	.359
75	.274	721	33.6	272	266	45	.254
85	.177	850	30.8	236	232	100	.155
95	.107	975	28	200	196		.096
105	.022	1001	25.2	164	162		.043
115	-	1007	22.4	120	126		-
WAVE 4 (q_{max} = 210 ℓ/sec/m , T = 30 mins)							
1	-	0	17.8	78	74	0	-
3	.003	0	19.4	98	90	0	-
5	.014	1.29	21.0	117	110	1	.002
7	.032	4.51	22.8	134	132	1	.032
9	.046	8.05	24.6	154	156	2	.059
11	.062	17.4	26.2	173	172	3	.08
13	.078	25.1	28	192	196	3	.107
15	.102	32.2	29.5	210	215	4	.129
17	.070	41.8	28.2	198	198	7	.107
19	.051	48.3	26.8	180	182	7	.085
21	.043	54.7	25.2	164	164	14	.054
23	.027	57.9	23.6	146	144	33	.032
25	.019	61.2	22.1	128	124	110	.022
27	.004	61.2	20.6	112	108	-	.002
29	-	61.2	19.1	90	86	-	-
WAVE 5 (q_{max} = 210 ℓ/sec/m , T = 60 mins)							
2	-	0	18.2	78	76	0	-
6	-	0	19.8	96	96	0	-
10	.006	1.29	21.5	114	116	10-	.002
14	.022	3.54	23	132	134	10-	.027
18	.040	10.3	24.7	152	156	10-	.048
22	.059	18.3	26.3	170	174	10-	.065
26	.078	32.2	28	189	196	10-	.091
30	.113	51.5	29.5	208	214	10-	.129
34	.088	69.8	28.2	193	198	10	.102
38	.065	83.7	26.7	176	180	20	.076
42	.037	90.1	25.3	160	164	30	.054
46	.027	93.3	24	144	148	90	.032
50	.006	96.6	22.4	126	128	-	.011
54	-	96.6	21.0	110	110	-	-
58	-	96.6	19.6	88	92	0	-

Table E.6 (Continued)

WAVE 6 (q_{max} = 210 ℓ/sec/m , T = 120 mins)							
5	-	0	18.4	80	78	0	-
15	.001	1.16	20.5	104	104	10-	.002
25	.016	7.08	22.6	128	130	10-	.022
35	.040	23.2	24.6	152	154	10-	.037
45	.062	57.9	26.6	176	180	10-	.076
55	.099	99.8	28.7	200	206	10+	.102
60	.110	133	29.6	214	218	10+	.118
65	.099	162	29.0	205	208	25	.107
75	.076	216	27.4	186	188	60	.080
85	.043	251	25.8	170	170	75	.048
95	.016	261	24.2	152	150	-	.022
105	.001	267	22.6	134	130		.005
115	-	270	20.5	110	104	-	-

Table E.7 - Mean Bed Levels - $\bar{z}(t)$ (cms)

Time	WAVES					
(mins)	W_1	W_2	W_3	W_4	W_5	W_6
0	6.00	5.86	5.89	6.04	5.90	5.89
5	5.94			5.94		
10	5.83	5.80		5.92	5.87	
15	5.80		5.87	5.69		5.80
20	5.61	5.69		5.69	5.67	
25	5.54			5.69		
30	5.54	5.53	5.54	5.66	5.57	5.74
40		5.46			5.57	
45			5.54			5.56
50		5.21			5.56	
60		5.16	5.16		5.51	5.54
75			5.04			5.33
90			4.93			5.30
105			4.86			5.33
115			4.70			5.26
120			4.66			5.24

Table E.8 - Non-Steady Average/Equivalent Steady Water Discharge

WAVES	W_1	W_2	W_3	W_4	W_5	W_6
T (mins)	30	60	120	30	60	120
q_{av} (ℓ/sec/m)	200	200	200	140	140	140
G_T (N/m)	235	412	1007	61	97	267
q_s (ℓ/sec/m)	210	218	230	154	150	160
q_{av}/q_s	.95	.92	.87	.91	.93	.88
$\frac{1}{2}$ T	15	30	60	15	30	60
q_{av}	200	200	200	140	140	140
G_T	109	161	399	32	52	135
q_s	212	200	215	145	148	152
q_{av}/q_s	.94	1.0	.93	.97	.95	.92
$\frac{1}{4}$ T	7.5	15	30	7.5	15	30
q_{av}	135	135	135	105	105	105
G_T	16.1	19.3	51	6.4	6.4	12.9
q_s	150	148	147	-	-	135
q_{av}/q_s	.90	.91	.92	-	-	.78
$\frac{1}{4}$ T	22.5	45	90	22.5	45	90
q_{av}	222	222	222	152	152	152
G_T	216	386	933	55	93	254
q_s	235	230	240	157	152	164
q_{av}/q_s	.95	.97	.93	.97	1.0	.93

E.8 BED RESPONSE EFFECTS

The differences in the sediment yields ΔG_T between the observed sediment hydrographs and those obtained under comparable conditions were found by measuring the area under the relevant plots with a planimeter. Thus

$$\Delta G_T \% = \frac{\text{Comparable hydrograph area - observed hydrograph area}}{\text{observed hydrograph area}}$$

Other parameters were determined directly from the experimental data.

Table E.9 - Bed Response Parameters

SERIES III

y_{crit} = 0.11 m S_o = 0.002 U_{*max} = 0.063 ($W_1 \rightarrow W_3$), 0.47($W_4 \rightarrow W_5$) m/sec.

WAVE	W_1	W_2	W_3	W_4	W_5	W_6
$\frac{y_{crit}}{u_* T} \times 10^{-4}$	10	5	2.5	13	6.6	3.3
ΔG_T %	26	14	6	30	15	9

SERIES I

y_{crit} = 0.056 m , u_{*max} = 0.069 m/sec , S_o = 0.0044

$\frac{y_{crit}}{u_* T} \times 10^{-4}$	13.5			6.8	3.4	
ΔG_T %	115			65	35	

E.9 STAGE-DISCHARGE RELATION

The stage discharge relation for Wave 3 of the Series III non-steady equilibrium transport runs and the steady flow rating are given in Table E.10. Both ratings were measured at the downstream recorder site (Fig. 4).

Table E.10 - Stage Discharge Relation for Wave 3
(Non-steady Equilibrium Transport)

q (steady flow)	y_s (steady flow)	y_s (non-steady flow)	
		Rising stage	Falling stage
$m^3/sec/m$	m	m	m
0.09	0.196	0.196	0.196
0.13	0.226	0.226	0.226
0.17	0.256	0.256	0.256
0.21	0.287	0.287	0.287
0.23	0.302	0.302	0.305
0.25	0.318	0.316	0.320
0.27	0.332	0.328	0.337
0.29	0.348	0.344	0.352
0.31	0.363	0.357	0.369
0.32	0.378	0.373	0.379
0.33	0.383	0.379	0.379

E.10 RESISTANCE VARIATIONS

The absolute variation in Manning's 'n' , between the steady flow value and the Wave 3 value, and Einstein's intensity of bedload transport (ϕ) is given in Table E.11.

Manning's 'n' was calculated from the expression

$$n = {}^{1}/_{q}\, y^{5/3}\, S_f^{1/2} \qquad \text{(metric units)}$$

where the steady or non-steady water stage (as appropriate) was used